# NOTE TO USERS

# Immune suppression by parasitoid wasps of *Drosophila*: studies on virus-like particles, virulence, and genome-wide expression analysis

by

Jorge Morales

A dissertation submitted to the Graduate Faculty in Biology
in partial fulfillment of the requirements for the degree of Doctor of Philosophy,

The City University of New York

2005

This manuscript has been read and accepted for the Graduate Faculty in Biology in Satisfaction of the dissertation requirement for the degree of Doctor of Philosophy.

Jan 21, 2005
Date

Chair of Examining Committee
Dr. Shubha Govind, City College

January 25 2005
Date

Executive Officer
Dr. Richard L. Chappell

Dr. Sally Hoskins, City College

Dr. Paul Gottlieb, City College

Dr. Robert DeSalle, American Museum of History

Dr. Christine Rushlow, New York University

Supervising Committee

The City University of New York

Abstract

IMMUNE SUPPRESSION BY PARASITOID WASPS OF *DROSOPHILA*: STUDIES ON VIRUS-LIKE PARTICLES, VIRULENCE, AND GENOME-WIDE EXPRESSION ANALYSIS

by

Jorge Morales

Adviser: Professor Shubha Govind

*D. melanogaster* has a primitive but powerful innate immune system consisting of humoral and cellular components. Cellular immune responses are mediated by plasmatocytes that carry out phagocytosis, crystal cells that mediate melanization, and lamellocytes which encapsulate large parasites. Encapsulation is the major defense of *Drosophila* larvae against eggs of parasitoid wasps. Parasitoid wasps, however, have evolved to either actively suppress, or passively avoid encapsulation. For instance, infection by the wasps *Leptopilina heterotoma* or *L. victoriae,* eliminates activated plasmatocytes and lamellocytes via apoptosis and lysis respectively. Virus-like particles (VLPs) produced by *L. heterotoma* mediate the lysis of lamellocytes and consequently suppress encapsulation. Avirulent strains of wasps, such as *L. boulardi-G486,* are less successful at parasitizing *Drosophila*, and their VLPs do not cause lamellocyte lysis. Our main goals are (1) To understand the nature of humoral and cellular immune responses of *D. melanogaster* infected by parasitoid wasps differing in the degree and mechanisms of virulence. (2) To understand virulence mechanisms adapted by these wasps, the structure of their VLPs, and to determine, how virulence factors disrupt host defense responses. We describe the

biogenesis and fine structure of previously undescribed VLPs found in *L. victoriae*. *In vitro*, these VLPs induce the lysis of lamellocytes but with slower kinetics than *L. heterotoma* VLPs. Purified VLPs from these two wasp species contain at least 4 major proteins. The most abundant proteins, p40 in *L. heterotoma* and p47.5 in *L. victoriae*, cross react with polyclonal antisera raised against *L. heterotoma* VLPs. Immuno-EM staining localizes these proteins to VLP surfaces. Significantly, anti-p40 antibodies block lamellocyte lysis induced by either *L. heterotoma* or *L. victoriae* VLPs. A comparison of changes in global gene expression patterns of *D. melanogaster* larvae in response to *L. heterotoma* versus *L. boulardi* infection reveals significant differences, both in the number and nature of genes. These differences in gene expression patterns will provide clues into the molecular mechanisms of virulence and immune suppression used by parasitoid wasps.

## ACKNOWLEDGEMENTS

I am grateful to my mentor Professor Shubha Govind who has guided me for the past two and a half years. I thank her for the valuable advisement and choices she gave me as I progressed through my work. It has been a privilege to work with her.

I also want to express my gratitude to the people who have been extremely helpful and influential during my years at CCNY. I would like to thank the late Dr. Sharon Cosloy with whom I did my first research rotation in molecular biology. I am also grateful to Dr. John J. Lee from whom I learned electron microscopy. I am grateful to Dr. Jane Gallagher, Dr. Jerry Guyden, Dr. Sally Hoskins, and Dr. Millicent Roth for their unconditional support, specially during my most difficult times.

I thank the members of my thesis defense committee, and also thank Dr. John Berriman and Dr. Mark Steinberg for serving as members of my second level examination committee.

The following programs made my career in science possible by providing financial support.

The Minority Biomedical Research Support Program (MBRS)
Program director: Professor Myer Fishman
Provided financial support while in the B.S. program.

The Bridges to the Doctorate Program, funded by the NIH
Program director: Professor Gail Smith
Provided financial support while in the M.A. program.

The RISE Program
Program director: Professor Michael Weiner
Provided financial support while in the Ph.D. program.

# TABLE OF CONTENTS

# LIST OF TABLES

## Chapter 1



## Chapter 3

# LIST OF FIGURES

## Chapter 1



## Chapter 2

**Chapter 3**

# Biogenesis, structure, and immune suppressive effects of virus like particles of a *Drosophila* parasitoid, *Leptopilina victoriae*

Jorge Morales[1,2], Hsiling Chiu[1], Thiri Oo[1], Rosemary Plaza[1], Sally Hoskins[1,2], and Shubha Govind[1,2]

[1]Department of Biology, The City College of New York
138th Street & Convent Avenue, New York, NY 10031

[2]The Graduate School and University Center
The City University of New York
365 Fifth Avenue, New York, NY 10016

Key words: *Drosophila*, parasitoid wasps, immune suppression, virus like particles, hemocytes, innate immunity

Abbreviations:

VLP: virus-like particle

PBS: phosphate buffered saline

BCA: bichinoic acid

nm: nanometers

## ABSTRACT

*Drosophila melanogaster* larvae are attacked by virulent strains of parasitoid wasps. Females of *Leptopilina heterotoma* produce virus-like particles (VLPs) that efficiently destroy lamellocytes, a major larval immune effector cell type. We report here that *L. victoriae*, a closely related wasp species, also produces VLPs that trigger immune suppression responses in fly hosts. We compare the ability of immune suppression of the two parasitoids using a mutant host strain *hopscotch*$^{Tumorous\text{-}lethal}$. *hopscotch*$^{Tumorous\text{-}lethal}$ larvae have two defects of hematopoietic origin: overproliferation of hemocytes and constitutive encapsulation of self tissue by lamellocytes. The encapsulation phenotype is suppressed weakly by *L. victoriae* and strongly by *L. heterotoma*. *In vitro* studies on *hopscotch*$^{Tumorous\text{-}lethal}$ lamellocytes show that VLP-containing fluid from either wasp species induces lamellocyte lysis, but with different kinetics.

Previously undocumented precursors of *L. victoriae* VLPs are synthesized in the long gland and are first visible within canals connecting secretory cells to the long gland lumen. VLP assembly occurs in the lumen. VLPs show multiple electron-dense projections surrounding a central core. Maturing particles appear segmented, singly or in arrays, embedded in the reservoir matrix. In sections, mature particles are pentagonal or hexagonal; the polygon vertices extending into spikes. Our results suggest that *L. victoriae* is likely to promote immune suppression by an active mechanism that is mediated by VLPs, similar to that used by *L. heterotoma*.

# INTRODUCTION

Insect species of the dipteran genus *Drosophila* serve as hosts to endoparasitoid wasps (Hymenoptera; referred to as parasitic wasps hereafter) and recognize them as "foreign". Parasitic wasps of the *Leptopilina* genus inject their eggs into the body cavity of the second instar larval host. If the host's innate immune responses of encapsulation and melanization are effective, the egg is encapsulated, parasite development does not progress and the fly develops into a fertile adult. If, however, the host is immune-incompetent, or if the parasite evades or suppresses the immune responses of the host, the parasite egg develops, consumes the host, and emerges from the fly pupa as an adult wasp (Rizki and Rizki; 1984; Carton and Nappi, 1997; Schmidt *et al.*, 2001).

A successful cellular immune response in *Drosophila* larvae is characterized by an increase in the number of mature circulating blood cells (hemocytes), and involves proliferation and differentiation of hematopoietic precursors in the larval lymph gland. Wasp infection results in the differentiation of large, disc-shaped lamellocytes and an increase in the number of smaller, phenol oxidase-bearing, crystal cells in the lymph gland (Lanot *et al.*, 2001; Sorrentino *et al.*, 2002). This increase is observed in third instar hosts. Lamellocytes are adhesive and rapidly aggregate around eggs of the parasite to form a cellular capsule. Crystal cells lyse and release substances that melanize the capsule (Rizki and Rizki, 1984a; Carton and Nappi; 1997; Nappi and Vass, 2001). The third and predominant cell type in circulation is the plasmatocyte. More than 90% of hemocytes in circulation are plasmatocytes (Rizki and Rizki, 1984a; Lanot *et al.*, 2001). Plasmatocytes are phagocytic cells that protect larvae from microbial infections (Rizki and Rizki, 1984a). While the specific role of plasmatocytes in the encapsulation

response is not entirely clear, we have recently found that there is a direct correlation between circulating hemocyte concentration (mainly plasmatocytes) and the efficiency of the encapsulation response (Sorrentino *et al.*, 2004). Successful encapsulation of parasite eggs by *Drosophila* larvae thus involves recognition of the parasite as non-self, proliferation of hematopoietic precursors, differentiation of lamellocytes and crystal cells, and death of the parasite egg.

Encapsulation of the parasite egg is not always fatal, as parasites have adopted both passive and active means to manipulate the host's immune system and avoid encapsulation (for review, see Schmidt *et al.*, 2001). Parasite evasion, an example of the passive mode of immune suppression is observed when the wasp produces molecules that are either not recognized as foreign or do not allow adhesion of host hemocytes. For example, Crp32, a protein synthesized in the calyx cells of the ovaries of the wasp *Cotesia rubecula*, coats the egg surface to form a protective layer against blood cells of its butterfly host, *Pieris rapae* (Asgari *et al.*, 1998). Many braconid and ichneumonid endoparasitic wasps harbor unusual DNA-containing insect viruses called 'polydnaviruses'. These viruses actively suppress the immune responses of the lepidopteran hosts, especially encapsulation by hemocytes (Webb, 1998; Schmidt *et al.*, 2001; Turnbull and Webb, 2002). In many cases, a combination of these active and passive approaches is employed by parasites to ensure their survival. A variety of factors thus determine whether the parasite will successfully infect and consume the host, or if instead, the immune system of the host can defend against this invasion.

Cynipid wasps of the cosmopolitan genus *Leptopilina* infect *Drosophila melanogaster* and related species (Schilthuizen *et al.*, 1998). The interactions of two

*Leptopilina* species (*L. boulardi* and *L. heterotoma*) with their *D. melanogaster* host, and the immune response of the host have been particularly well studied (Rizki *et al.*, 1990; Russo *et al.*, 1996; 2001; Lanot *et al.*, 2001; Sorrentino *et al.*, 2002, 2004). Two distinct types of *L. boulardi* strains have been identified: virulent strains (e.g., L104 and G431) that are able to suppress encapsulation (no more than 5% of wild type or other control larvae respond by forming egg capsules), and avirulent strains (e.g., G486), that allow variable levels of encapsulation in control or "resistant" host strains (Carton *et al.*, 1992; Dupas *et al.*, 1996; Labrosse *et al.*, 2003; Sorrentino *et al.*, 2004). Eggs of *Leptopilina boulardi* strain L104 resist the immune responses of the host by lodging in or around host organs where host lamellocytes cannot fully access the egg (Rizki *et al.*, 1990). In addition, both avirulent and virulent strains of *L. boulardi* possess virus like particles in their long gland/reservoir structures (Dupas *et al.* 1996; Labrosse *et al.*, 2003). Differences in VLP morphology correlate with the difference in virulence between the two classes of *L. boulardi* wasps: VLPs from the virulent (immune suppressive) strains are round with several vesicles, whereas those from the avirulent (non-immune suppressive) strains are elongate, with fewer vesicles (Dupas *et al.*, 1996; 1998). VLPs in virulent strains are believed to act as factors that suppress the hosts' immune responses. While host lamellocytes are not destroyed upon infection by *L. boulardi* or treatment with VLP-containing wasp fluid, lamellocyte morphology and adhesive properties are modified. Furthermore, the melanization pathway is impaired (Labrosse *et al.*, 2003).

In contrast, lamellocyte destruction has been clearly documented when *Drosophila* larvae are infected by independent isolates of *L. heterotoma* (Rizki and

Rizki, 1992). In addition, both the "suppression of tumor formation" assay as well as the *in vitro* "biopolar cell formation" assay indicate that fluid from *L. heterotoma* wasps promotes lamellocyte destruction (Rizki and Rizki, 1984; Rizki *et al.*, 1990; see below). Mutant larvae with melanotic tumors have an overabundance of lamellocytes in their hemocoel, and melanotic 'tumors' themselves contain melanized capsules of lamellocytes layered around larval self-tissues (Rizki and Rizki, 1986). Observations as early as 1959 showed that wasp infection of mutant *D. melanogaster* strains carrying melanotic tumors caused suppression of the tumor phenotype (Walker, 1959). Subsequent reports of infection of other tumor-bearing strains by *L. heterotoma* confirmed these early observations (Nappi, 1975; Nappi *et al.*, 1984; Rizki and Rizki 1984; 1990; Rizki *et al.*, 1990).

In a series of elegant experiments (Rizki and Rizki 1984, 1990, 1991, 1992 and 1994), Rizki and Rizki showed that virus-like particles (VLPs) from *L. heterotoma* interfere directly with the cellular defense system of *Drosophila* to ensure optimal developmental opportunity for the wasp's progeny. VLPs are manufactured in the *L heterotoma* long gland and stored in the reservoir, organs associated with the female reproductive structures. Transmission electron microscopy revealed that mature VLPs are 300 nm in diameter, with electron-dense cores and surface spikes (Rizki and Rizki, 1990, 1994). It is believed that VLPs are released into the host hemocoel during oviposition and prevent encapsulation of the parasite egg by targeting lamellocytes for destruction (Rizki and Rizki 1984, 1991). Two to four hours after infection, lamellocytes in the hemocoel simultaneously lose their discoidal appearance and their ability to adhere. They become bipolar, and undergo degenerative changes as cytoplasm is lost at

the tips of elongating cells (Rizki and Rizki 1984, 1990, 1991 and 1994; Rizki *et al.*, 1990).

Unlike *L. heterotoma* VLPs, VLPs from virulent strains of *L. boulardi* have no surface spikes but contain multiple internal vesicles (Dupas *et al.*, 1996). Our goals here are to determine if *L. victoriae*, the closest reported relative of *L. heterotoma* (Schilthuizen *et al.*, 1998), harbors VLPs like those found in *L. heterotoma*, and to understand the molecular mechanisms by which such particles mediate immune suppression in *D. melanogaster*. We compared the immune suppressive effects of *L. heterotoma* and *L. victoriae* and performed a fine-structural analysis of the *L. victoriae* long gland/reservoir complex. Here we present the first description of *L. victoriae* VLP structure and biogenesis. Our results suggest that even though there are significant differences in their virulence, the two wasp parasites *L. heterotoma* and *L. victoriae* share overall biological, and possibly molecular mechanisms of immune suppression.

## METHODS

**Insect stocks** Parasitic wasps: *Leptopilina heterotoma* was obtained from Dr. P. Chabora, Queens College, CUNY, whereas *Leptopilina victoriae* was a gift of Dr. J.J.M. van Alphen, Leiden University. Both strains were grown on *D. melanogaster* host as previously described (Chiu *et al.*, 2001).

**Tumor suppression** To compare the relative degrees to which *L. heterotoma* and *L. victoriae* infection can promote the suppression of melanotic tumors, larvae of the mutant host strain of *D. melanogaster*, *y v* $hop^{Tum\text{-}l}/Y$ were infected by 6-day old naïve wasps as described in Chiu *et al.* (2001). Even though almost all *y v* $hop^{Tum\text{-}l}/Y$ larvae contain melanotic tumors, the size of the tumors and the number of free lamellocytes in these individuals is highly variable (Hanratty and Dearolf, 1993; Sorrentino *et al.*, 2002). Thus, effects of wasp infections, even under the most controlled experimental conditions, on the presence and size of the tumors, are at best qualitative. Egg lays were carried out for 4-6 hours in glass vials containing 5 ml of fly food. More than 100 second instar larvae were infected 48 hours later with ten *L. heterotoma* or *L. victoriae* females for 6 hours. Infected third instar larvae were first inspected for the presence of egg capsules and melanotic capsules six days after the initiation of egg lay. They were then dissected to check for infection or the degree of superinfection. Under these conditions of infection, a majority of the host larvae were parasitized with only one egg. Uninfected hosts were not included in the experiment.

To compare immune suppression *in vitro*, hemolymph from ten $hop^{Tum\text{-}l}/Y$ mutant larvae was pooled in 200 µl phosphate buffered saline containing bovine serum albumin. Aliquots (40-60 µl) of hemolymph were placed in humidified chamber slides. Fifty *L.*

*heterotoma* and *L. victoriae* long glands and reservoirs were dissected and crushed into 50 µl of phosphate buffered saline (PBS), pH 7.2 and protein concentration was determined using the BCA method (Smith *et al.*, 1985). At the equivalent ages, glands of both wasps contain approximately equal amounts of total protein. Fluid containing equal amounts of total protein was added to the hemocytes in culture at time zero. Two experiments in which extracts were prepared from different groups of wasps were performed. In one experiment, 20 µg of protein was used per chamber. In the other experiment, 2.4 µg of protein was used per chamber. An equivalent volume of PBS was added to control samples in place of wasp fluid. Some lamellocytes with bipolar morphology were observed in control samples, possibly in response to culture conditions. Only those lamellocytes with clear bipolar morphology was recorded. Cell numbers were recorded manually at different time points using an inverted Nikon Eclipse TE200. Recording of cellular morphology took 15-30 minutes per sample; the midpoint of this duration was plotted against percent bipolar cells. Lamellocyte morphology was scored for roughly 6 hours after the addition of fluid.

To determine if the differences between proportions observed at equivalent timepoints in both the in vivo (percentage of animals) and in vitro (percentage of bipolar cells) assays are significantly different, we performed a two-tailed z test where the difference between the two independent proportions is divided by the standard error of the difference (Dawson and Trapp, 2004). The standard error of each percentage was calculated using each proportion as the mean as described in Dawson and Trapp (2004).

**Ultrastructural analysis of *L. victoriae* VLPs** To examine stages of VLP biogenesis, the long gland reservoir complex was dissected in PBS, and fixed in 3.5% glutaraldehyde prepared in 0.2 M sodium cacodylate buffer pH 7.2, for 2 hrs at 4°C. Tissues were postfixed for 30 min in 1% osmium tetroxide at 4°C. Tissues were embedded in EMBeb-812 and samples were sectioned at different locations, indicated by numbers in Fig. 3a. Sections were stained with 4% uranyl acetate for 4 hrs, followed by 0.6% lead citrate for 30 min, similar to the method described by Rizki and Rizki (1990). To study morphology of mature VLPs, we dissected 200 glands and reservoirs in PBS (pH 7.2), extracted VLP-containing fluid by homogenization, and purified VLPs on a 10-50% Nycodenz gradient. VLPs were pelleted in one 30-min centrifugation step. Pellets were processed for fixation, sectioning and staining as described previously (Rizki and Rizki, 1984, 1990). A Zeiss transmission electron microscope (EM902) was used to visualize stained preparations. Images were photographed on Kodak SO-163 film and scanned at 600 dpi using an Epson Perfection 1640 Photo scanner and Adobe Photoshop v. 6. Images were saved as "TIF" files. Measurements were made using options available in Image-Pro Plus v. 4.0 (circle function for diameter, or line and angle tools). For each scanned image, spatial calibration was done using the scale bar on the original negative. Data were exported into an Excel file and the final measurements are presented as averages of all images in a specific class.

## RESULTS

Wild type host larvae rarely encapsulate the eggs of *L. heterotoma* or *L. victoriae*; thus in these hosts, free parasitoid is observed inside the host hemocoel. To compare the immune-suppressive capacities of *L. heterotoma* and *L. victoriae*, we infected host larvae carrying a mutation in the JAK-kinase-encoding gene *hopscotch*$^{Tumorous\text{-}lethal}$ (*hop*$^{Tum\text{-}l}$). This mutation causes a drastic over-proliferation of hematopoietic precursors and as a result hemocyte concentration in mutants is five to ten times higher than in wild-type larvae (Hanratty and Dearolf, 1993). In almost all (98/99) *hop*$^{Tum\text{-}l}$ larvae, hemocytes (chiefly lamellocytes) aggregate around self tissues to form melanotic capsules (tumors) that can be clearly observed through the transparent cuticle (Hanratty and Dearolf, 1993). Infection of *hop*$^{Tum\text{-}l}$ larvae by either *L. heterotoma* or *L. victoriae* would be expected to decrease tumor formation due to the effect of infection on lamellocyte survival. At the same time, the high concentration of circulating lamellocytes in these mutants makes encapsulation of parasite wasp eggs likely. Both these outcomes were used to compare the immune-suppressive capacities (virulence) of the two wasps.

Infection by either wasp resulted in a clear reduction in the number of *hop*$^{Tum\text{-}l}$/Y animals carrying melanotic tumors as compared to uninfected controls (Fig. 1, 2). In the case of *L. heterotoma* 53.4% (n = 118) of the infected animals exhibited tumors (all uninfected *hop*$^{Tum\text{-}l}$/Y larvae have tumors) and these animals did not encapsulate the wasp egg. Another 7.6% of these infected cases encapsulated a wasp egg, and exhibited small tumors or no tumors (Fig. 1, 2b). When infected with *L. victoriae,* only 10.8% of the infected *hop*$^{Tum\text{-}l}$/Y larvae exhibited melanotic tumors without egg encapsulations.

An additional 74.6% of these infected animals encapsulated the wasp egg and carried a small tumor or had no tumor (n = 193; Fig. 1, 2c). The size of melanotic capsules in infected mutant larvae is strikingly smaller than that seen in uninfected mutants (Fig. 2: compare tumor sizes in panels b and c, relative to a; white arrows). The z test for independent proportions revealed that the difference in tumor suppression (MC) and egg encapsulation (EC) between *L. heterotoma* and *L. victoriae* infected larvae is statistically significant ($p < 0.003$ for both tests). Taken together, these results suggest that relative to *L. heterotoma*, *L. victoriae* is less effective in suppressing the $hop^{Tum\text{-}l}$ tumors and is also less efficient at protecting its eggs from encapsulation.

**Morphology of the long gland-reservoir complex**

*L. victoriae* females harbor the long-gland/reservoir complex equivalent to that described for *L. heterotoma* (Rizki and Rizki, 1984, 1990). We stained these structures with Hoechst 33258, a fluorescent nuclear dye and found that the long glands of *L. heterotoma* and *L. victoriae* are similar in size, but the anterior-most portion of the long gland, called the nose (N, Fig. 3a-d), of the *L. victoriae* gland is round, while that of the *L. heterotoma* gland is triangular (compare N in Fig. 3c and d). In both cases, the nose leads to the central, long gland lumen. A single "intimal" layer of cells (I, Fig. 3b) surrounds the lumen. A concentric layer of much larger, peripheral, presumably secretory cells surrounds the intimal layer and constitutes the body of the gland (S, Fig. 3b). In ultrastructual studies, we find that these cells contain extensive rough endoplasmic reticulum, characteristic of cells engaged in protein synthesis and secretion (Figs. 5a and 6a, below). Proximal to the ovipositor, the long gland narrows into a tube

called the connecting duct (CD, Fig. 3a, c), which opens into a wider reservoir. The reservoir lumen is largely acellular and has one layer of peripheral cells with flattened nuclei (R, Fig. 3c, e). The reservoir is connected to the ovipositor, the chitinous structure through which the female wasp injects her eggs into the *Drosophila* larva (O, Fig. 3a).

**_In vitro_ effects on host lamellocytes**

*In vivo*, *L. heterotoma* has stronger effects on the *Drosophila* host than does *L victoriae* (Fig. 1). To examine whether this difference might, in part, arise due to quantitative differences in the effects of wasp secretions, we compared directly the relative effects of fluid produced by the long gland-reservoir complex of these two wasps on lysis of host lamellocytes. Previous studies have demonstrated that *in vitro*, lamellocytes undergo reproducible changes in response to exposure to fluid from either wasp (Rizki and Rizki, 1990; Chiu and Govind, 2002). Cell morphology changes from round or oblong to bipolar. Bipolar cells then lose cytoplasm at the tips and ultimately die. Furthermore, the reservoir fluid from *L. heterotoma*, that is responsible for lamellocyte lysis *in vitro,* is heat sensitive (Rizki and Rizki, 1990). This suggests that one or more component mediating lamellocyte lysis may be proteinaceous in nature. To determine if *L. heterotoma* fluid induces lamellocyte lysis more rapidly than does fluid from *L. victoriae*, we introduced wasp fluid containing equal concentrations of total protein on hemocytes of $hop^{Tum\text{-}l}$ male larvae *in vitro*, and monitored the morphological changes induced over a six-hour period. At time zero, lamellocytes are the largest cells in culture, shaped roughly oval or oblong, flattened against the bottom of the dish (Fig.

4a). Nuclei with prominent nucleoli are often visible. Plasmatocytes in contrast are smaller, rounder, and have cytoplasm that appears granular (Fig. 4c). In two experiments testing different protein amounts of wasp fluid on hemocyte cultures, lamellocytes underwent the morphological changes typically observed in response to infection, becoming bipolar (Fig. 4b). In both experiments, *L. heterotoma* fluid had a significantly stronger effect earlier than *L. victoriae* fluid, with morphological changes first apparent within 4 hours after application of the fluid (Fig. 4d, e, and legend). These *in vitro* results parallel the differential effects of *L. heterotoma* and *L. victoriae* infection on melanotic tumors of $hop^{Tum\text{-}l}$. Thus, *L. heterotoma* suppresses melanotic tumors more strongly *in vivo* (Fig. 1) and its fluid acts faster on host cells in culture.

**Biogenesis of VLPs occurs in secretory cells of the long gland**

To examine the structure of immature and mature *L. victoriae* VLPs at high resolution and to compare their morphology with that of *L. heterotoma* VLPs described before (Rizki and Rizki, 1990), we prepared ultrathin sections of the long gland and reservoir at locations 1-5, indicated in Fig. 3a. Electron dense structures, resembling immature VLPs, are first apparent in the large secretory cells just below the nose region (position "1", Fig. 3a; Fig. 5a). The example in Fig 5a harbors a large nucleus (Nu; Fig. 5a) and the extensive rough ER and Golgi apparatus typical of an animal cell engaged in protein synthesis (Fig. 5e-g) Adjacent secretory cells are held together by desmosome-like structures, with electron-dense plaque on the cytoplasmic face (Fig. 5c). We were surprised to find specialized canal-like structures (Fig. 5a, C) within the cytoplasm, with immature, membrane-bound structures that we refer to as VLP

precursors (Fig. 5b, VLPp; Fg. 5j). The canal-like structures are surrounded by cylindrical membrane processes, with microvilli-like appearance. These invaginations give the canals a rough appearance (Fig. 5 b, d, i, k). We therefore refer to these canals as "rough" canals. Closer to the long gland lumen, the rough canals (RC) abruptly transition into canals that are not surrounded by membranous processes, but which also contain VLP precursors (Fig. 5l, bracket). The smooth canals (SC) are continuous with the long gland lumen (Fig. 5o), presumably emptying their contents, including the VLP precursors, into the lumen.

As noted above, a thin layer of intimal cells resides between the lumen and the secretory cells (Fig. 3b and 5h). Sections along the long gland revealed that the rough/smooth canals that emerge from the secretory cells into the lumen traverse through cells of the intimal layer (Fig. 5m, n, o) at position "1" (Fig. 3a) as well as more proximally (not shown). Many immature VLP precursors that are morphologically similar to structures in the rough canals, are also similar to structures present within the smooth canals and in the lumen of the long gland (Fig. 5i-l, p). Two populations of VLP precursors are observed in the lumen at position "1". Particles in the first class are spherical and 88.25 $\pm$ 16.59 nm in diameter (n = 12). These are the smallest precursors observed in our studies. The second class of particles has a more complex morphology with spherical structures (88.90 $\pm$ 15.05 nm; n = 20) connected to each other by electron dense linkers or segments, 98.10 $\pm$ 17.56 nm in length (n = 20). As many as five spherical structures can be observed within one such VLP precursor (Fig. 5p). Relative to each other, the segments and spheres are arranged in a regular geometric order, suggesting that this is the first step in the extracellular subassembly of the precursors.

**Subassembly of VLP continues within the long gland lumen**

Next, we consider VLP morphology at position "2" of the long gland, where the diameter of the long gland lumen is narrower than at position "1" (Fig. 3a for orientation). The secretory cells (S) in this region also contain protein components of VLP precursors (Fig. 6a). These cells possess the rough/smooth canal complex through which secretory products are delivered into the long gland lumen, much like that described for anterior region at position "1". The smooth canal negotiates through the cell of the intimal layer (not shown). Electron dense spherical VLP precursors (roughly 90 nm in diameter) are also observed within these canals (Fig. 6b), as are electron-dense structures containing electron-light vesicles (Fig. 6b, white arrowhead). A third kind of structure consists of electron dense spheres, variable in volume (Fig. 6a, c, d, black arrowhead). The significance of these latter two types of structures is not known.

Within the long gland lumen at position "2", VLP precursors begin to self-assemble to yield particles that are morphologically more diverse and complex than VLP precursors in the lumen at position "1" (Fig. 6d, Table 1). Some particles exhibit projections extending away from the core and acentric vesicles within the VLP core (compare Fig. 6d with Fig. 5p). These VLP intermediates appear to be surrounded by a lipid bilayer. At higher magnification, VLPs in the lumen show distinct stages of sub-assembly. Five subclasses of morphologically different intermediates are recognized. VLP cores of the first four subclasses are electron-light (Fig. 6e-h), whereas the core of VLPs in the last subclass is electron-dense (Fig. 6i-k and Table 1). VLP intermediates in subclasses I (Fig. 6e) and II (Fig. 6f) have semicircular or circular electron dense

segments that end in spherical structures (Fig. 6e, f, stars). VLP intermediates in classes III (Fig. 6g) and IV (Fig. 6h) exhibit peripheral electron-dense projections (Fig. 6g, h, arrows). In the fifth subclass of VLP intermediates, the VLP core is electron-dense and some particles contain one or more electron-light vesicles within them (Fig. 6i, j, k, arrowheads).

Various dimensions of these VLP intermediates were measured as described in Fig. 7j-l. Averages are shown in Table 1. Several points are worth noting. (1) The overall average size of the VLP intermediates is 280 nm. (2) The average diameter of the spherical electron-dense spherical structures (Fig. 6e-j, asterisks) in all five subclasses is 96.74 nm $\pm$ 10.37 nm (n = 27). This dimension is in the same size range as spherical VLP precursors in region "1" (roughly 90 nm; see previous section). (3) The average lengths of electron-dense projections in VLP intermediates of subclasses III and IV are very similar (130.1 and 137.2 nm; see arrows, Fig. 6g, h). The equivalent structures in the subclass V intermediates (Fig. 6j, k arrows), however, are significantly shorter, less than 50 nm (Table 1). (4) Electron-dense cores and vesicles appear to be retained during the next stages of VLP biogenesis and differentiation.

**Structures of maturing and mature VLPs**

At positions "3" and "4", biogenesis of VLPs progresses; VLPs appear embedded in electron-light matrix (Fig. 6l-p). At high magnification (Fig. 6n-o), Sectioned VLPs appear stellate, are 263 $\pm$ 38.91 nm in diameter (n = 10), with five or more vertices from which short spikes emanate. Vesicles are occasionally observed in the core of these VLPs.

At position "5", the reservoir contains single VLPs or arrays of VLPs that are clearly surrounded by a lipid bilayer. VLP arrays observed contain 1-6 particles (Fig. 7c-d). At this stage of biogenesis, the average diameter of the VLP core is more than 300 nm (Fig. 7a-d, Table 2). The VLP cores are segmented by, what appear to be double, parallel lipid bilayers, dividing them into equal or unequal segments (Fig. 7 a-d, arrows; 7o; Table 2). The segmenting bilayers merge with the surrounding electron-light matrix. In spite of the clustered arrangement of the VLPs and the segmented nature of the core, individual VLPs are distinct. The cores of some VLPs in the reservoir contain electron-light vesicles (Fig. 7c, d, arrowheads). Only two of the eight solitary VLPs studied in detail contained vesicles, whereas 7 of the 13 VLPs present in the four clusters analyzed in detail possessed 1-2 vesicles. These vesicles were variable in size (Table 2) and appeared circular or oblong in sections.

Sections of mature VLPs prepared after gradient purification are pentagonal or hexagonal in shape and have a roughly 300 nm core diameter (Table 3). The core of these particles extends into 5-6 electron-light spikes. In a few sections, round knobs are present at the termini of spikes (Fig. 7h, i, arrows). These knobs are more clearly visible in scanning electron micrographs (Fig. 7e, f). These knobs are adhesive and may mediate interactions between VLPs (Fig. 7e) and between VLPs and lamellocytes (data not shown). The angles between two adjacent sides range from 91-127° for pentagons and 97-139° for hexagons. The distance between termini of spikes that extend from opposing vertices exceeds 500 nm.

## DISCUSSION

Like *L. heterotoma*, the endoparasitoid *L. victoriae* is extremely successful at subduing the immune responses of its host *Drosophila melanogaster*. Previous work from our laboratory (Chiu and Govind, 2002) has shown that infection of *D. melanogaster* by *L. victoriae* or *L. heterotoma* leads to depletion of the cells in the larval lymph glands. These glands harbor precursors of mature immune effector cells – lamellocytes and crystal cells – the cells responsible for encapsulation and melanization of wasp eggs (Lanot *et al.*, 2001; Sorrentino *et al.*, 2002). Destruction of the precursor population is likely to underlie the absence of new lamellocytes and crystal cells in infected larvae, and also the failure of encapsulation of the wasp egg. Additional mechanisms of immune suppression have been observed *in vitro*, for both wasp species. These include the ability of wasp fluid to induce apoptosis of plasmatocytes in culture (Chiu and Govind, 2002) and lamellocyte lysis by mechanisms not involving programmed cell death (Rizki and Rizki, 1990; 1992; Chiu and Govind, 2002). Thus, a variety of strategies are involved in deleting the cellular immune responses of the host and it appears that a combination of strategies is responsible for the high degree of virulence exerted by both *L. heterotoma* and *L. victoriae*.

### Steps in *L. victoriae* VLP biogenesis

In this study, we provide evidence for the existence of *L. victoriae* VLPs within the long gland-reservoir complex, an organ associated with ovaries. The VLP structure in mature *L. victoriae* wasps reveals significant similarities with VLPs produced by *L. heterotoma*. Our observations outline four steps in VLP biogenesis and morphogenesis.

The first three of these occur in the long gland, whereas the final event takes place in the reservoir. (1) VLP precursors are secreted from the secretory cells as 90 nm electron dense spheres. VLPs move into the lumen via novel structures connecting secretory cells and lumen. We have found very similar, previously-undescribed canals in the *L. heterotoma* long glands as well (Morales and Govind, unpublished results). (2) Once in the lumen, VLP precursors appear to be linked to each other via straight or curved electron-dense segments to form larger intermediates with electron-light cores and peripheral electron-dense projections. (3) The internal VLP core becomes electron dense and may contain one or more electron-light vesicles. (4) VLPs in the reservoir, either singly or in arrays, undergo additional morphogenesis. The particles, surrounded by one lipid bilayer are also intersected with bilayers, dividing the VLP core into segments.

Virus-like particles from *L. heterotoma* were first described by Rizki and Rizki (1990, 1994). Like the *L. victoriae* VLPs, *L. heterotoma* VLPs are produced in the long gland lumen. Gradient-purified VLPs have an electron-dense, asymmetric coat with surface projections. Recently, we have also analyzed *L. heterotoma* VLP structure and biogenesis (Morales and Govind, unpublished results; see also below). Our studies of VLPs from both wasp species extend the earlier findings of the Rizkis (Rizki and Rizki, 1990; 1994), and provide a comprehensive view of the biogenesis of *L. victoriae* and *L. heterotoma* VLPs. Several new insights emerge from our observations reported here: First, VLP precursors, synthesized in the long gland secretory cells are secreted into the rough-smooth canal structures and are deposited into the long gland lumen. Second, the long gland lumen, site of VLP subassembly, contains VLPs in a variety of progressive stages of assembly. Small vesicles within some VLPs are observed during biogenesis

and these vesicles appear to be retained through maturation. Third, the reservoir lumen contains segmented, single VLPs or VLP clusters. The significance of the segmented VLP morphology and of the arrangement of maturing VLPs in the reservoir matrix is not understood. Finally, mature isolated particles have a pentagonal/hexagonal core, with multiple spikes. The size of the mature VLP from one end to another exceeds 500 nm. VLPs are deposited into host hemocoel as single or composite particles. In other studies, we have found that the particles interact with each other and with host hemocytes via spike ends (Morales and Govind, unpublished results). Given the close phylogenetic relationship between these species, the parallels between *L. heterotoma* and *L. victoriae* VLP structure and biogenesis are not surprising; nevertheless, they raise interesting questions about the similarities and differences in the two wasps' virulence on different hosts.

**Differences in virulence in *D. melanogaster***

Despite the structural similarities between *L. victoriae* and *L. heterotoma* VLPs, we note clear and measurable differences between virulence of these parasitic wasps. Using an established *in vivo* bioassay of mutant hosts, we show that infection by *L. victoriae* suppresses constitutive melanotic tumor formation (encapsulation) of self-tissue in $hop^{Tum\text{-}l}$ hosts, but this suppression is not as strong as that seen after infection by *L. heterotoma*. In other words, the immune-competent mutant $hop^{Tum\text{-}l}$ strain is more successful at defending itself against *L. victoriae* than against *L. heterotoma*. The high encapsulation level of *L. victoriae* eggs (relative to *L. heterotoma* eggs) by the $hop^{Tum\text{-}l}$ strain (Fig. 1) suggests that *L. victoriae* cannot suppress the cellular encapsulation

response triggered in the "supercompetent" *hop*$^{Tum\text{-}l}$ strain. The differences in virulence in the melanotic tumor suppression assay can be explained in part by differences in the rates at which virulence factors of the two species destroy the host immune cells. First, *L. victoriae* infection brings about apoptosis of lymph gland cells at a slower rate than does *L. heterotoma* infection. Both lymph gland atrophy and the appearance of TUNEL positive cells are seen 24 hours earlier in larvae infected with *L. heterotoma* than in those infected with *L. victoriae* (Chiu and Govind, 2002). Second, the present study demonstrates that primary cultures of lamellocytes undergo morphological transformations more rapidly when treated with VLP-containing *L. heterotoma* than with *L. victoriae* fluid (Fig. 4). Whether this difference is due to the *heterotoma* species containing more VLPs per gland, the *heterotoma* VLPs being individually more effective, or an unidentified factor in the wasp fluid, remains to be determined. The difference in relative virulence of the two wasp strains is likely to, at least in part, reflect differences in molecular affinities between VLPs and their receptors on target cells in the host. As outlined below, we have begun pursuing this question by examining the molecular mechanisms that underlie the VLP attack on the host immune system.

We have identified major protein components of the VLPs of both wasp species (Govind *et al.*, unpublished results). In *L. victoriae*, an abundant 47.5 kDa protein is localized to the VLP surface, including the spikes. In *L. heterotoma*, a 40 kDa protein shows a similar distribution. Significantly, antibodies to p40 cross react with *L. victoriae* VLPs in addition to staining *L. heterotoma* VLPs and their precursors. Cross reactivity suggests conservation of molecular structure and possibly also of the molecular mechanism of virulence within the sister species. Our studies demonstrate functional

(introduction of VLP with egg in both cases), morphological (VLP core plus spike structure) and molecular (similarities in major proteins) shared derived traits in these two species of parasitic wasps. The existence of such shared derived traits suggests that the mechanism of virulence in these closely related sister species evolved prior to or during speciation and that differences in their virulence may reflect differences in their natural host range.

**Evolution of virus like particles in *Leptopilina***

The genus *Leptopilina* has three species groups (the *longipe*s group, the *heterotoma* group and the *boulardi* group). Molecular and morphological phylogenetic studies have revealed the relationships of the species within these groups (Schithuizen *et al.*, 1998). To date, immune-suppressive virus-like particles have been described from species of the latter two groups. These VLPs are introduced into the host hemocoel during oviposition, and are considered to be non-infectious as there is no indication of lateral transmission of VLPs neither from one infected host to another nor from one individual wasp to another. Females of specific *Leptopilina* strains studied to date appear to produce VLPs of the same morphology. Because the VLP phenotype exhibits high penetrance and expressivity in morphology and function, it is reasonable to assume that genetic information housed within the wasp genome dictates to some extent the consistent degree of host immune suppression observed in different strains. Our studies showing similarities in the morphologies and modes of action of *L. heterotoma* and *L. victoriae* VLPs and corresponding differences with *L. boulardi* VLPs (Dupas *et al.*, 1996; Labrosse *et al.*, 2003; see Introduction) demonstrate for the first time that VLPs

from closely-related *Leptopilina* species are morphologically and functionally more similar to each other than to those found in distantly-related wasps. Studies by others have shown that closely-related braconid parasitoids carry morphologically similar immune-suppressive polydnaviruses (see Whitfield and Asgari, 2003 and primary references therein). As a result of these and other observations, it has recently been proposed that polydnaviruses can be conceptualized as character states of their wasps and not as separate life forms (Fedirici and Bigot 2003; Whitfield and Asgari, 2003; Drezen *et al.*, 2003). These authors suggest that the evolution and function of polydnaviruses be considered almost entirely within the context of their wasps. Our studies here are consistent with this idea and suggest that the relationships of *Leptopilina* species and their VLPs will broaden our insights into the evolutionary relationships between parasitoid wasps and their viruses/VLPs in general. Unlike the polydnaviruses, where the presence and function of DNA in immune suppression has been established (Webb, 1998; Turnbull and Webb, 2002), it is still not known if VLPs from the *Leptopilina* species harbor functional nucleic acid. Future studies in this respect as well as investigating VLP morphologies in additional *Leptopilina* species will have a great impact in elucidating patterns and processes of the evolution of virulence in this clade.

## ACKNOWLEDGEMENTS

We dedicate this paper to the contributions of Drs. Rose and Tahir Rizki whose work on *L. heterotoma* VLPs guided our findings described here. We are grateful to Drs. J.J.M. van Alphen and P. Chabora for sharing the *L. victoriae* and *L. heterotoma* strains, respectively. We specially thank Dr. G. Nordlander, who suggested studying immune suppression in *L. victoriae* and Drs. John Lee and R. Nehm for stimulating discussions. This work was supported by grants from American Heart Association, Heritage Affiliate, Inc., American Cancer Society RPG 98-228-01-DDC and NIGMS S06 GM08168. Support from NIH-RCMI RR03060, and PSC-CUNY is also gratefully acknowledged.

## REFERENCES

Asgari, S., Theopold, U., Wellby, C., Schmidt, O. 1998. A protein with protective properties against cellular defense reactions in insects. Proceedings of the National Academy of Sciences. USA 95, 3690-3695.

Carton, Y., Frey, F., Nappi, A. 1992. Genetic determinism of the cellular immune reaction in *Drosophila melanogaster*. Heredity 69, 393-399.

Carton, Y., Nappi, A.J. 1997. *Drosophila* cellular immunity against parasitoids. Parasitology Today 13, 218-227.

Chiu, H.L., Sorrentino, R.P., Govind, S. 2001. Suppression of the *Drosophila* cellular immune response by *Ganaspis xanthopoda*. Advances in Experimental Medicine and Biology 484, 161-167.

Chiu, H.L., Govind, S. 2002. Natural infection of *D. melanogaster* by virulent parasitic wasps induces apoptotic depletion of hematopoietic precursors. Cell Death and Differerentiation 12, 1379-1381.

Dawson, B., Trapp, R.G. 2004. *Basic and Clinical Biostatistics*. Fourth Edition, McGraw Hill, New York.

Dupas, S., Brehelin, M., Frey, F., Carton, Y. 1996. Immune suppressive virus-like particles in a *Drosophila* parasitoid: significance of their intraspecific morphological variations. Parasitology 113, 207-212.

Dupas, S., Frey, F., Carton, Y. 1998. A single parasitoid segregating factor controls immune suppression in Drosophila. Journal of Heredity 89, 306-311.

Federici, B.A., Bigot, Y. 2003. Origin and evolution of polydnaviruses by symbiogenesis of insect DNA viruses in endoparasitic wasps. Journal of Insect Physiology 49, 419-432.

Hanratty, W.P., Dearolf, C.R. 1993. The *Drosophila* Tumorous-lethal hematopoietic oncogene is a dominant mutation in the hopscotch locus. Molecular and General Genetics 238, 33-37.

Labrosse, C., Carton, Y., Dubuffet, A., Drezen, J.M., Poirie, M. 2003. Active suppression of D. melanogaster immune response by long gland products of the parasitic wasp *Leptopilina boulardi*. Journal of Insect Physiology 49, 513-522.

Lanot, R., Zachary, D., Holder, F., Meister, M. 2001. Post-embryonic hematopoiesis in *Drosophila*. Developmental Biololgy 230, 243-257.

Nappi, A.J. 1975. Inhibition by parasites of melanotic tumor formation in *Drosophila melangaster*. Nature 255, 402-404.

Nappi, A.J., Kmiecik, J., Silvers, M. 1984. Cellular immune competence of a *Drosophila* mutant with neoplastic hematopoietic organs. Journal of Invertebrate Pathology 44, 220-227.

Nappi A.J., Vass, E. 2001. Cytotoxic reactions associated with insect immunity. Advances in Experimental Medicine and Biology 484: 329-348.

Rizki, R.M., Rizki, T.M. 1984. Selective destruction of a host blood cell type by a parasitoid wasp. Proceedings of the National Academy of Sciences USA 81, 6154-6158.

Rizki, T.M., Rizki, R.M. 1984a. The cellular defense system of *Drosophila melanogaster*. *In* Insect Ultrastructure. Vol 2. R.C. King, and H. Akai, editors. Plenum Publishing, New York. 579-604.

Rizki, T. M., and Rizki, R. M. 1986. Surface changes on hemocytes during encapsulation in *Drosophila melanogaster* Meigen. *In* "Hemocytic and Humoral Immunity Immunity in Arthropods.: (A. P. Gupta, Ed) pp157-190. Wiley, New York.

Rizki, T.M., Rizki, R.M., Carton. Y. 1990. *Leptopilina heterotoma* and *L. boulardi*: Strategies to avoid cellular defense responses in Drosophila melanogaster. Exp. Parasitol. 70, 466-475.

Rizki, R. M., and Rizki, T. M. 1990. Parasitoid virus-like particles destroy *Drosophila* cellular immunity. Proceedings of the National Academy of Sciences USA 87, 8388-8392.

Rizki, R.M., Rizki, T.M. 1991. Effects of lamellolysin from a parasitoid wasp on *Drosophila* blood cells in vitro. Journal of Experimental Zoology 257, 236-244.

Rizki, T.M., Rizki, R.M. 1992. Lamellocyte differentiation in *Drosophila* larvae parasitized by *Leptopilina*. Developmental and Comparative Immunology 16, 103-110.

Rizki, T.M., Rizki R.M. 1994. Parasitoid-induced cellular immune deficiency in *Drosophila*. Primordial Immunity: Foundations for the Vertebrate Immune system. Annals of the New York Academy of Sciences 712, 178-194.

Russo, J., Dupas, S., Frey, F., Carton, Y., Brehelin, M. 1996. Insect immunity: early events in the encapsulation process of parasitoid (*Leptopilina boulardi*) eggs in reactive and non reactive strains of *Drosophila*. Parasitology 112, 135-142.

Russo, J., Brehelin., Carton, Y. 2001. Haemocyte changes in resistant and susceptible strains of *D. melanogaster* caused by virulent and avirulent strains of the parasitic wasp *Leptopilina boulardi*. Journal of Insect Physiology 47, 167-172.

Schilthuizen, M., Nordlander, G., Stouthamer, R., van Alphen, J.J.M. 1998. Morphological and molecular phylogenetics in the genus *Leptopilina* (*Hymenopter*; *Cynipoidae*; *Eucoilidae*) Systematic Entomology 23, 253-264.

Schmidt, O., Theopold, U., Strand, M. 2001. Innate immunity and its evasion and suppression by hymenopteran endoparasitoids. BioEssays 23, 344-351.

Smith, P.K., Krohn, R.I., Hermanson, G.T., Mallia, A.K., Gartner, F.H., Provenzano, M.D., Fujimoto, E.K., Goeke, N.M., Olson, B.J., Klenk, D.C. 1985. Measurement of protein using bichinoic acid. Analytical Biochemistry 150, 76-85.

Sorrentino, R.P., Carton, Y., Govind, S. 2002. Cellular immune response to parasite infection in the *Drosophila* lymph gland is developmentally regulated. Developmental Biology 243, 65-80.

Sorrentino, R.P., Melk, J.P., Govind, S. 2004. Genetic contributions of dorsal group and JAK-Stat92E pathway genes to larval hemocyte concentration and the egg encapsulation response in *Drosophila*. Genetics 166, 1343-1356.

Turnbull, M., Webb, B. 2002. Perspectives on polydnavirus origins and evolution. Advances in Virus Research 58, 203-254.

Walker, I. 1959. Die abwehrreakion des wirtes *Drosophila melanogaster* gegen die zoophage cynipide *Pseudocoila bochei* Weld. Revue Suisse de Zoologie 66, 569-632.

Webb, B.A. 1998. Polydnavirus biology genome structure and evolution. In *The Insect Viruses*. Eds. Ball, E. A. & Miller, L. K. (Plenum Press, New York), pp. 105-139.

Whitfield, J.B. and Asgari, S. (2003) Virus or not? Phylogenetics of polydnaviruses and their wasp carriers. 49, 397-405.

**Table 1.** Measurements of dimensions of VLP intermediates at region "2" of the long gland lumen. See Fig. 3**a** for orientation relative to the entire long gland reservoir complex, Fig. 6**e-k** and Fig. 7 **j**, **k**, **l** for VLP morphologies and parameters measured, respectively. Five different morphological subclasses are described in the text. Intermediates in VLP subclasses I-IV have electron light cores (Table 1a); VLP intermediates in subclass V have electron dense cores and electron light vesicles (Table 1b). The number of VLP images from which measurements were made is indicated in column 2. Inner horizontal and vertical and outer horizontal and vertical dimensions for particles in subclasses II and III are as shown in Fig. 7**j** and **k**. Measurements for intermediates in subclasses I and IV were made similarly. Long and short diameters for VLP intermediates in subclass V, average vesicle dimension, length of the electron dense projections and diameter of the spheres were measured as shown in Fig. 7**l**. NA = not applicable.

Table 1a

| Morphological class | # VLP images | Inner vertical (nm) | Inner horizontal (nm) | Outer vertical (nm) | Outer horizontal (nm) | Diagonal (nm) | Electron-dense projections (nm) |
|---|---|---|---|---|---|---|---|
| I (Fig. 6e) | 4 | 137.09 ± 25.02 | 130.35 ± 35.0 | 278.50 ± 42.7 | 238.72 ± 38.12 | NA | NA |
| II (Fig. 6f) | 5 | 195.588 ± 37.718 | 165.177 ± 46.420 | 311.5924 ± 58.351 | 306.891 ± 45.789 | NA | NA |
| III (Fig. 6g) | 5 | 138.768 ± 15.429 | 135.765 ± 31.478 | 290.283 ± 55.010 | 270.330 ± 48.870 | NA | 130.10 ± 3.68 (n = 10) |
| IV (Fig. 6h) | 3 | 154.776 ± 49.442 | 140.841 ± 38.917 | 274.978 ± 39.412 | 243.786 ± 33.859 | 230.884 ± 26.338 | 137.23 ± 34.84 (n = 6) |

Table 1b

| Morphological class | VLP images | VLP long diameter (nm) | VLP short diameter (nm) | Internal vesicle diameter (nm) | Electron-dense projection |
|---|---|---|---|---|---|
| V (Fig. 6i-k) | 7 | 326.86 ± 68.85 | 266.76 ± 42.08 | 107.91 ± 41.66 | 46.87 ±18.09 (n = 12) |

**Table 2.** Measurements of dimensions of VLPs in reservoir (position "5" Fig. 3**a**, Fig. 7**b-d, o**). VLPs found singly showed simpler morphology. Side lengths and segment lengths were measured for eight solitary VLPs. The body of each VLP is bisected completely by lipid bilayers dividing the core into two segments. To determine the ratio of the segment diameters (S1, S2; Fig. 7**o**), only continuous lipid bilayers that crossed the VLP core from one end to the other were considered. This S2/S1 ratio ranged from 1.02 to 1.91 and the average ratio was 1.24. For VLPs in clusters, four clusters were examined, one cluster with two particles, two clusters with three particles each and one cluster with five particles. Vesicle dimensions are recorded as long and short diameters.

Table 2

| VLPs in group | # of images | # of VLPs | VLP diameter (nm) | Vesicle long diameter (nm) | Vesicle short diameter (nm) | Average side length |
|---|---|---|---|---|---|---|
| 1 | 8 | 8 | 351.06 ± 55.68 | 133.22 ± 40.91 | 110.08 ± 23.84 | 157.35 ± 18.70 |
| 2 to 5 | 4 | 12 | 361.28 ± 32.78 | 122.53 ± 25.65 | 68.14 ± 22.73 | Not determined |

**Table 3.** Measurements of dimensions of mature VLPs. Measurements of various parameters (Fig. 7**g-i**, **m**, **n**) were done from pentagonal and hexagonal VLP sections separately. (Table 3a) Average measurements for side length, diagonal length and spike length, and variation (standard deviation of the means) are indicated. The length of the spike is likely to be an underestimation as the termini and the knobs are electron light and not always visible. (Table 3b) Spike widths of 51 spikes arising from pentagons and hexagons were measured at a distance of 30 nm from the body of the VLPs. These spikes terminate in electron light knobs that are not always observed in transmission electron micrographs. The numbers of knobs for which measurements was made is therefore low (n = 9).

Table 3a

| VLP type | # of images | Average side length (nm) *[n]* | Average diagonal length (nm) *[n]* | Average spike length (nm) *[n]* |
|---|---|---|---|---|
| Pentagon | 11 | 175.09 ± 9.84 *[55]* | 282.53 ± 15.89 *[55]* | 73.19 ± 14.58 *[50]* |
| Hexagon | 10 | 170.59 ± 15.53 *[60]* | 309.64 ± 28.55 *[90]* | 84.369 ± 22.31 *[49]* |

Table 3b

| VLP type | Spike width (nm) *[n]* | Knob diameter (nm) *[n]* | Range of angles (degree) |
|---|---|---|---|
| Pentagon | 39.06 ± 6.71 *[51]* | 64.185 ± 22.33 *[5]* | 91-127 |
| Hexagon | 46.03 ± 8.02 *[51]* | 51.227 ± 12.33 *[4]* | 97- 139 |

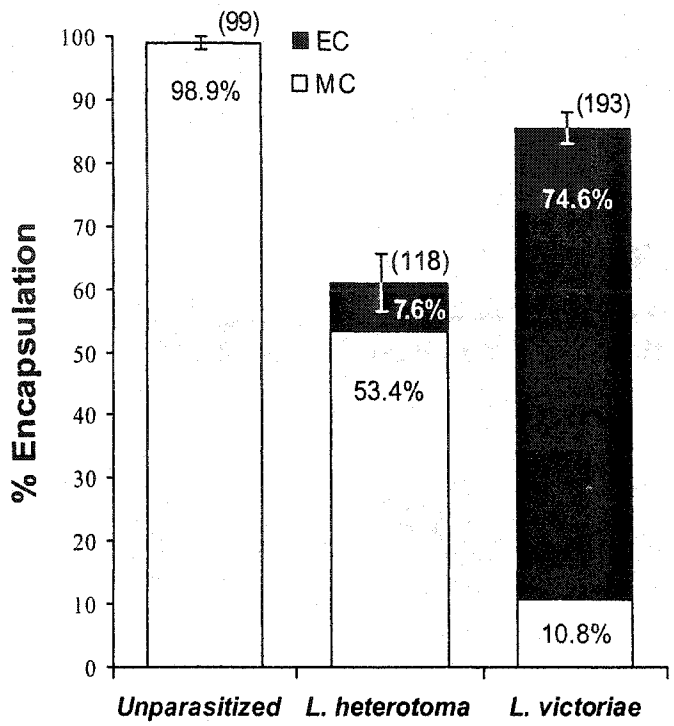


**Fig. 1.** Evidence for immune suppression *in vivo*. Percentage of 6-day-old *hopTum-l* larvae carrying either melanotic capsules (unparasitized controls) only, or melanotic capsules plus egg capsules, when parasitized by either *L. heterotoma* or *L. victoriae*. The breakdown of larvae carrying melanotic capsules only (MC) and those carrying egg capsules (EC, with or without melanotic capsules) is shown. Numbers of host larvae examined are atop each bar. The z value is 4.9 ($p < 0.003$) when total percentages (EC + MC) are compared between *L. heterotoma* and *L. victoriae*; $z = 8.2$ ($p < 0.003$) when melanotic capsules (MC) are compared, and $z = 11.5$ ($p < 0.003$) when egg capsules (EC) are compared.

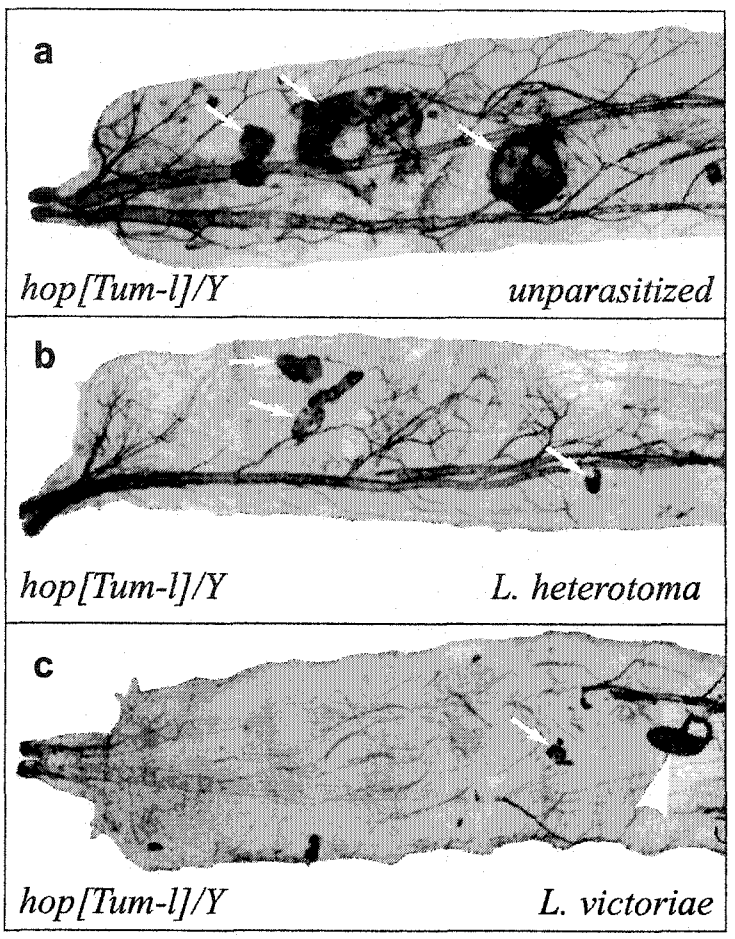


**Fig. 2.** Uninfected 6-day-old *hopTum-l* mutants (**a**) contain many more and larger melanotic tumors around self tissues than do mutants infected by *L. heterotoma* (**b**) or *L. victoriae* (**c**). White arrows indicate melanotic tumors, white arrowhead indicates an encapsulated egg of *L. victoriae*. The stalk of the egg is visible to the right.

**Fig. 3.** Morphology of the long gland-reservoir complex from *L. victoriae* (panels **a, b, d** and **e**) and *L. heterotoma* (panel **c**). Samples in panels **b-e** were stained with Hoechst 33258 to reveal size and position of nuclei. (**a**) Long gland (LG) is distal to the ovipositor, and is continuous with the reservoir (R) via the connecting duct (CD). The distal-most portion of the long gland, the nose (N) tapers into a tubular lumen (white arrow). On the proximal end (to the right in panel **a**), the reservoir opens into the ovipositor (O). Locations 1-5 (circled) indicate the positions from which sections were prepared for transmission electron microscopy. Positions 1, 2 and 3 are within the long gland. Position 4 is in the connecting duct, and position 5 is in the reservoir. (**b**) Combined phase and fluorescent view of the long gland revealing the morphology of the nose (N) and the long gland lumen. Large cells composing the main body of the gland are secretory (S) and contain a large nucleus. Cells of the intimal layer (I) are narrow and provide a lining to the long gland lumen (black arrowhead). (**c**) Organization of the long gland reservoir complex from *L. heterotoma*. (**d**) *L. victoriae* long gland for comparison with panel **c**. Note difference in nose morphology. (**e**) Higher magnification of surface of *L. victoriae* reservoir showing nuclei of cells surrounding the internal matrix. As in the reservoir of *L. heterotoma* (panel **c**), a single cell layer is found peripherally. Labeling for panels **b-e** is as described in panel **a**.

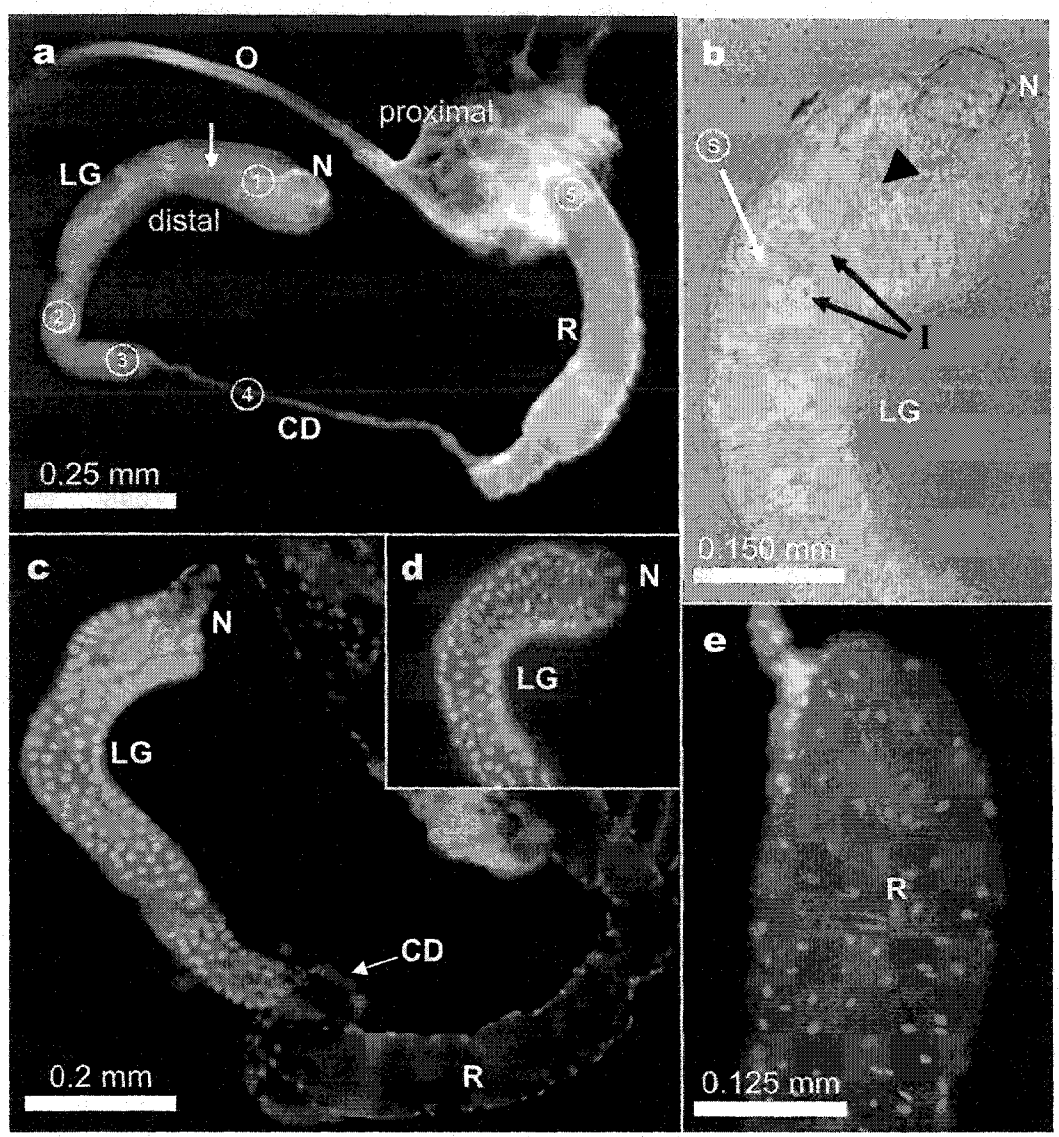

**Fig. 4.** (**a-c**) Morphology of *hopTum-l* lamellocytes after application of wasp fluid. Lamellocyte (L) with normal (**a**) or bipolar (**b**) morphology. (**c**) Other hemocytes are also observed in the field including round plasmatocytes (P), next to a bipolar lamellocyte (L). (**d**, **e**) Kinetics of bipolar cell formation after exposure to wasp fluid. Total protein concentration of wasp fluid used in the two experiments per aliquot of hemocytes was 20 mg (**d**) and 2.4 mg (**e**). Cellular morphology was scored manually and recording was staggered over time. For each time point, the number of lamellocytes included in the observations is indicated along with the standard error bars. Pair-wise comparisons were done in separate *z* tests for each time point. At the second time point in the experiment shown in panel **d** (3-4 h), values of *L. heterotoma* versus *L. victoriae*, and *L. heterotoma* versus control, are significantly different ($p < 0.003$), whereas values for *L. victoriae* versus control are different at $p = 0.096$. By six hours, all three pair-wise comparisons are significantly different ($p < 0.003$). In the experiment shown in panel e (lower protein concentration), all three pair-wise comparisons are statistically significant ($p < 0.05$) by 3-4 hours after the addition of the fluid. By six hours, the difference between *L. victoriae* /*L. heterotoma* versus control values are statistically significant ($p = 0.007$, $p < 0.003$ respectively). This difference is not significant when values for *L. victoriae* and *L. heterotoma* are compared with each other ($p = 0.162$).

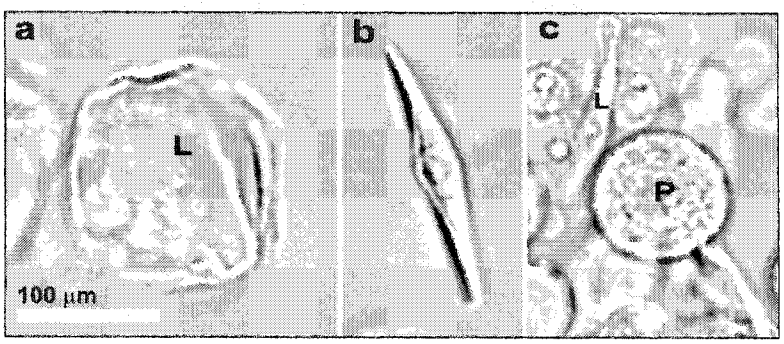


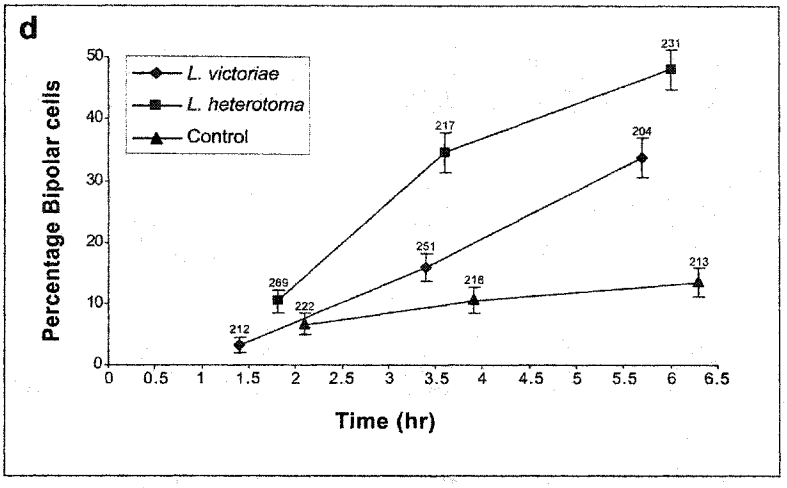


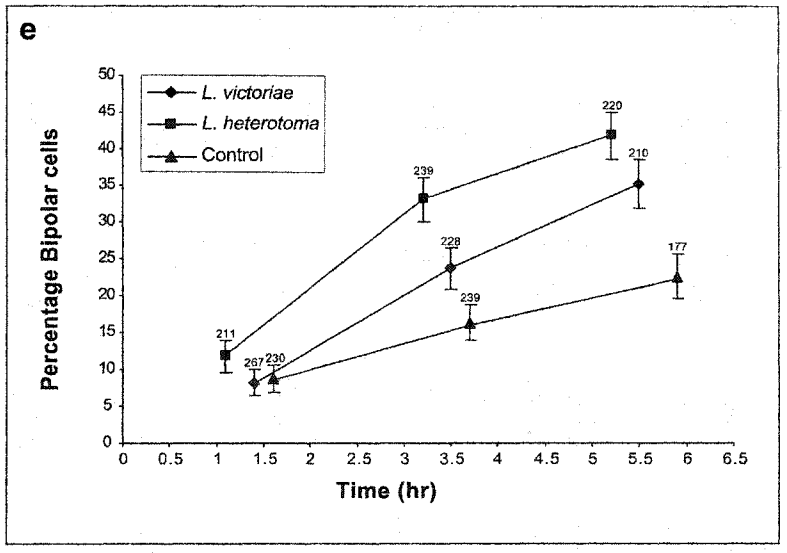

**Fig. 5.** Fine structure of the long gland from region "1" of the long gland reservoir complex. (a) Electron micrograph of a portion of a large secretory cell (S) with portion of the cytoplasm and a nucleus (Nu). An electron-light canal (C) that contains VLP precursors can be seen in the cytoplasm. The canals protrude through the cells of the intimal layer (I), to open into the long gland lumen (L). VLP precursors (VLPp) are also observed in the lumen. Nuclei of cells of the intimal layer are much smaller (N, top right of panel a) than the nuclei of secretory cells (Nu, top left of panel a). (b, d) Cross-section of a rough canal (RC) found within a secretory cell. Spherical VLP precursors are first observed in these rough canals (panel b). (c) Electron-dense structures similar to desmosomes are present between adjacent secretory cells. (d) Higher magnification shows extensive, microvilli-like, cylindrical processes in the rough canal. (e-g) Higher magnification of cytoplasm of a secretory cell shows a mitochondrion (M), nucleus (Nu), rough endoplasmic reticulum (box in panel e, enlargement in panel f) and the Golgi apparatus (panel g). (h) Enlarged section of a cell of the intimal layer (I, its nucleus, N), which is adjacent to a secretory cell (S) and the long gland lumen (L). Lumen has VLP precursors. (j) High magnification view of a membrane-bound VLP precursor within the rough canal. (i-p) Delivery of VLP precursors from secretory cells (S) into the lumen (L) occurs via the rough (i-l) and smooth canals (l-o). (i-k) Two classes of VLP precursors, spherical particles with or without linkers, are observed. (l) A clear transition from rough (RC) to smooth canal (SC) structure is observed within a secretory cell. A bracket indicates transition zone. (m-o) Smooth canals (SC) are observed to traverse through the narrow cells of the intimal layer. Intimal cell nucleus (N) is identified in panels m-o. In each of these panels, secretory cell is to the left, long gland lumen (L) to the right. Smooth canals (SC, longitudinal sections, panels m, o) negotiate through the intimal layer cell (I). The cytoplasm of the intimal layer cell is seen surrounding the smooth canal (panel n). (p) Spherical particles with or without linkers, also seen in the rough canals (panel k), are observed in the long gland lumen (L).

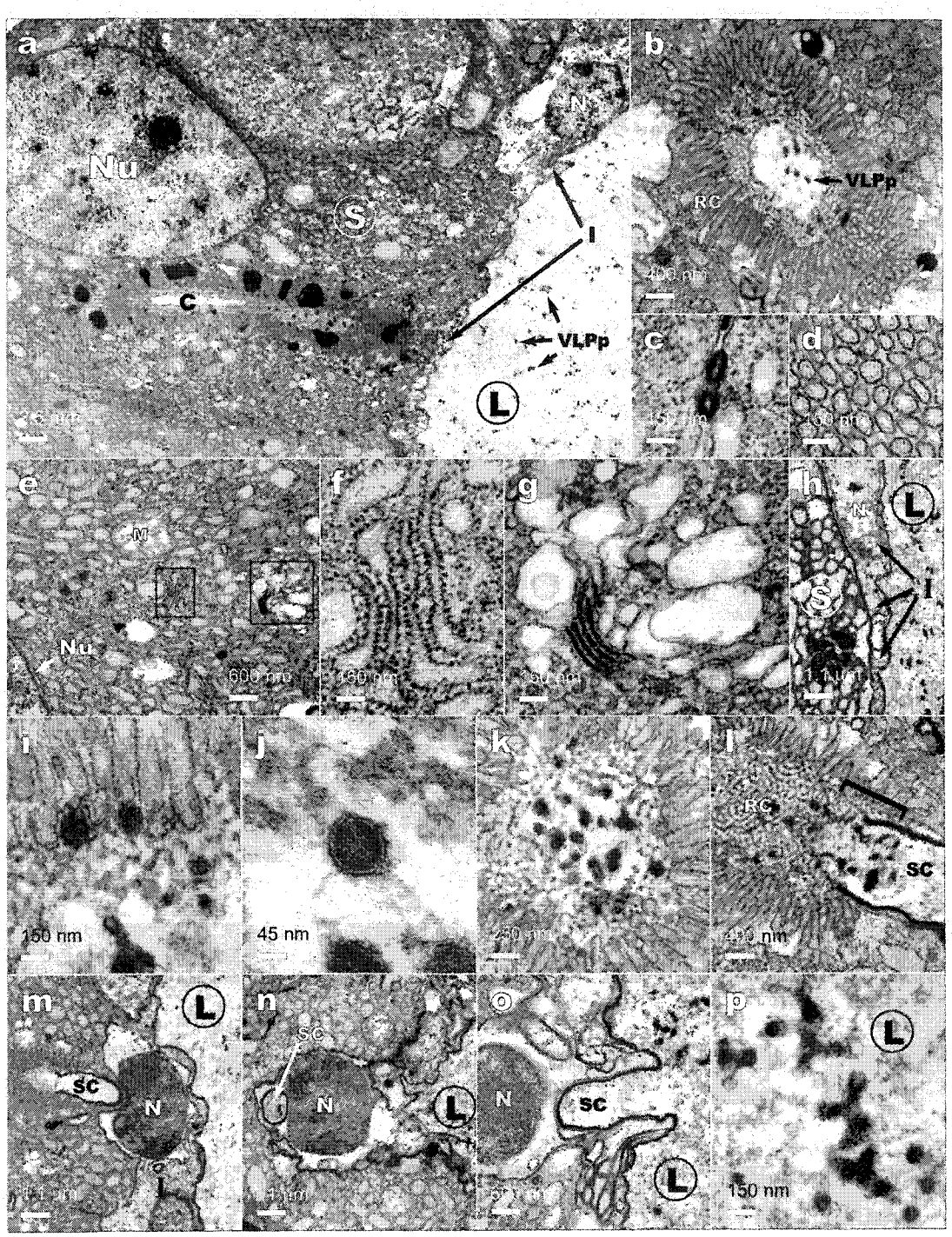

**Fig. 6.** Fine structure of the *L. victoriae* long gland from region "2" (**a-k**) and region "3" (**l-o**) of the long gland reservoir complex. **(a)** Secretory cells (S), adjacent to the long gland lumen (L). The lumen contains VLP precursors (VLPp). In addition, electron-dense spheres of variable diameter (black arrowheads) are observed. **(b)** Higher magnification of a secretory cell with cross section of rough canal (RC). Notice invaginated membrane around the circumference of the rough canal and presence of VLP precursors (VLPp). Also notice electron-dense structures with electron-light vesicles (white arrowheads) along the membrane invaginations. **(c)** Large spherical, electron-dense spheres (arrowhead) are also found within the rough canal. **(d)** A number of immature VLPs in the long gland lumen (L) at low magnification. **(e-h)** VLPs in the lumen, at higher magnification. Different stages of sub-assembly are evident. **(e-g)** High magnification view of VLPs undergoing or completing circularization. Spherical structures (asterisk) are at the termini (**e**, subclass I) or also in the vicinity of the VLP intermediate (**f**, subclass II). **(g, h)** Some intermediate particles (subclasses III and IV) assume an electron-light circular core and have electron-dense projections (arrows in **g, h**) extending outward from the core. Extensions terminate in spheres (asterisks). **(i-k)** Class V membrane-bound VLP intermediates have shorter electron-dense projections (arrows) that terminate in spheres (asterisks), and electron-dense cores, with electron-light vesicles (arrowheads in panels **i-k**). Samples in panels **l-o** were prepared from region "3", just anterior to the connecting duct. The margins of the lumen (L) are visible (arrows). **(m)** VLPs (arrows) appear to be embedded in electron-light matrix (M). **(n, o)** At higher magnification, VLPs appear stellate and angular, with five or more vertices from which projections emerge. **(p)** Cross section of the narrow interconnecting duct in region "4". VLPs (arrows) occupy this region as they move into the reservoir.

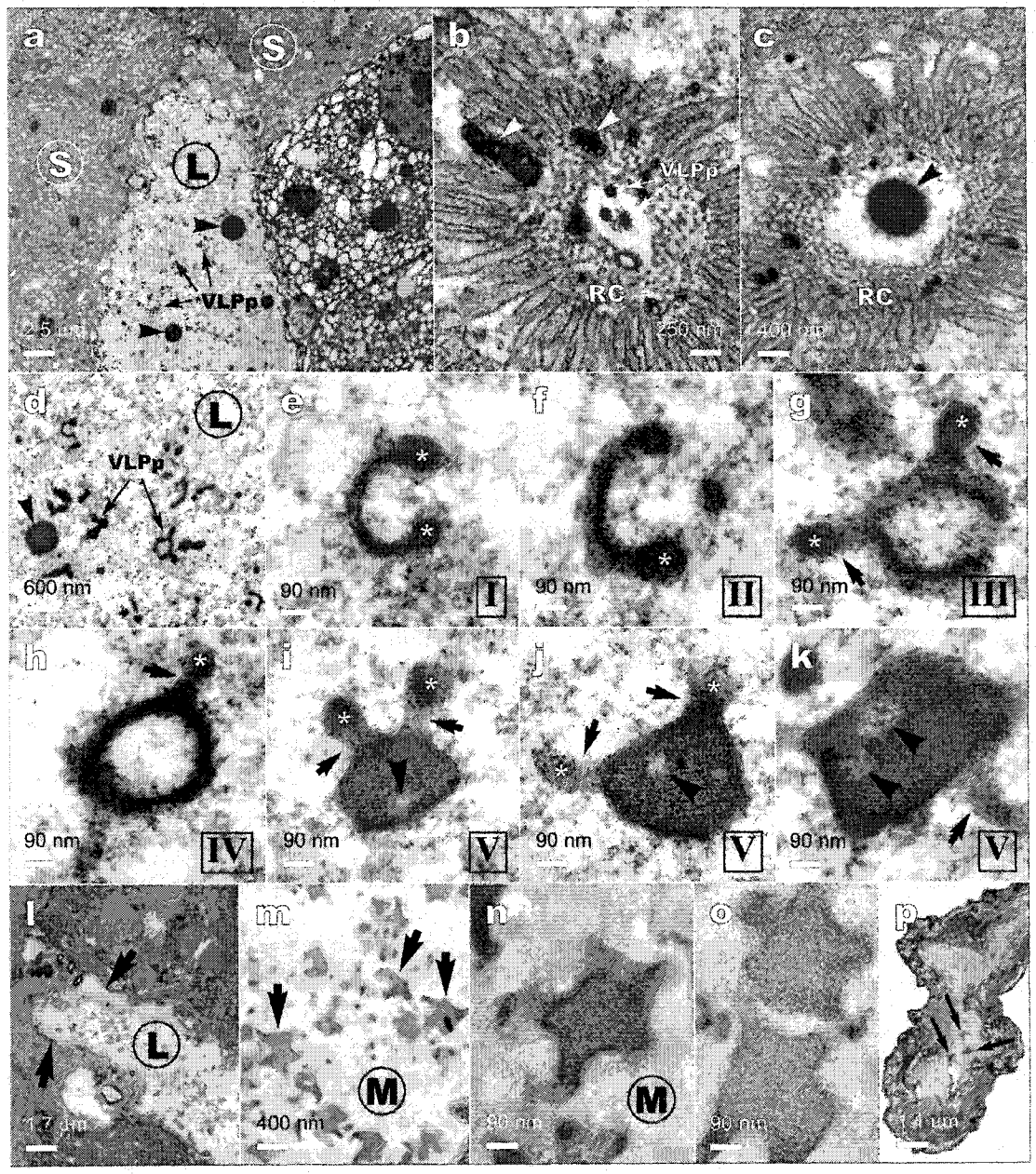

**Fig. 7.** (**a-d**) Transmission electron micrographs of VLPs in the reservoir (region 5). (**a**) Maturing VLPs (arrows) are arrayed in electron light matrix (M). VLPs are found singly (**b**) or in clusters of 2-6 particles (**c, d**). The VLP core is segmented by one or more lipid bilayers (arrows, b, **c, d**). Vesicles are also visible in some VLPs (arrowheads, **c**, **d**). (**e, f**) Scanning electron micrographs of *L. victoriae* VLPs. In (**e**), a cluster of 10-20 VLPs is shown. In (**f**), a single particle from the gradient-purified preparation is shown at higher magnification. Both VLP preparations show typical stellate morphology and spiky projections tipped by knobs. (**g-i**) Sections through mature particles may show five (**g, h**) or six (**i**) sides in sections. The section in panel **g** passes through a large vesicle (arrowhead), whereas those in panels **h** and **i** do not. Knobs are present at the ends of spikes (arrows in **h**, **i**). (**j-o**) White lines indicate various dimensions measured. The diameters of spherical structures in section were measured using the circle function (**j**, **k**, **l**). VLPs in intermediate stages of assembly (**j**, **k**) were measured as shown: inner or outer vertical, or inner or outer horizontal diameters (Table 1). The diameters of irregular structures (VLP cores, vesicles, or knobs panels; **l, n, o**) were averaged using the line function from one point to another as indicated (averages of more than six measurements were made; only two are shown for illustration). (**m**, **n**) Sides, diameter, spike lengths and angles were measured for pentagonal and hexagonal sections of mature particles as illustrated. Spike width was measured 30 nm away from the vertices. Data are summarized in Table 3. (**o**) The length of the sides of VLPs in reservoir was averaged for solitary particles as indicated. The relative segment sizes of the core were computed by measuring S1, S2 (heavy lines) and dividing the length of the longer segment (S2) by that of the shorter one (S1, Table 2).

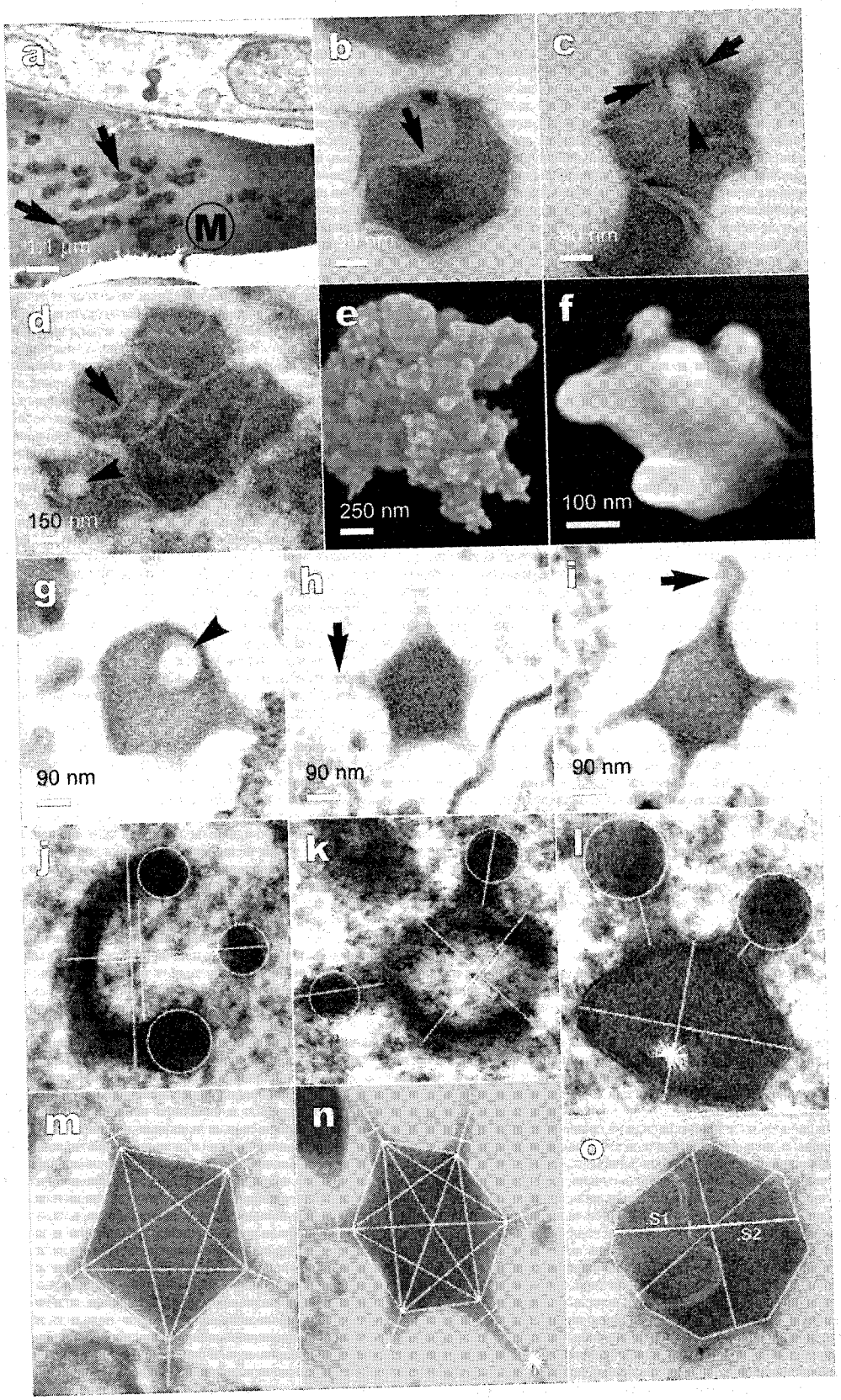

# Identification of virulence factors from parasitoid wasps of *Drosophila*

Hsiling Chiu[1,3], Jorge Morales[1,2,3], and Shubha Govind[1,2]

[1]Department of Biology, The City College of New York
138th Street and Convent Avenue, New York, NY 10031

[2]The Graduate School and University Center
The City University of New York
365 Fifth Avenue, New York, NY 10016

[3]Contributed equally to this work

Key words: *Drosophila*, parasitoid wasps, immune suppression, virus like particles, hemocytes, innate immunity

Abbreviations:
VLP: virus-like particle
EM: electron microscopy
SEM: scanning electron microscopy
TEM: transmission electron microscopy

## ABSTRACT

When infected by avirulent strains of parasitoid wasps such as *Leptopilina boulardi G486*, *Drosophila melanogaster* larvae mount an encapsulation response in which larval blood cells called lamellocytes form a multicellular capsule around the parasite egg. However, large virus-like particles (VLPs) from two closely-related virulent parasitoid wasp species, *Leptopilina heterotoma* and *L. victoriae* suppress the host encapsulation response by promoting lysis of lamellocytes. VLP precursors are produced in secretory cells of the long gland of the female wasp. Precursors are deposited into the long gland lumen via novel, cytoplasmic canals lined with filamentous actin. Mature VLPs are composed of at least four major proteins. Polyclonal antisera against the most abundant *L. heterotoma* VLP protein, p40, cross-react with the most abundant *L. victoriae* VLP protein, p47.5. Immuno-electron microscopy of the long gland-reservoir complex reveals that p40 is expressed early in VLP biogenesis and is detected along with VLP precursors within the cytoplasmic canals and the long gland lumen. In the reservoir, VLPs have an angular core, resemble mature particles, and p40 is detected outside the VLP cores. Immuno-EM staining of mature VLPs from both species localizes the p40 and p47.5 proteins largely to the periphery of the VLPs and along the VLP spike-like projections. *In vitro*, anti-p40 antibody almost completely blocks the ability of *L. heterotoma* VLPs to promote lamellocyte lysis. Anti-p40 antibody blocks lysis by *L. victoriae* VLPs by more than half. We propose that VLP surface proteins p40 and p47.5 share antigenic determinants and contribute significantly to the strong virulence of their Hymenopteran hosts.

# INTRODUCTION

In nature, *Drosophila* serves as host for a number of different microbial commensals, pathogens, pests and parasites (Ashburner, 1989). When avirulent strains of parasitoid wasps introduce eggs into the hemocoel of *Drosophila* larvae, a strong and specific innate immune response of encapsulation is observed. This encapsulation reaction is characterized by the proliferation and differentiation of hematopoietic precursors in the lymph gland, and the appearance of immune effector cells that quickly surround the wasp egg within many cell layers (Russo et al., 1996; Lanot *et al.*, 2001; Sorrentino *et al.*, 2002). The immune effector cells in the *Drosophila* hemolymph are plasmatocytes, lamellocytes and crystal cells, collectively referred to as hemocytes (Rizki and Rizki, 1984; Carton and Nappi, 1997). Plasmatocytes are primarily phagocytic, but are also thought to be involved in recognition of the parasite egg. Lamellocytes are disc-shaped adhesive cells and form the bulk of the capsule. Crystal cells are thought to carry enzymes for melanization reactions and to participate in the melanization of the capsule. Ultimately, encapsulation and melanization lead to death of the parasite.

Parasitoid wasp eggs can, by a variety of mechanisms, often escape or evade this encapsulation, leading to their evolutionary success (Schmidt *et al.*, 2001). *L. heterotoma* and *L. victoriae*, Cynipid wasp species of the genus *Leptopilina*, are sister species (Schilthuizen et al., 1998) and are both highly virulent. These wasps actively suppress the encapsulation reaction in their *Drosophila* hosts by two mechanisms: Infection by either wasp leads to the apoptotic depletion of hematopoietic precursors, although it is not known how the observed apoptosis is triggered (Chiu and Govind,

2002). Wasp infection is thought to introduce virus-like particles (VLPs) into the host hemocoel, which promote the lysis of mature lamellocytes (Rizki and Rizki, 1984a, 1990, Morales et al., 2005). VLP-induced lysis of lamellocytes does not appear to involve apoptosis (Chiu and Govind, 2002). These strategies of active immune suppression allow the wasp to inactivate and neutralize the cellular defense system of *Drosophila* and ensure optimal developmental opportunity for the wasp's progeny.

In *L. heterotoma* and *L. victoriae,* VLP precursors originate in cells of the long gland, an organ present in female wasps. Precursors undergo assembly within the long gland lumen and transit into the lumen of the reservoir via a connecting duct. In the reservoir lumen, VLPs undergo morphogenesis (Rizki and Rizki, 1984a; Morales et al., 2005). The reservoir in turn is connected to the ovipositor, which is inserted by the female into the body cavity of the *Drosophila* larval host, during the process of egg-laying. Transmission electron microscopy of *L. heterotoma* and *L. victoriae* VLPs revealed that mature VLPs have electron-dense cores that are roughly 300 nm in diameter. The core of some VLPs has defined electron-light regions that are not surrounded by a membrane. Several surface projections that have been previously referred to as spikes arise from the core (Rizki and Rizki, 1990; Morales et al., 2005). A lipid bilayer is present around the core and continues into the spikes. The size of the mature *L. victoriae* VLP from one spike end to another exceeds 500 nm (Morales et al., 2005). VLP morphology is complex and variable; VLPs can be found singly or in groups of two or more. Such particles with more than one core element within a cluster are referred to as compound particles.

When incubated with intact *L. heterotoma* or *L. victoriae* VLPs *in vitro*, lamellocytes lose their typical discoidal appearance as well as their ability to adhere. Instead, they become bipolar in shape and undergo degenerative changes, leaking cytoplasm at the elongating tips (Rizki and Rizki, 1990; Chiu and Govind, 2002). While VLPs of *L. heterotoma* and *L. victoriae* are similar in morphology and appear to act in a similar manner *in vitro*, we have recently found that *L. heterotoma* is more virulent than *L. victoriae* both *in vivo* and in *in vitro* assays (Morales et al., 2005). The molecular mechanisms by which VLPs promote lamellocyte lysis and the molecular basis for differences in virulence between *L. heterotoma* and *L. victoriae* are not understood. In this study, we have begun to analyze the molecular basis of host-parasite interactions by characterizing the basic constituents of VLP proteins. We report that the most abundant VLP proteins, p40 of *L. heterotoma* and p47.5 of *L. victoriae*, share antigenic determinants and play an important role in promoting the lysis of lamellocytes. Based on immuno-EM observations of *L. heterotoma*, we show that p40 is expressed early in VLP biogenesis, and is associated with VLP precursors throughout VLP biogenesis and assembly. It becomes localized to the VLP surface during VLP morphogenesis in the reservoir. Both p40 and p47.5 appear to be localized to the surface and spikes of mature VLPs. Finally, anti-p40 antibody made against *L. heterotoma* VLPs inhibits the ability of VLPs from both *L. heterotoma* and *L. victoriae* to promote lamellocyte lysis, suggesting that VLPs from both wasp species share antigenic determinants that contribute to virulence of the parasitoids.

## METHODS

**Insect stocks** Parasitoid wasps: *Leptopilina heterotoma* was obtained from Dr. P. Chabora, Queens College, CUNY. *Leptopilina victoriae* was a gift of Dr. J. J. M. van Alphen, Leiden University. Both strains were grown on *Canton S* and $ry^{506}/ry^{506}$ of *D. melanogaster* host as previously described (Chiu and Govind, 2002, Morales et al., 2005, Sorrentino *et al.*, 2002). Hemocytes from *D. melanogaster* strain *y v* $hop^{Tum-l}$*/Basc* were used to evaluate the *in vitro* effect of VLPs on hemocytes.

**Antibody production, protein analysis and immuno-detection of p40** VLP-containing fluid was extracted from 100–200 glands and reservoirs dissected in PBS. This crude lysate has been previously referred to as "raw fluid". Raw fluid was used for VLP purification on a Nycodenz gradient as described previously (Rizki and Rizki, 1984a; 1990). Ultraviolet absorbance at 280 nm and the Bradford method (Bradford, 1976) were used to quantify proteins. A purified VLP preparation from *L. heterotoma* was used as an antigen to inject mice. Injections and bleeding (polyclonal serum) were performed at the Antibody Facility of Princeton University. Proteins present in VLPs and fluid were processed for SDS-PAGE analysis on a 9%, 0.75 mm-thick, acrylamide minigel, according to standard protocols (Laemmli *et al.*, 1970; Sambrook *et al.*, 1989). Proteins were either stained with silver stain (BioRad) or were transferred to nitrocellulose membranes. Membranes were probed with the anti-p40 antibody followed by treatment with alkaline phosphatase-linked secondary antibody (Sigma). Bound antibody was detected using NBT and BCIP substrates (Promega).

To visualize VLPs on host cells, live hemocytes from *y v hop*$^{Tum\text{-}l}$*/Basc* or from *y v hop*$^{Tum\text{-}l}$*/Y* larvae were treated for 2 – 4 hours with either gradient-purified VLPs or from VLPs present in raw fluid, in PBS. Larvae carrying the sex-linked semi-dominant *hop*$^{Tum\text{-}l}$ mutation show an overabundance of plasmatocytes and lamellocytes in their hemocoel (Hanratty and Dearolf, 1993). The presence of the *yellow* marker (*y* mutation results in yellow mouth hooks of larvae) allows for genotyping mutant and control larvae. Using this marker, mutant males were sorted from control males and mutant animals were bled on a slide for examining VLP-hemocyte interaction *in vitro* or for antibody staining experiments. For antibody staining experiments, hemocytes were incubated with purified VLPs (or with raw fluid), the medium was removed and cells were air dried for 30 minutes. Cells were fixed, washed, blocked and probed with primary anti-p40 antibodies, that were visualized by a FITC-labeled secondary goat anti-mouse IgG (Immunotech) or HRP conjugated goat anti-mouse IgG (Vectastain). Either a Zeiss Axioplan compound fluorescent or Biorad Confocal microscope were used for imaging stained cells.

**Scanning electron microscopy** To determine if VLPs are associated with the wasp egg soon after oviposition, *Drosophila* larvae were dissected 20-30 min. after infection and prepared for SEM as described below. To study VLP-lamellocyte interaction, hemocytes from hop$^{Tum\text{-}l}$/Y larvae were incubated with *L. heterotoma* VLP fluid *in vitro* for 30 minutes. Samples for scanning electron microscopy (wasp eggs, VLP-treated hemocytes, or VLPs) were mixed with 10 times the volume of freshly-prepared cold fixative (0.4 ml 10X phosphate buffered saline pH 7.2, 1.1 ml of $dH_2O$, 0.5 ml 16%

paraformaldehyde, 1 ml 8% glutaraldehyde, 1 ml 4% osmium tetroxide). After 20-30 minutes on ice, 10 ml of cold distilled water were added, and 3mL were filtered onto a 10 mm polycarbonate filter (0.22 μm pore size). The filtered sample was covered with a second moistened filter and clamped between O-rings. The sandwiched sample was rinsed five times in cold distilled water and dehydrated at room temperature in a graded series of ethanol, followed by two rinses (5-10 min each) in amyl acetate. After rinsing the sample seven times in liquid $CO_2$, the sample was critical point dried. The dried sample was coated with gold and observed with a Zeiss DSM 940.

To examine VLP structure and analyze the distribution of p40 in wasp tissues and mature VLPs at high resolution, the long gland-reservoir complex or purified VLP pellets were fixed in glutaraldehyde, formaldehyde and picric acid and embedded in LR White Resin as described in Newman *et al.* (1982). Ultra-thin sections were treated with primary anti-p40 antibodies and then stained in goat anti-mouse secondary antibodies linked to 6 nm gold beads according to the manufacturer's instructions (Aurion). A Zeiss transmission electron microscope (EM902) was used to visualize immuno EM results. Negatives of electron micrographs were scanned at 600 dpi on an Epson 1640 scanner and the contrast of the images was adjusted using Adobe Photoshop v. 6. Fine structure analysis of *L. victoriae* long gland/reservoir complex and VLPs for transmission electron microscopy was done as described in Morales *et al.*, 2005.

**Inhibition of bipolar cell formation by primary antibody** VLP-containing fluid containing 30 μg of protein in 10 μl of PBS dissected from either *L. heterotoma* or *L.*

*victoriae* glands was treated with the primary antibody or non-immune mouse serum. The amount of protein in the antibody sera from immune and non-immune mice ranged from 70 μg/μl to 80 μg/μl. These mixtures were gently agitated for 30 minutes at room temperature. Hemocytes obtained from 10 $hop^{Tum\text{-}l}/Y$ animals were pooled in 210 μl of 10% fetal bovine serum, separated into 7 equal portions and treated as follows (25°C): portions 1 and 2 were treated with either *L. heterotoma* or *L. victoriae* fluid (positive controls, No antibody); portions 3 and 4 with 5 μl of anti-p40 antibody-treated fluid from either of the wasps (experimental, immune); portions 5 and 6 with non-immune mouse serum treated fluid; portion 7 with PBS (negative controls, non-immune). In order to obtain a high fraction (> 80%) of bipolar lamellocytes and allow comparison of equivalent VLP activities, blood cells were incubated with *L. victoriae* fluid for 8 hours and with *L. heterotoma* fluid for 4-5 hours. The number of bipolar cells formed was counted using a Nikon inverted microscope. Standard error and *z* tests for independent proportions were performed as described in Dawson and Trapp, 2004.

# RESULTS

Virus-like particles in both *L. heterotoma* and *L. victoriae* are synthesized in the long gland and are thought to be stored in the reservoir (Rizki and Rizki, 1984; Morales *et al.*, 2005; Fig. 1a, b, d-f). The overall morphology of the *L. heterotoma* long gland (Fig. 1a-b, e) is similar to that of *L. victoriae* (Fig. 1d, f). A series of large, peripheral secretory cells (Fig. 1b, arrows) surround an internal, narrow concentric lumen (Fig. 1a, b, labeled with "L"). In between the lumen and the secretory cells, a layer of small endothelial-like cells (intimal layer) is clearly seen (Fig. 1 a, b, arrowheads). At the distal end, the lumen expands into a sac-like structure referred to as the "nose" (Fig. 1a-f, N).

## Actin-lined cytoplasmic canals link secretory cells to the long gland lumen

We have recently described the fine structure of the *L. victoriae* long gland (Morales *et al.*, 2005). In that study, we described clear canals that originate within the cytoplasm of secretory cells, connecting these cells to the long gland lumen. These canals show a bipartite organization: at their proximal ends, the canals are surrounded by membranous microvilli-like projections. Presence of projections makes the canals to appear rough, and we refer to this portion of the canals as the "rough" canal. Within the cytoplasm of the secretory cells, these rough canals of *L. victoriae* glands abruptly transition into smooth canals, where microvilli-like projections are not present (see Fig. 5, Morales et al., 2005). The smooth canals penetrate through the cells of the intimal layer and open into the long gland lumen. Throughout their course, these canals are lined with electron-dense filaments (see Fig. 5 in Morales *et al.*, 2005).

To determine if similar canals exist in the *L. heterotoma* long gland and if these structures might be lined with f-actin, we stained dissected long glands from both *L. heterotoma* (Fig. 1e) and *L. victoriae* (Fig. 1d, f) with rhodamine-labeled phalloidin. These preparations were counterstained with the nuclear dye Hoechst (blue) to define the identity of cells (Fig. 1f). Fig. 1 d-e clearly shows the presence of continuous, phalloidin-positive parallel tracks connecting the cytoplasm of the secretory cells and the long gland lumen. The phalloidin tracks are separated by a narrow phalloidin-negative space (see Fig. 1e, arrow), which presumably corresponds to the lumen of the canals. While these observations do not prove that the phalloidin-stained structures observed here correspond to the electron-dense filaments observed within the canals in EM images (see also EM images of *L. heterotoma* glands, Fig. 4b4, Fig. 5c3, arrowhead), our results support the possibility that canals may be lined with bundles of polymerized actin that provide structural integrity to the canals.

**Three-dimensional structure of VLPs: SEM studies**

In transmission EM studies, it was previously reported that *L. heterotoma* and *L victoriae* VLP spikes sometimes terminate into larger knob like structures (Rizki and Rizki, 1994; Morales et al., 2005). To determine if this is the case and to examine the general three-dimensional structures of mature VLPs, we prepared VLP samples for scanning electron microscopy. These preparations confirm the general organization and variability observed in TEM analysis of VLP morphology (Rizki and Rizki, 1994; Morales et al., 2005). At lower magnification in the SEM, VLPs from the long gland/reservoir complex appear in small groups, aligned in rows. In such preparations,

VLPs appear to adhere to each other via the ends of their spikes. These spike ends (knobs) are more enlarged relative to the average width of the spikes. However, in contrast to TEM images where only some spikes seem to terminate in knobs, SEM images reveal the presence of knobs on all spikes (See Fig. 2 c). This apparent difference in morphology could be due to differences in fixation (osmium/glutaraldehyde/formaldehyde or glutaraldehyde/formaldehyde) or in preparation (critical point drying or embedding) of materials in SEM and TEM methods respectively.

To determine if VLPs are associated with the wasp egg soon after oviposition, we dissected newly-infected wild type host larvae and fixed eggs for observations with the SEM. We found that a few VLPs were indeed present on the egg surface (Fig. 2 b, c). In several cases, we found a clear association of the VLP spike with the egg surface (e.g. Fig. 2 c, white arrowhead). Both single particles (Fig. 2c) and compound particles (not shown) are associated with wasp eggs.

To examine VLP lamellocyte binding, we incubated purified VLPs with lamellocytes from *hop*$^{Tum\text{-}l}$ mutant larvae *in vitro*. Thirty minutes following this incubation, VLP–treated hemocyte samples were fixed and processed for SEM. In these preparations, we found clusters of VLPs adhering to the lamellocyte membrane. At high magnification, VLPs in these clusters appear to adhere to the lamellocyte membrane via spikes/knobs (Fig. 2d, e). Together, these results suggest that VLP spikes and possibly the knobs have an adhesive function and may harbor molecules involved in VLP-hemocyte interactions.

**VLP proteins**

To estimate the number and size of proteins that make up the VLPs, gradient-purified VLPs from *L. heterotoma* and *L. victoriae* were separated by SDS-PAGE and visualized by silver staining (Fig. 3a, lanes 1, 2). The silver stain is 10-50 times more sensitive than the Coomassie brilliant blue protein stain and as little as 0.1 ng/mm$^2$ of protein can be visualized by silver staining (Merril et al., 1981). Four major protein bands (apparent molecular mass 87.5, 75, 72.5, and 40 kDa) were observed in VLPs of *L. heterotoma*. There are at least 8 major proteins in the *L. victoriae* VLP preparation (arrowhead, stars, dots, Fig. 3a, lane 2). Several proteins present in lower abundance are also observed in both VLP preparations (dots, Fig. 3a, lanes 1, 2). The most abundant *L. heterotoma* VLP protein is 40 kDa, whereas in *L. victoriae* it is roughly 47.5 kDa (arrows, Fig. 3a, lanes 1, 2). Since VLPs are synthesized and stored in the long gland and reservoirs respectively, we also examined the protein composition of the fluid obtained from these organs by silver staining. All the major VLP proteins observed in lanes 1 and 2 (Fig. 3a) also appear to be represented in the raw fluid prepared from dissected long glands and reservoirs (lanes 3 and 4), although their relative proportions are different. As expected, the number of proteins in the raw fluid is higher.

Mouse polyclonal antibodies against purified intact *L. heterotoma* particles react specifically with the predominant p40 protein of *L. heterotoma* VLP (called anti-p40 antibody hereafter; Fig. 3b, lanes 1, 2). This anti-p40 antibody also cross-reacts with p47.5 of *L. victoriae* VLPs (Fig. 3c). This observation suggests that these predominant VLP components have common antigenic determinants.

VLPs have also been reported in *L. boulardi*, where like the *L. heterotoma/L. victoriae* particles, they are synthesized, secreted, and injected with the egg into the host hemocoel (Dupas *et al.*, 1996; Labrosse et al., 2003). However, unlike the *L. heterotoma/L. victoriae* VLPs that induce lamellocyte lysis, *L. boulardi* VLPs do not appear to have a similar role: First, when fluid obtained from a virulent *L. boulardi* strain was placed on $hop^{Tum\text{-}l}$ lamellocytes *in vitro*, a change to bipolar shape was not observed. Second, In ELISA or Western blot analyses, anti-p40 antibody showed no detectable cross-reactivity with proteins within crude lysate prepared from glands of *L. boulardi* (H. Chiu and S. Govind, unpublished results).

**Expression of p40 in wasp tissues**

To determine if p40 protein is expressed during early stages of VLP biogenesis in the long gland and to examine how p40 distribution is modified as VLPs undergo maturation, we first dissected the long gland-reservoir complex and stained it with anti-p40 antibody (Fig. 1c). While the main body of the long gland showed clear and intense staining, the "nose" of the long gland was not stained (Fig. 1c). In addition, staining of the reservoir was much less intense than that of the long gland (Fig. 1c). Other organs of the female wasp (such as ovaries) or even host tissues (e.g., larval fat body) remain completely unstained (not shown).

To examine the distribution of p40 protein at higher resolution, we performed immuno-electron microscopy on thin sections through the long gland "nose" (position "A"), main body of the long gland (positions "B" and "C") and the reservoir (positions "D", see Fig. 1g for orientation). p40 protein was visualized by secondary antibodies

linked to gold beads. In negative controls where primary antibody was not included in the staining protocol, background levels of adhering gold beads were never observed (Fig. 4, panels a4, b4, and b8; Fig. 5, panels c2, c9, and d4).

The "nose" of the long gland (location "A", Fig. 1g), is an expanded region of the lumen, surrounded only by small endothelial-like cells. The nose contains many small vesicle-like structures but lacks electron-dense particles resembling immature VLPs. Consistent with whole mount staining result (Fig. 1c), immuno-gold staining shows very low, if any, p40 protein in this region (Fig. 4; compare panels a1-a3 with a4). However, within secretory cells located around position "B" of the long gland (see Fig. 1g for orientation), the level of p40 protein is very high (compare panels b1-b3 with a1-a3 in Fig.4, panel b4 represents negative control). Furthermore, p40 is clearly associated with VLP precursors (electron-dense structures found within canals and long gland lumen; see Morales et al., 2005 for more details) being secreted into the rough canals (surrounded by membranous projections; see Fig. 4 panel b3; arrows point to clusters, whereas membranous projections are apparent in panel b4). As mentioned before, these canals connect the secretory cells to the lumen. At the same location, but within the lumen adjacent to the secretory cells (position "B", lumen is wide), we found a very high level of p40 protein assembled onto electron-dense clusters of immature VLPs (Fig. 4 compare b5-b7 with b8). Significantly, vesicles-like structures present in the "nose" are not present in the lumen of position "B", even though this region is continuous with the "nose".

At a more proximal position, where the lumen tapers into the body of the long gland, (position "C", Fig. 1g), we found clusters of immature VLPs in the secretory cell

canals and lumen, and, as described above, strong anti-p40 staining. Anti-p40 binding is especially strong around the VLPs present within the smooth canals and the lumen (Fig. 5, panel c1, and panels c6-c8 respectively). Immature particles in the lumen at position "C" (Fig. 5, panels c6-c10) are morphologically slightly more complex than particles in the lumen at position "B" (Fig. 4, panels b5-b8). Some particles at position "C" appear to have spikes, have acentric electron-light regions, and resemble particles described by Rizki and Rizki (1984a). Morphologically these particles are intermediate in complexity between the simpler precursors found in the secretory cells and the mature particles found in the reservoir. VLP precursors and maturing VLPs observed in Fig. 5 are structurally comparable to those observed in the *L. victoriae* study (Morales *et al.*, 2005; Fig. 6) although the resolution of the images of VLPs in this study is somewhat limited presumably due to the differences in immuno-EM and standard EM protocols.

To examine VLP morphology and p40 staining in the reservoir, sections were prepared from position "D" (panels d1-d4, Fig. 5). In this region, the morphology of the VLPs is more complex, the particles appear more differentiated; and morphologically, begin to resemble mature VLPs. Individual VLPs appear continuous with one another, separated by electron-light "tracks". These "tracks" merge with the electron-light matrix surrounding the VLPs. The number of gold particles that bind to sections prepared from the reservoir is not as high as that observed in the long gland sections, an observation that is consistent with the whole mount staining result (Fig. 1c). However, the gold particles are clearly present above background levels (compare panels d2-d3 with d4, Fig. 5) and localize the p40 protein mostly to the immediate vicinity of the

maturing particles. One interpretation of these results is that the reservoir is not merely a storage organ; instead, VLPs continue to undergo morphogenesis. While in the reservoir, it is possible that p40 protein is not as accessible to the anti-p40 antibody as it is in the long gland, resulting in a lowered signal in both whole mount and immuno-EM experiments. The composition of the electron-light matrix surrounding the VLPs in the reservoir is not known.

**p40 and p47.5 are localized to VLP surface and spikes**

To confirm that p40 and p47.5 proteins are part of mature VLPs and to determine their distribution on the VLPs, we performed immuno-electron microscopy on sections of gradient-purified VLPs isolated from female wasp reservoirs, and counted the number of gold beads present on the VLP surface and inside each VLP. We found that while some p40 and p47.5 protein is localized within the VLPs, most of it is distributed to the surfaces of the VLPs (Fig. 6a-d). The number of gold beads per VLP present on the VLP surface is significantly higher ($P < 0.001$) than that within the VLP core (Fig. 6e) for both *L. heterotoma* (15.9/20; n = 22) and *L. victoriae* (9.9/11.1; n = 22). Further, each VLP has 4-6 spikes and roughly 20% of the secondary antibody-linked gold bead signal is associated with the spikes. Because this "peripheral" anti-p40 signal accounts for the majority of the total anti-p40 antibody binding, we conclude that p40 and p47.5 proteins are primarily located on the surface and spikes of the VLPs.

**p40 and p47.5 in *Drosophila* hemocytes**

Because p40 protein is present on mature VLPs, and mature VLPs interact with lamellocytes or are internalized by plasmatocytes (Rizki and Rizki, 1994), we expected p40 to be present in association with both cell types. To test this idea, we probed $hop^{Tum\text{-}l}$ larval hemocytes with *L. heterotoma* or *L. victoriae* fluid with anti-p40 antibody. Lamellocytes exposed to VLPs from either species become bipolar in shape before undergoing lysis (Fig. 7a, c, e arrows). When such fluid-treated lamellocytes were incubated sequentially with primary anti-p40 antibody and FITC-linked secondary antibody, immuno-reactivity to the p40 and p47.5 proteins was clearly observed (Fig. 7d, f). As expected, there was no binding of antibody to PBS-treated lamellocytes and these lamellocytes retained their discoidal shape throughout the incubation period (Fig. 7a, b). When a confocal microscope was used to visualize p40 protein, antibody binding signal was present within *L. heterotoma* fluid-treated plasmatocytes (Fig. 7g, h). In this experiment, the fluorescent signal from lamellocytes was not as strong possibly because lamellocytes are extremely thin and flat or because p40 protein remains on lamellocyte surface.

**A role for p40 and p47.5 in lamellocyte lysis**

Having established that p40 and p47.5 proteins are associated with VLPs when they interact with plasmatocytes and lamellocytes, we tested if p40 and p47.5 proteins play a role in immune suppression. We examined whether the anti-p40 antibody can interfere with VLP-induced cell lysis. Anti-p40 antibody was added to long gland/reservoir fluid prior to its addition to hemocytes. We controlled for differences in

the activity levels of the *L. heterotoma* and *L. victoriae* VLPs by imposing conditions so that VLP samples exhibit similar activity (*i.e.*, ~ 85% of lamellocytes became bipolar). We found that anti-p40 antibody strongly reduces the percentage of lamellocytes that become bipolar (Fig. 7i). Only 7% of lamellocytes become bipolar in response to *L. heterotoma* VLP in the presence of the antibody, as compared to control experiments, in which over 85% of lamellocytes assume bipolar morphology (Fig. 7i). Consistent with its cross-reactivity, anti-p40 significantly reduces the percentage of lamellocytes made bipolar by *L. victoriae* VLP (from 87.3 and 82.8% in control experiments to 45.8%), although this effect is weaker than that observed on *L. heterotoma* VLP (Fig. 7i). These results directly link VLP proteins from both wasp species to the lysis of *Drosophila* lamellocytes. Because they are functionally involved in promoting morphological changes in lamellocytes, these proteins may play a direct role either in the initial recognition of lamellocytes, or at a subsequent step, in altering lamellocyte cell surface properties or lamellocyte shape change. The observation that anti-p40 antibody blocks bipolar cell formation *in vitro* is thus consistent with the idea that VLP surface proteins p40 and p47.5 are somehow involved in VLP-lamellocyte interaction.

# DISCUSSION

In recent years, remarkable progress has been made in our understanding of processes and mechanisms governing innate immune responses of *Drosophila* (reviewed in Bodian et al., 2004; Brennan and Anderson, 2004). A variety of microscopic and macroscopic pathogens may infect *Drosophila* at specific stages of its life cycle. The host in turn counteracts infection by activating a specific set of local or systemic immune responses. These responses include initiating transcription of genes that encode antimicrobial peptides (humoral responses) and altering hemocyte population through proliferation and differentiation (cellular responses). Genetic and genome-wide molecular studies designed to reveal mechanisms underlying the specific immune response to bacterial and fungal infections suggest a central role for signal transduction and gene expression (DeGregorio et al., 2002; Boutros et al., 2002; Roxstrom-Lindquist et al., 2004, and references therein). Our understanding of *Drosophila* immunity in response to infection by eukaryotes and macroscopic pathogens such as parasitoid wasps is, however, still limited. It is not known whether the same genetic mechanisms that regulate antimicrobial defense in adult flies also participate in defending *Drosophila* larvae against parasites.

*Drosophila* hosts and their obligate parasitoid wasps of the *Leptopilina* species are among the best-studied host-parasitoid systems. When infected by the non-virulent *L. boulardi* strain *G486*, cellular immune responses involving proliferation and differentiation of hemocytes are activated and, in resistant infected hosts, egg development is halted in an encapsulation response (Meister and Lagueux, 2003; Russo et al., 2001; Sorrentino et al., 2004). The primary hemocyte type responsible for

blocking the development of the wasp egg is the lamellocyte. Proliferation and differentiation of hematopoietic precursors residing in the lymph glands is thought to precede encapsulation of the wasp egg (Lanot et al., 2001; Sorrentino et al., 2002). In contrast to the avirulent *G486* strain, virulent strains of *L. boulardi* nearly always successfully infect and overcome the host's immune response. These virulent *L. boulardi* strains suppress egg encapsulation by producing VLPs that do not induce lamellocytes to become bipolar. Instead, *L. boulardi* VLPs are thought to modify lamellocyte morphology and functional capacity, compromising the host's ability to encapsulate the egg (Labrosse et al., 2003).

**The origin, development and delivery of *L. heterotoma* VLPs**

In this study we present a detailed immuno-EM analysis of VLP biogenesis within the *L. heterotoma* long gland reservoir complex, outlining distinct steps in VLP biogenesis and morphogenesis that were previously unreported. Both the steps in VLP biogenesis and the way the VLPs are delivered into the long gland lumen via actin-lined canals are largely similar between *L. heterotoma* and *L. victoriae* (see Morales et al., 2005). It is not known if similar canals are present in long glands of other *Leptopilina* species and in equivalent organs in non-parasitoid wasps. The numerous microvilli-like projections at its proximal end presumably increase the available surface area of the canal, enabling a higher efficiency of VLP protein secretion from the cytoplasm of the secretory cells into the long gland lumen.

In the lumen, *L. heterotoma* VLP precursors appear to increase in size, progressing through different stages of differentiation (VLPs with electron light cores

and peripheral spikes, Fig. 5, c6-c10), much like *L. victoriae* VLPs (see Morales et al., 2005; Fig. 6). In both wasp species, VLPs in the reservoir exhibit higher complexity in organization than do those in the long gland. In the reservoir, *L. heterotoma* VLPs are present either singly or in arrays, and are surrounded by a lipid bilayer. VLP cores are intersected with bilayers that divide the particles into segments. Mature, gradient-isolated particles have a pentagonal/hexagonal core, with multiple spikes.

Not all species of the genus *Leptopilina* produce VLPs with spikes. In *L. boulardi*, the only other species from which VLPs have been reported, spikes are absent (Dupas et al., 1996), but these particles are believed to carry out the same biological function (Labrosse et al., 2003). The presence of spikes in VLPs from both *L. heterotoma* and *L. victoriae* (but not in VLPs from *L. boulardi*) constitutes a clear morphological parameter for VLP classification. Scanning electron micrographs of VLPs show that VLP spikes enlarge into structures that we refer to as "knobs". However, knobs are not frequently observed in transmission electron micrographs (see Morales et al., 2005 for details). Scanning electron micrographs of freshly-deposited wasp eggs (from the host hemocoel) confirm that VLPs are associated with the eggs and suggest that the association may be mediated by VLP spikes/knobs. Furthermore, SEM of VLPs incubated with lamellocytes confirming that VLPs interact with these cells via spike and knobs. Together, these observations suggest that spikes on the VLPs may play an adhesive role or may mediate recognition and/or contact between VLPs and wasp eggs and between VLPs and lamellocytes. Understanding the nature of these interactions is clearly of great importance, as they represent the interface between host and parasite.

**Expression of p40 in *L. heterotoma***

To address the mechanism by which VLPs interact with host lamellocytes, we characterized purified *L. heterotoma* and *L. victoriae* VLPs biochemically. In polyacrylamide gels of purified VLPs we consistently observed strong protein bands of 40 kDa and p47.5 kDa. Staining studies show that p40 expression is restricted to the tissues where VLPs originate and develop. p40 expression was not detected in wasp ovaries or in extracts prepared from male wasps (data not shown).

Immuno-staining experiments revealed that, within the long gland, p40 is not detected in the "nose" of the long gland, but is expressed within canals of secretory cells proximal to the "nose". The expression of p40 is coincident with the site at which the first electron-dense VLP precursors are seen. p40 expression is continuously observed thereafter during stages of VLP biogenesis, morphogenesis and maturation. Immuno-electron micrographs through the long gland and the reservoir suggest that the presence of p40 protein is not restricted to the electron-dense cores of the maturing VLPs. Instead, gold particles are also observed within the matrix surrounding the VLP cores and spikes. This localization of p40 in the vicinity of developing VLPs is consistent with p40's likely presence on the surface and spikes of mature VLPs. Our results also show that p40 expression can be used as a means to track the presence of VLPs. The presence of intact VLPs within plasmatocytes and lamellocytes has been observed by electron microscopy after their incubation with VLPs (Rizki and Rizki, 1994), and it is therefore not surprising that we can identify the presence of p40 (or

p47.5) proteins in these cells after treatment with VLPs *L. heterotoma* or *L. victoriae* (Fig. 7).

**Functional conservation of VLP surface proteins**

VLPs from both *L. victoriae* and *L. heterotoma* are made up of several proteins. However, when mice were injected with intact *L. heterotoma* VLPs, we were initially surprised to find that the polyclonal serum developed by the mouse cross-reacted specifically with the most abundant protein, p40. In retrospect this can be explained by the fact that p40 being an abundant surface protein, was the primary antigen sensed by the mouse immune system. The cross-reactivity of *L. heterotoma* anti-p40 with p47.5 from *L. victoriae* on the western blot, as well as surface localization of p47.5 on mature *L. victoriae* VLPs argue for structural, and possibly functional, conservation between the most abundant proteins of each VLP. Results from antibody inhibition experiments support this idea, where we found that not only do the anti-p40 antibodies almost completely inhibit the effect of *L. heterotoma* VLPs to promote bipolar cell formation, but that they also have the same effect on *L. victoriae* VLPs. Based on these antibody cross-reactivity and antibody inhibition experiments, we propose that p40 and p47.5 proteins are structurally and functionally related and contribute to the high degree of virulence conferred by the VLPs. An alternative interpretation of the antibody inhibition experiments is that the anti-p40 antibodies cluster VLPs, masking lamellocyte-binding sites, thereby preventing VLPs from acting on lamellocytes.

The molecular function and mode of action of p40 and p47.5 are currently not known. Because these proteins appear to be localized to the VLP spikes and surface,

one possibility is that VLPs are a vehicle for p40/p47.5 delivery and p40/p47.5 are directly involved in lamellocyte lysis. An alternative idea is that these two abundant proteins provide structure to VLPs themselves, and mediate VLP-lamellocyte interactions. We are in the process of characterizing the molecular structures of p40 and p47.5, with the goal of shedding light on their molecular functions and providing insight into the role of VLP proteins in lamellocyte lysis.

In conclusion, *Drosophila* hosts and their obligate parasitoid wasps of the *Leptopilina* species constitute an ideal system for analyzing host parasitoid interactions and coevolution. Our recent studies (Morales et al., 2005 and this study) define a new group of VLPs, whose biogenesis, structures, biochemical constituents, and mode of action are now known. The most abundant proteins in each VLP shares structural and functional similarities, suggesting that that the *L. heterotoma/L. victoriae* VLPs first arose in the common ancestor of their wasps. These VLPs form a synapomorphy for the two taxa, and serve as phylogenetically informative characters for this clade. Further morphological studies of VLPs and molecular analysis of VLP proteins in different species of this genus and will shed light on the mechanisms and evolution of virulence in this clade.

## ACKNOWLEDGEMENTS

We are grateful to Drs. J.J.M. van Alphen and Peter Chabora for sharing the *L. victoriae* and *L. heterotoma* strains, respectively. We thank Drs. J. Berriman, S. Hoskins, J.J. Lee, R. Nehm, and P. Gottlieb for stimulating discussions and help with experiments. This work was supported by grants from American Heart Association, Heritage Affiliate, Inc., American Cancer Society RPG 98-228-01-DDC and NIGMS S06 GM08168. Support from NIH-RCMI RR03060, and PSC-CUNY is also gratefully acknowledged.

## REFERENCES

Ashburner, M. 1989. *Drosophila* A Laboratory Handbook. Cold Spring Harbor Laboratory Press.

Bodian, D.L., S. Leung, H. Chiu, and S. Govind. 2004. Cytokines in Drosophila hematopoiesis and cellular immunity. Prog Mol Subcell Biol. 34:27-46.

Bradford, M. M. 1976. A rapid and sensitive method for the quantitiation of microgram quantities of protein utilizing the principle of protein dye binding. Analyt. Biochem. 72:248-254.

Brennan, C. A., and K. V. Anderson. 2004. Drosophila: the genetics of innate immune recognition and response. Ann. Rev. Immunol. 22:457-483.

Boutros, M., H. Agaisse, and N. Perrimon. 2002. Sequential Activation of Signaling Pathways during innate immune responses in Drosophila. Developmental Cell 3:711-722.

De Gregorio, E., P. T. Spellman, P. Tzou, G. M. Rubin, and B. Lemaitre. 2002. The Toll and Imd pathways are the major regulators of the immune response in Drosophila. EMBO J. 21(11):2568-2579.

Carton, Y., and A. J. Nappi. 1997. *Drosophila* cellular immunity against parasitoids. Parasitology Today. 13:218-227.

Chiu, H. L., and S. Govind. 2002. Natural infection of *D. melanogaster* by virulent parasitic wasps induces apoptotic depletion of hematopoietic precursors. Cell Death Differ. 12:1379-1381.

Dawson, B., and R. G. Trapp. 2004. *Basic and Clinical Biostatistics*. Fourth Edition, McGraw Hill, New Yok.

Dupas, S., M. Brehelin, F. Frey, and Y. Carton. 1996. Immune suppressive virus-like particles in a *Drosophila* parasitoid: significance of their intraspecific morphological variations. Parasitology 113:207-212.

Hanratty, W. P., and C. R. Dearolf. 1993. The *Drosophila* Tumorous-lethal hematopoietic oncogene is a dominant mutation in the hopscotch locus. Molec. gen. Genet. 238:33-37.

Labrosse, C, Y. Carton, J. M. Drezen, and M. Poirie. 2003. Active suppression of D. melanogaster immune response by long gland products of the parasitic wasp Leptopilina boulardi. J. Insect Physiology 49:513-522.

Laemmli, U. K. 1970. Cleavage of structural proteins during the assembly of the head of bacteriophage T4. Nature 227:680-685.

Lanot, R., D. Zachary, F. Holder, and M. Meister. 2001. Post-embryonic hematopoiesis in *Drosophila*. Dev. Biol. 230:243-257.

Merril, C.R., D. Goldman, S. A. Sedman, and M. H. Ebert. 1981. Ultrasensitive stain for proteins in polyacrylamide gels shows regional variation in cerebrospinal fluid proteins. Science 211:1437-1438.

Meister, M., and M. Lagueux. 2003. *Drosophila* blood cells. Cellular Microbiology 5(9):573-580.

Morales, J., H. L. Chiu, R. Plaza, T. Oo, S. Hoskins, and S. Govind. 2005. Biogenesis, structure, and immune suppressive effects of virus-ike particles of a Drosophila parasitoid, Leptopilina victoriae. J. Insect Physiology, Special Issue "Physiological and biochemical relationships among non-poly-DNA viruses, parasitic wasps, and Their hosts". In press.

Newman, G. R., B. Jasani, and E. D. Williams. 1982. The preservation of ultrastructure and antigenicity. J. Microscopy. 127:RP5-RP6.

Rizki, T. M., and R. M. Rizki. 1984. The cellular defense system of *Drosophila melanogaster*. *In* Insect Ultrastructure. Vol 2. R.C. King, and H. Akai, editors. Plenum Publishing, New York. 579-604.

Rizki, R.M., and T. M. Rizki. 1984a. Selective destruction of a host blood cell type by a parasitoid wasp. Proc. Natl. Acad. Sci. USA 81:6154-6158.

Rizki, R. M., and T. M. Rizki. 1990. Parasitoid virus-like particles destroy *Drosophila* cellular immunity. *Proc. Natl. Acad. Sci.* USA 87, 8388-8392.

Rizki, T. M., and R. M. Rizki. 1992. Lamellocyte differentiation in *Drosophila* larvae parasitized by *Leptopilina. Dev. comp. Immunol.* 16:103-110.

Rizki, T. M., and R. M. Rizki. 1994. Parasitoid-induced cellular immune deficiency in *Drosophila*. Primordial Immunity: Foundations for the Vertebrate Immune system. Annals of the New York Academy of Sciences 712:178-194.

Roxstrom-Lindquist, K., O. Terenius, and I. Faye. 2004. Parasite-specific immune response in adult Drosophila melanogaster: a genomic study. EMBO reports 5(2):207-212.

Russo, J., S. Dupas, F. Frey, Y. Carton, and M. Brehelin. 1996. Insect immunity: early events in the encapsulation process of parasitoid (*Leptopilina boulardi*) eggs in reactive and non reactive strains of *Drosophila*. Parasitology 112:135-142.

Russo, J., M. Brehelin, and Y. Carton. 2001. Haemocyte changes in resistant and susceptible strains of *D. melanogaster* caused by virulent and avirulent strains of the parasitic wasp *Leptopilina boulardi*. Journal of Insect Physiology. 47:167-172.

Sambrook J., E. F. Fritsch, and T. Maniatis. 1989. Molecular Cloning, A Laboratory Manual, Cold Spring Harbor Laboratory Press.

Schilthuizen, M., G. Nordlander, R. Stouthamer, and J. J. M. van Alphen. 1998. Morphological and molecular phylogenetics in the genus *Leptopilina* (*Hymenopter*; *Cynipoidae*; *Eucoilidae*). Systematic Entomology. 23:253-264.

Schmidt, O., U. Theopold, and M. Strand. 2001. Innate immunity and its evasion and suppression by hymenopteran endoparasitoids. BioEssays. 23:344-351.

Sorrentino, R. P., Y. Carton, and S. Govind. 2002. Cellular immune response to parasite infection in the *Drosophila* lymph gland is developmentally regulated. Dev. Biol. 243 :65-80.

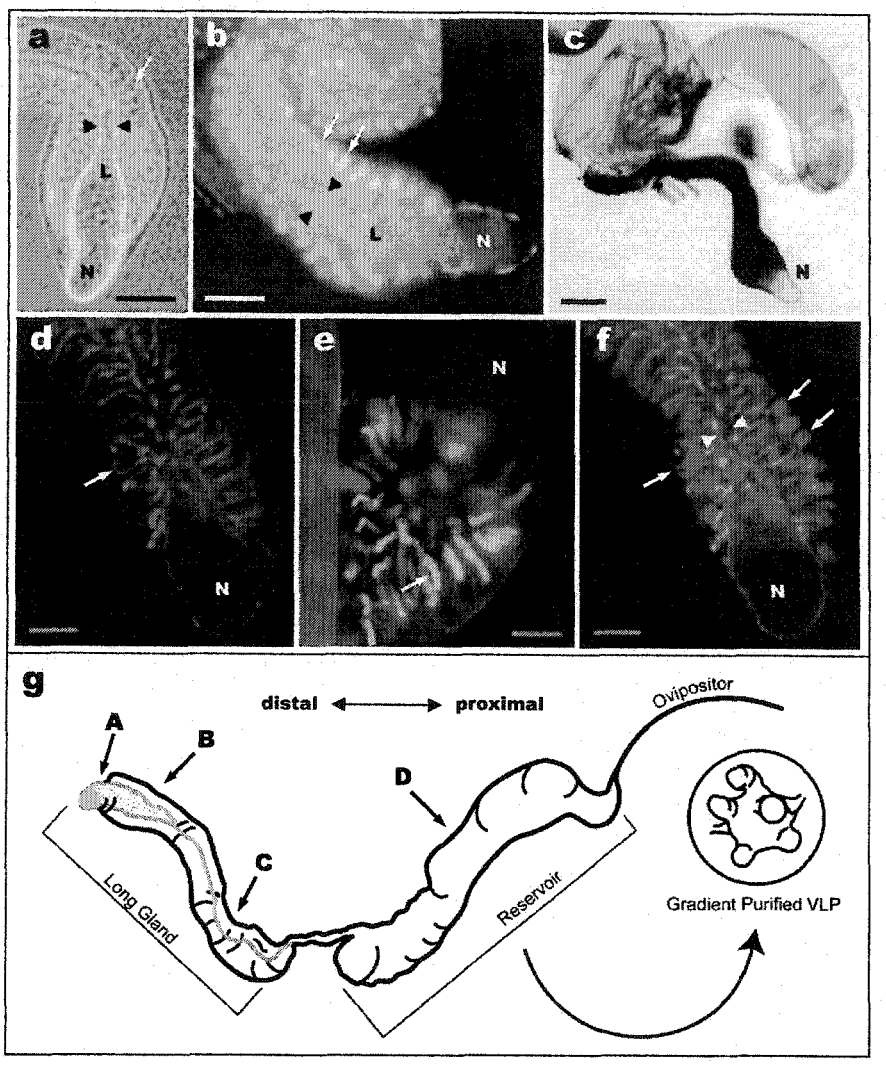


**Fig. 1.** (a) Phase contrast and (b) Hoechst-stained micrographs showing morphology of *L. heterotoma* long gland. Arrows point to secretory cells, arrow heads to lumen (L). Note that the lumen expands into the "nose" (N) and is surrounded by a thin layer of smaller cells of the intimal layer. Scale bars in a and b is 100 μm. (c) Indirect immuno-detection of p40 protein in the long gland-reservoir complex of *L. heterotoma* by anti-p40 antibody. An Equal Opportunity Employer

Anti-p40 antibody is detected by secondary antibody linked to alkaline phosphatase (purple reaction product). Long gland shows strong staining, reservoir shows weaker staining. Scale bar in c is 200 μm. Distal portions of *L. victoriae* (d, f) and *L. heterotoma* (e) long glands dissected and stained with phalloidin (d-f) and counterstained with Hoechst (f) to visualize the overall organization of the cytoplasmic canals at lower magnification. Arrows point to secretory cells, arrowheads to the lumen, scale bars in d-f is 100 μm. (g) Schematic representation of the long gland-reservoir complex indicating the positions from where sections were prepared for immuno-electron microscopy (Fig. 4, 5).

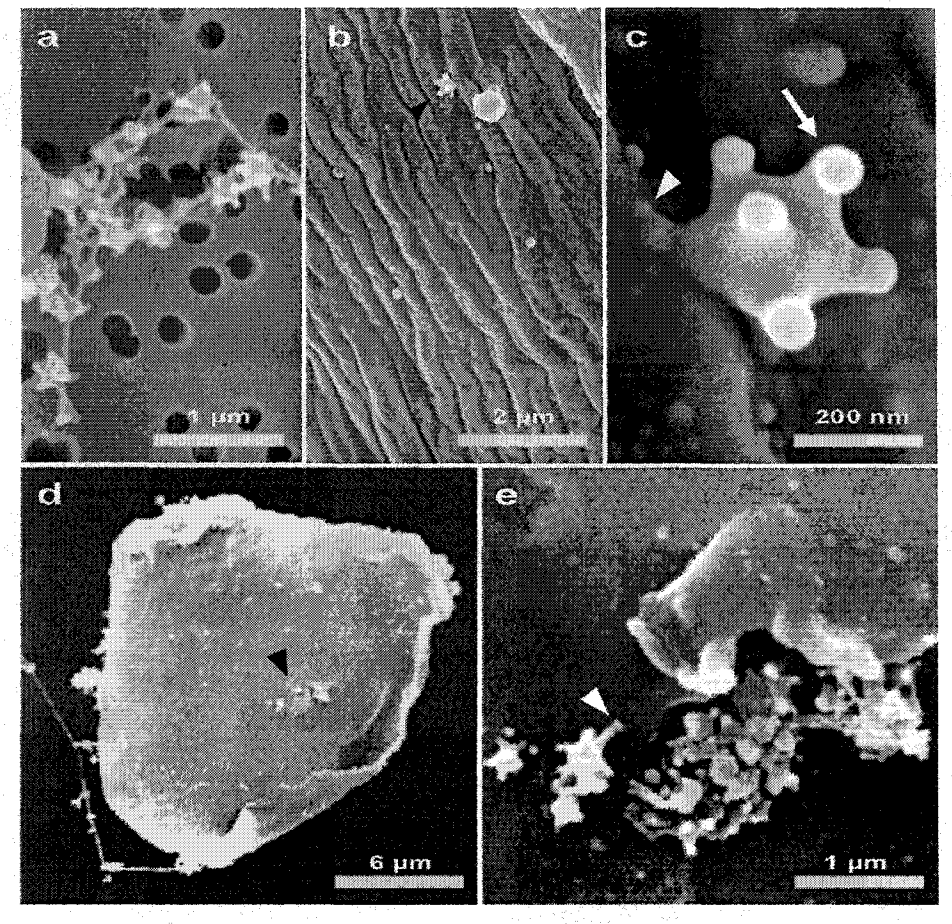


**Fig. 2.** Scanning electron micrographs of *L. heterotoma* VLPs. (a) In raw fluid, VLPs remain connected to one another. (b, c) Panels show VLPs on the surface of a wasp egg, 10 to 15 min after wasp infection. Panels d and e show binding of VLPs to a lamellocyte after 30 min of incubation. Arrowhead in d shows a cluster of VLPs; this area is enlarged in panel e. White arrowheads in panels c and e show the spike/knob structure of a VLP in contact with the surface of a wasp egg (c), and the surface of a lamellocyte (e), respectively. Arrowheads in b and d point to areas enlarged in c and e respectively.

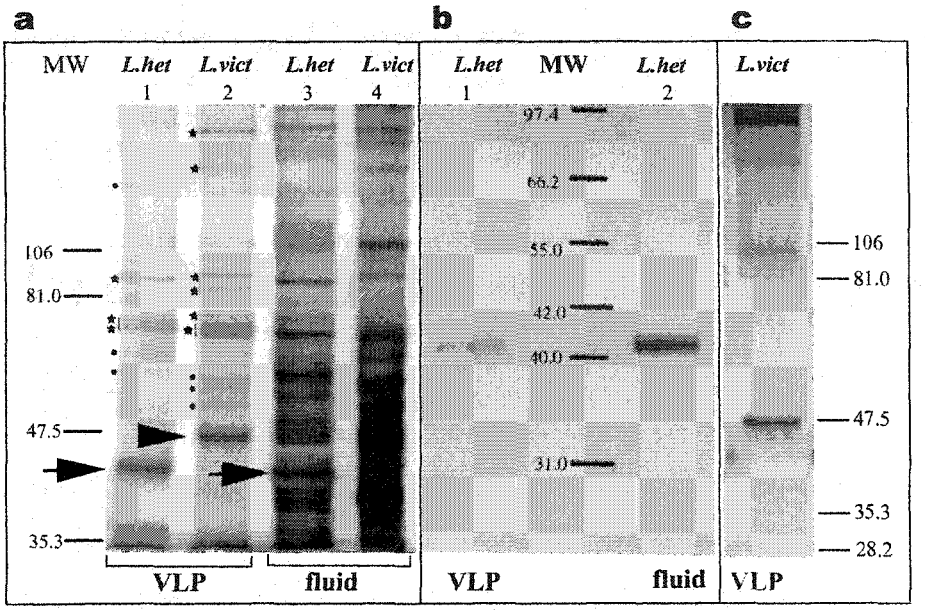


**Fig. 3**. (a) Silver-stained SDS-PAGE of *L. heterotoma* and *L. victoriae* VLP proteins. Stars and dots along lanes 1 and 2 indicate major and minor protein bands respectively that are reproducibly observed. Arrow indicates the *L. heterotoma* p40 protein, whereas the arrowhead points to the *L. victoriae* p47.5 protein. Micrograms of protein loaded in lanes 1 and 2: 2.1; lanes 3 and 4: 12. (b, c) Western analysis using anti-p40 antibody. Lanes 1 and 2 each have 1.0 mg of *L. heterotoma* VLP or fluid proteins. Lane in panel c contains 8 mg of *L. victoriae* VLP proteins. The blot was over-stained with substrates of alkaline phosphatase.

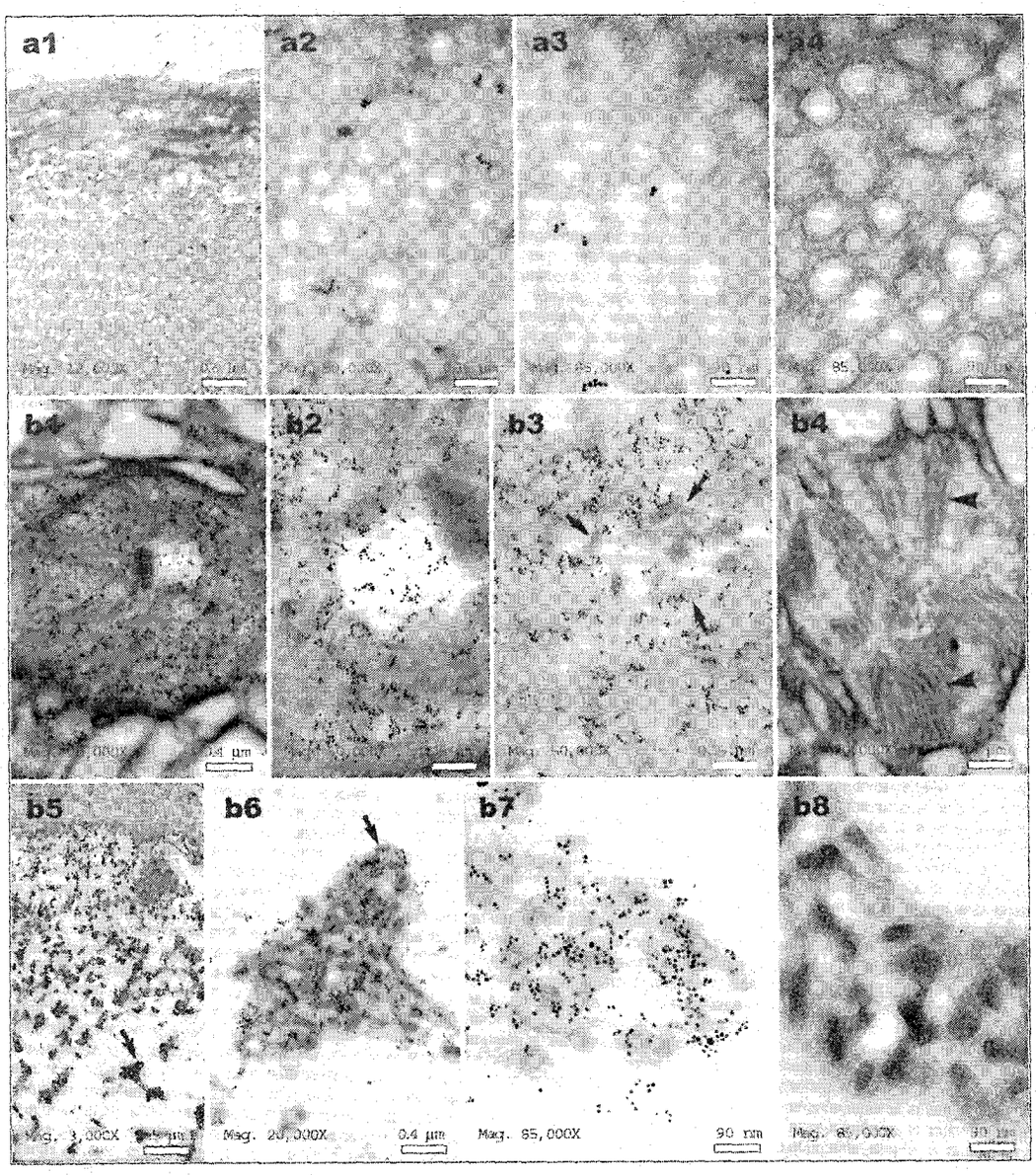


**Fig. 4**. Immuno-electron micrographs of thin sections prepared from positions "A" and "B" of *L. heterotoma* long gland (see Fig. 1g for orientation). Panels a1-a4 show preparations derived from the "nose", and b1-b4 through the "rough" canals within secretory cells, and b5-b8 through the lumen of the long gland. Panels a4, b4 and b8 are negative controls (no primary antibody). Arrows in panels b3, b5 and b6 point to clusters of immature VLPs. Arrowheads in panel b4 point to membranous projections found around the "rough" canals into which immature VLPs are first secreted. Similar structures are found in secretory cells in the long gland at position "C" (see Fig. 5, panel c3, black arrowhead).

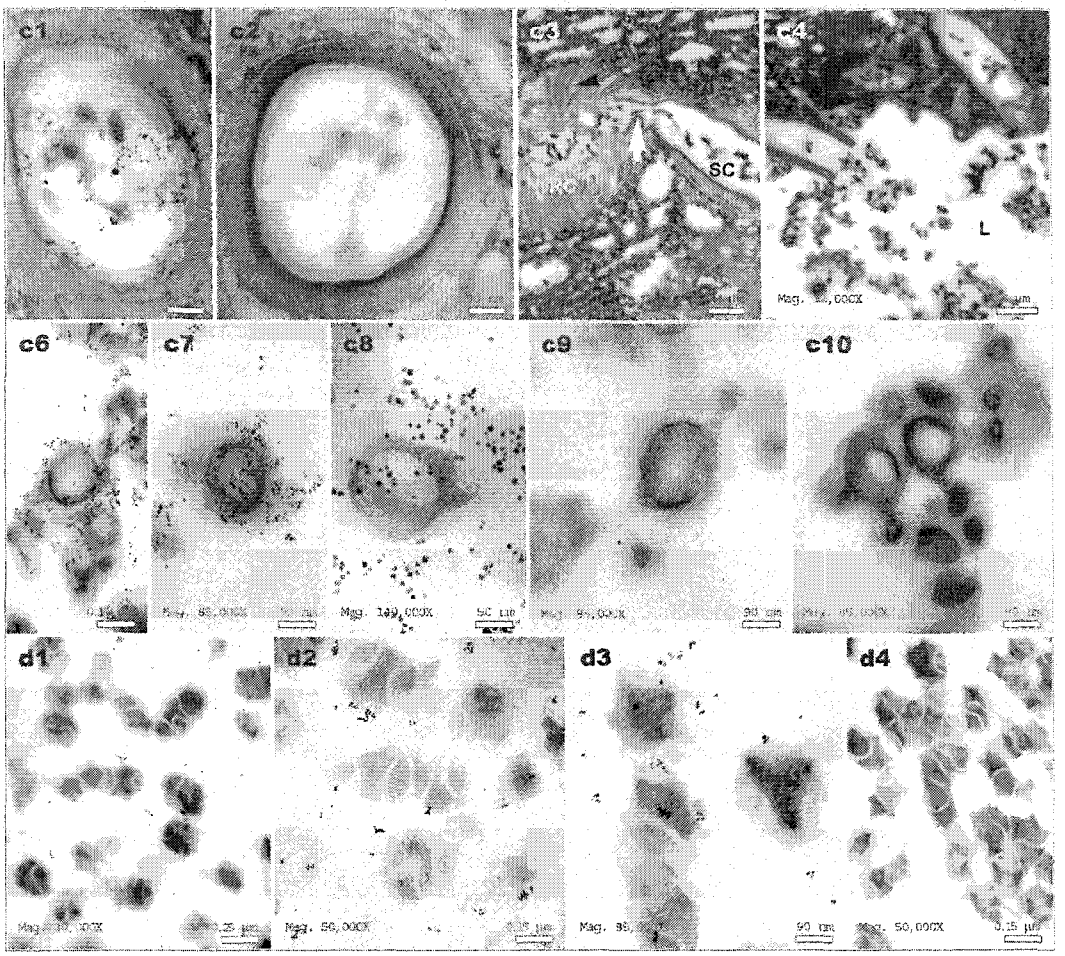


**Fig. 5.** Electron micrographs of thin sections prepared from positions "C" and "D" of *L. heterotoma* long gland and reservoir respectively, as noted in Fig. 1g. Panels c1 and c2 show immature VLPs within the "smooth" canals (transverse sections). Notice that these canals are surrounded by concentric layers of materials, much like the "smooth" canals found in cells at the same position in *L. victoriae* (Morales et al., 2005). Smooth canals appear to be directly connected to "rough" canals (see white arrow in panel c3). The "smooth" canal empties into the long gland lumen ( L = lumen, panel c4). Panels c6-c10 show VLPs within the long gland lumen at position "C". Notice that some VLPs are spiked and have acentric electron-light regions inside the VLP body. At this stage of VLP biogenesis, high levels of p40 are associated with developing VLPs (panels c6-c8). (d1-d4) VLPs in the reservoir at position "D" (Fig. 1g). Panels c2, c9 and d4 are negative controls (primary antibody omitted), whereas samples in panels c3, c4 and c10 were not immuno-stained.

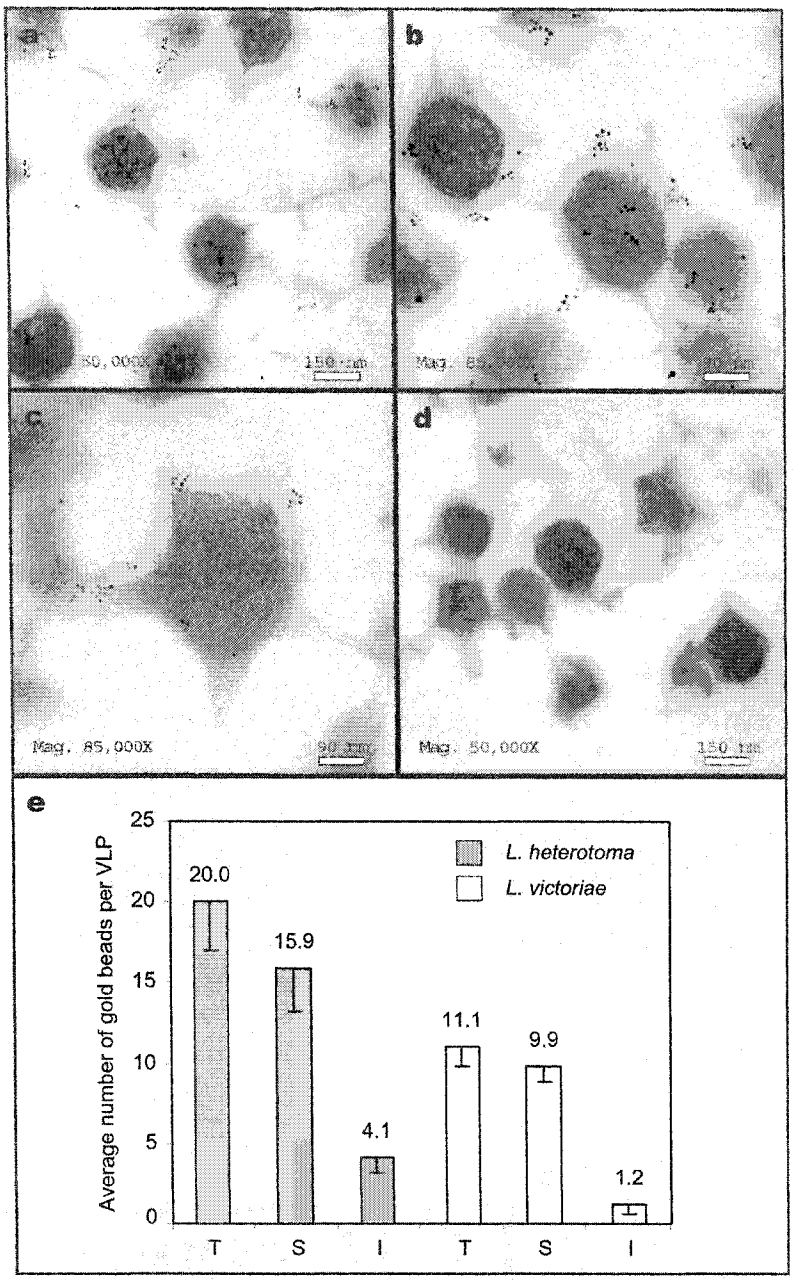


**Fig. 6.** (a-d) Immuno-electron micrographs of thin sections of VLPs. Localization of p40 protein on *L. heterotoma* VLPs (a, b) and p47.5 on *L. victoriae* VLPs (c). (d) Negative control where incubation with the primary anti-p40 antibody step was omitted. (e) Binding of the primary antibody as measured by counting number of gold beads adhering to the "surface" (S) or "internal" (I) regions of 22 VLPs from either wasp species. The sum of these two numbers is represented with the "total" (T) binding of gold beads to the VLPs.

**Fig. 7.** (a-h) Detection of p40 and p47.5 proteins by indirect immunofluorescence using anti-p40 antibodies. All hemocytes used were from *hopTum-l* /Y larvae and they were treated either with *L. heterotoma* (a-d, g-h), or *L. victoriae* fluid (e, f). (a, b) Negative control (incubation with primary antibody omitted). (a, c, e) Phase view of cells in panels b, d, f, where anti-p40 antibodies were visualized by FITC-linked secondary antibody. Arrows point to tapering ends of lamellocytes as they assume bipolar morphology prior to their lysis. Treated cells reveal adherence of VLP p40 and p47.5 to plasmatocytes and lamellocytes. Untreated lamellocytes do not become bipolar (not shown). (g, h) Confocal images of *hopTum-l* hemocytes showing association of anti-p40 antibody within plasmatocytes treated with the *L. heterotoma* fluid. Cells are counterstained with nuclear dye TOTO-3. (i) Inhibition of formation of bipolar cells by anti-p40 antibodies. Percentage of lamellocytes that became bipolar cells is noted on top of each bar. Total number of lamellocytes examined is in parenthesis. Non-immune: mouse serum was used as a negative control. Immune: anti-p40 antibody-treated fluid from *L. heterotoma* or *L. victoriae*. Suppression of bipolar cell formation by the anti-p40 antibody was highly significant ($z > 16$, $p < 0.003$) in pairwise $z$ tests for independent proportions between the no antibody/non-immune (negative controls) and the immune (experimental) *in vitro* assays with fluid from either wasp.

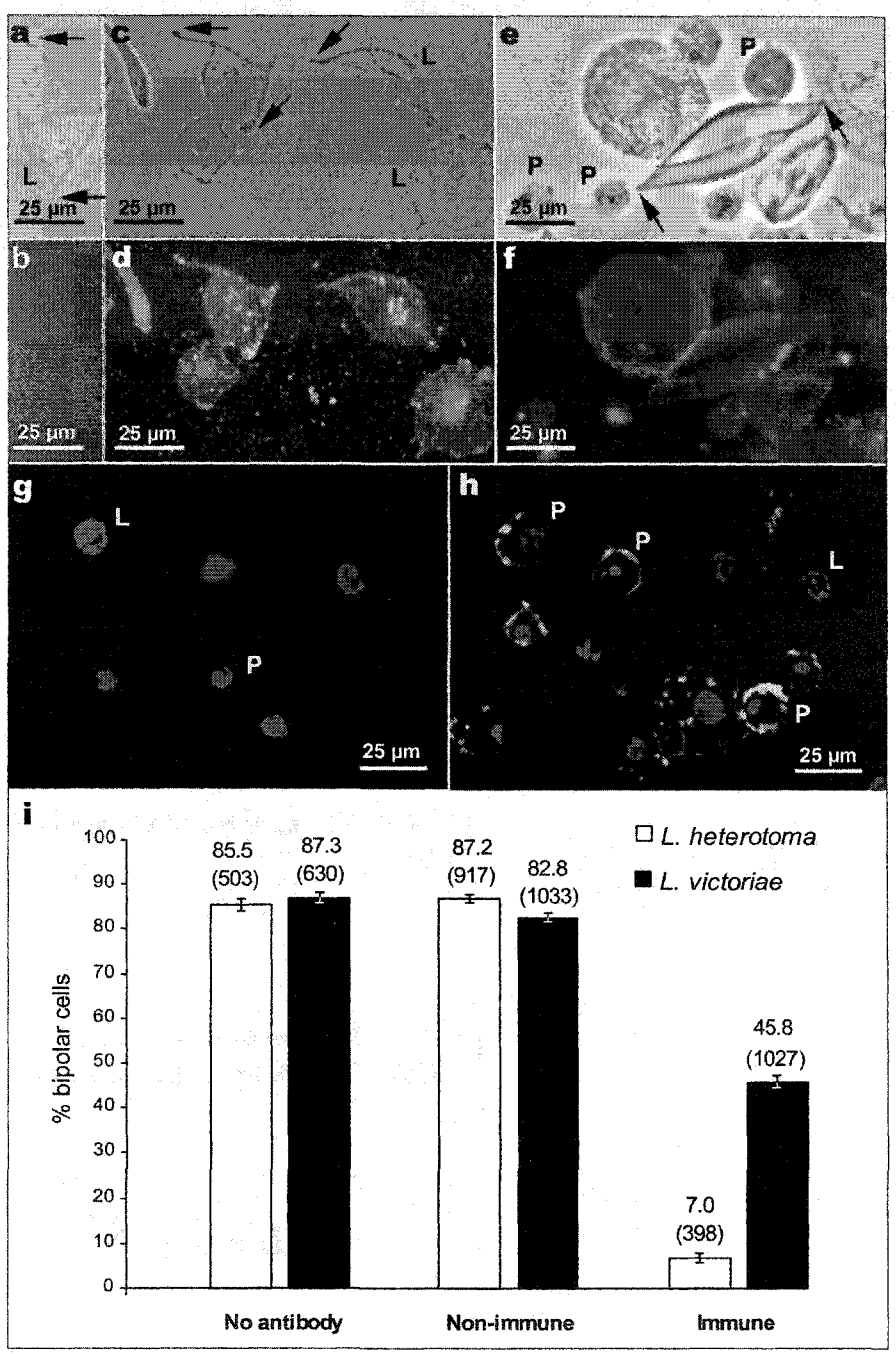

# Expression analysis of *Drosophila melanogaster* infected by parasitoid wasps with differing virulence

Jorge Morales[1], Todd Schlenke[2], Andrew Clark[2], and Shubha Govind[1]

[1]The Graduate School and University Center
The City University of New York
365 Fifth Avenue, New York, NY 10016

[2]Department of Molecular Biology and Genetics
Cornell University
227 Biotechnology Building, Ithaca, NY 14853

## ABSTRACT

The cellular immune responses of *Drosophila* are mediated by plasmatocytes (phagocytosis), crystal cells (melanization), and lamellocytes (encapsulation of large foreign objects). When resistant strains of *Drosophila* are infected by non-virulent strains of wasps, eggs are efficiently encapsulated by lamellocytes. Virulent wasps either avoid encapsulation or block encapsulation. Infection by virulent wasps *L. heterotoma* or *L. victoriae* eliminates these immune-active plasmatocytes and lamellocytes. *D. melanogaster* also has a potent humoral immune response, geared for combating bacterial or fungal infections. Previous studies have shown that microbial pathogens modulate the expression of 283 genes in *D. melanogaster*, including genes encoding antimicrobial peptides. This regulation of gene expression is largely under the control of either the Toll/NF-κB or the Imd/NF-κ pathways. It is however not known if infection by avirulent wasps results in significant gene expression changes, and if the Toll/Imd pathways are also involved in this process. Furthermore, it is not known, if virulent wasps, in addition to compromising cell-mediated immunity, interfere with gene expression programs, including the expression of humoral immunity genes. We present gene expression results of larval hosts infected by *L. boulardi-17* and *L. heterotoma-14*, wasps that differ in their degree and mechanism of virulence. We found that both wasps trigger a mild immune response, characterized by expression of several antimicrobial peptide genes. However, *L. boulardi* infection regulates the expression of many more immunity genes (79 of 81), as compared to infection by *L. heterotoma* (16/81 genes). Significantly, 33 of the 80 wasp-induced immunity genes identified in our study have been shown to be regulated by the Toll

and Imd pathways, and the expression of 29 of these 33 genes has been shown to be partially or completely Toll-dependent. Expression of the antifungal peptide gene *Drosomycin*, a target of the Toll pathway, is activated by *L. boulardi* infection, but not by *L. heterotoma* infection. This result was validated *in vivo*.

## INTRODUCTION

Fruit flies can be infected by a wide range of microscopic and macroscopic pathogens such as viruses, bacteria, fungi, and protozoa. In addition, many parasitoid wasps (*Hymenoptera*) reproduce by parasitization of *Drosophila* larvae (*Diptera*) (Hoffman, 2003). *Drosophila* lacks adaptive immunity, but it has an efficient innate immune system consisting of humoral and cellular components. In the *Drosophila* larvae, epithelial borders (cuticle), trachea, fat body, and blood cells (hemocytes) constitute some of the major host defense systems (Govind and Nehm, 2004). In the larval hemocoel, pathogen associated molecular patterns (PAMPs), present on the surface of microbes, are recognized by soluble recognition factors (Brennan and Anderson, 2004; Hoffmann, 2003). Gram negative binding proteins (GNBPs) and peptidoglycan recognition proteins (PGRPs) are examples of pattern recognition receptors (PRRs) that recognize bacteria and other microbes.

Fungi or gram positive bacteria are recognized by PGRP-SA, PGRP-SD, or GNBP-1 (Brennan and Anderson, 2004; Hoffmann, 2003). The serine protease Persephone and the protease inhibitor necrotic (*nec*) are involved in processing of Spatzle and Toll activation. Cleaved Spatzle binds to the Toll receptor, present on the surface of larval and adult fat body, activating an intracellular cascade mediated by Tube, Pelle, and Cactus. Phosphorylation of Cactus results in its degradation and the release and translocation of the NF-κB transcription factors Dorsal and Dif. Nuclear Dorsal and Dif induce the expression of antimicrobial peptide (AMP) genes such as *Drosomycin (Drs)* and M*etchnikowin (Mtk)* specific to fungi and gram positive bacteria.

Activation of the "Imd" pathway by gram negative bacteria results in the nuclear translocation of the NF-κB transcription factor Relish and the production of specific antimicrobial peptides such as *Diptericin (Dpt)* and *Attacin (Att)*. Imd stands for "immune deficiency", and the Imd protein regulates Relish cleavage and function independently of the Toll pathway (Brennan and Anderson, 2004 and references therein). The pattern recognition proteins for the Imd pathway are thought to be PGRP-LC and PGRP-LE (Takehana *et al.*, 2004). Thus, the Toll and Imd pathways play critical roles in the humoral immune response of *D. melanogaster*. Inactivation of these pathways by loss of function mutations results in immune deficiency in the fly, characterized by higher susceptibility to bacterial or fungal infection (Lemaitre *et al.*, 1996; Hoffmann, 2003; Hultmark, 2003; Lemaitre, 2004; Brennan and Anderson, 2004).

Cellular immunity in the *Drosophila* larva is carried out by three types of hemocytes: plasmatocytes which are macrophage-like, and carry out phagocytosis of microbes; lamellocytes which are large, discoidal, and adhesive, and surround large foreign objects; and crystal cells which mediate melanization reactions (Rizki and Rizki, 1984a; Meister and Lagueux, 2003; Bodian *et al.*, 2004). Infection by egg(s) of avirulent wasps such as *L. boulardi* strain G486, causes a rapid increase in the number of hemocytes in the larval hemocoel, and the appearance of activated lamellocytes. Newly-differentiated crystal cells and lamellocytes surround the wasp egg forming a capsule which may block parasite development (Rizki *et al.*, 1990; Lanot *et al.*, 2001; Russo *et al.*, 1996; Sorrentino *et al.*, 2002).

Proliferation of hemocytes and differentiation of lamellocytes after wasp infection is thought to be mediated by the Toll/NF-κB and JAK/STAT pathways (Sorrentino *et al.*, 2004). Mutations in components of both the Toll and JAK/STAT pathway genes result in immune deficiency, as these animals show significant reduction in their ability to mount an immune response (Sorrentino *et al.*, 2004). However, loss-of-function mutations in *Toll* and *tube* do not compromise lamellocyte differentiation, but instead lead to a reduction in circulating hemocyte concentration (Sorrentino *et al.*, 2004). In contrast, loss of function mutations in *hopscotch* do not compromise circulating hemocyte concentration, but block lamellocyte differentiation in the lymph gland (Sorrentino *et al.*, 2004). Gain-of-function mutations in the Toll receptor ($Toll^{10b}$) and the JAK-kinase receptor ($hopscotch^{Tum-l}$) result in the constitutive over-proliferation of hemocytes and the induced differentiation of lamellocytes (Qiu *et al.*, 1998; Luo *et al.*, 1995). In both of these mutant backgrounds, visible tumor masses are formed by abnormal encapsulation of self tissues. Recent studies support the idea that other signaling pathways control proliferation and differentiation of hematopoietic precursors (Asha *et al.*, 2003; Zettervall, *et al.*, 2004).

When a *Drosophila* larva is infected by a parasitoid wasp, two outcomes are possible: either the wasp egg is encapsulated (if the immune response is successful), or the parasite develops in the host (if the host immune responses are suppressed). In order to be successful parasites in *Drosophila*, different species of wasps have developed passive or active means to counteract or subvert their host immune responses. For example, *Asobara tabida* evades the immune defenses by injecting an egg which adheres tightly to host tissues. The egg quickly gets enveloped by the host

basement membrane and as a result, avoids detection by recognition proteins and hemocytes (Eslin *et al.,* 1996).

Several species of parasitoid wasps of *Drosophila* posses active means of immune suppression. Two closely-related, highly virulent, species of *L. heterotoma* and *L. victoriae* produce morphologically similar virus-like particles (VLPs) with immune suppressive qualities (Rizki and Rizki, 1994; Morales *et al.*, 2005, Chap.1). These VLPs specifically target lamellocytes, altering their cytoskeleton and membrane properties and leading to changes in cell shape and their lysis. This effect of wasp infection on lamellocytes can be seen clearly when tumor-carrying mutants are infected by either *L. heterotoma* or *L. victoriae* (Rizki and Rizki, 1984b; Morales et al, 2005). The tumor phenotype is rescued, even though the host animal dies due to other effects of the mutation. *In vitro*, the effect of purified VLPs (or fluid containing VLPs) can be observed upon incubation of lamellocytes and VLPs. Within hours, lamellocytes become bipolar and lyse by losing cytoplasm from their ends (Rizki and Rizki 1984b; Morales *et al.*, 2005).

In addition to these effects on lamellocytes, infection by *L. heterotoma* or *L. victoriae* causes the apoptosis of hemocyte precursors present in the lymph gland, 1-3 days after infection (Chiu and Govind, 2003). Furthermore, mature plasmatocytes in culture also undergo apoptosis when incubated with wasp fluid (Chiu and Govind, 2003). Whether VLPs are responsible for these apoptotic effects is currently not known. However, it is clear that different components of the fly larval hematopoietic system are destroyed by the wasps to ensure their development. Strains of *L. heterotoma* and *L. victoriae* are highly virulent (Rizki *et al.*, 1990; Morales, *et al.*,

2005). Their high virulence is ascribed in part to the presence of VLPs, as described above (Rizki and Rizki, 1994; Morales *et al.*, 2005).

The virulence of various *L. boulardi* strains has also been studied, and virulence among different strains is variable (Rizki *et al.*, 1990; Dupas *et al.*, 1996). Some *L. boulardi* strains are thought to be highly virulent (e.g., G431), and exhibit 0% encapsulation on a "resistant" host stain. Eggs of other, avirulent strains (e.g., G486), are encapsulated with 85% efficiency by the same "resistant" *Drosophila* hosts (Labrosse *et al.*, 2003). Infection by the same G486 strain promotes an increase in proliferation and differentiation of hemocytes (Sorrentino *et al.*, 2002).

While VLPs from virulent and avirulent *L. boulardi* strains have been identified, their biogenesis or biological effects are not as strong as that of *L. heterotoma/L. victoriae.* Bipolar cells are not observed when lamellocytes are treated with fluid extracted from *L. boulardi* glands (Rizki and Rizki, 1992; Labrosse *et al.*, 2003). A mild reduction in hemocyte numbers as well as morphological changes on lamellocytes was reported in *Drosophila* infected with virulent *L. boulardi* (Russo *et al.*, 2001). Virulence was correlated to morphological differences in VLPs from virulent and avirulent *L. boulardi* (Dupas *et al.*, 1996). It is not clear whether the virulent *L. boulardi* strains passively avoid encapsulation or actively suppress encapsulation or other immune responses. Strains of *L. boulardi* appear to form a second group of "less" virulent wasps (Rizki and Rizki, 1990, Rizki *et al.*, 1992, Chiu *et al.*, 2002).

In this study, we use Affymetrix expression array experiments on *D. melanogaster* larvae infected with recently captured *L. hetertoma* and *L. boulardi*

parasitoid wasps to study the effect of wasp infection on the regulation host immunity genes. First, we establish that there are measurable differences in the virulence of the wasps used in this study. We then investigate global gene expression patterns with a focus on immunity genes.

## METHODS

**Wasp virulence and long gland morphology** In order to compare virulence between the wasps to be used in array experiments, both an encapsulation assay (*in vivo*) and a bipolar cell assay (*in vitro*) were performed. For the encapsulation assay, early second instar (72-76 hr old at 25°C) *hopscotch*$^{Tum\text{-}l}$ larvae were infected by *L. boulardi-17* (LB17) or *L. hetertoma-14* (LH14) using a slightly higher ratio of wasp to larvae than in the array experiments (9 female wasps / 60 fly larvae). A third group of larvae were left uninfected (control). Five days after infection (8 days after the egg lay), larvae were dissected and the encapsulation of dominant and supernumerary parasite larvae was recorded. The uninfected larvae were not dissected but were observed for the presence of tumors.

For the bipolar assay, 50 female wasp long glands and their reservoirs were dissected from each wasp (LB17 and LH14) and separately crushed in 50 µl of PBS (pH 7.0) to obtain wasp gland fluid (venom) protein. Protein estimation was done on venom extracts using the Pierce Micro BCA Protein Assay Kit (Smith, *et al.*, 1985). Hemocytes were obtained from 12 *hopscotch*$^{Tum\text{-}l}$ larvae, bled in a spot plate well containing 300 µl of PBS (pH 7.0) with 7% bovine serum albumin. Equal volumes (70 µl) of medium containing hemocytes were aliquoted into three slide wells (Lab-Tek Chamber Slide). Equal amounts of protein (2.1 µg) from each wasp were added to separate wells containing hemocytes, PBS was added to a third well (control). Samples were kept at 25°C in with gentle rotation (12 rpm). The number of bipolar and normal lamellocytes was recorded at 2 and 4 hr after the addition of venom fluid.

In order to visualize the morphology of the long gland and verify the presence of F-actin-lined canals characteristics of these wasp species (Morales *et al.*, 2005), glands from LB17 and LH14 females were dissected in PBS (pH 7.0), fixed in 4% paraformaldehyde for 5 min, rinsed 3 times in PBS, stained with rhodamine-labeled phalloidin for 20 min (0.5 μg/ml), rinsed 3 times in PBS, and counterstained with Hoechst 33258 for 1 min (0.5 μg/ml, Molecular Probes). Observations were done using a fluorescence microscope.

**Wasp infections** Wasps were collected in California during the fall of 2002 and were maintained on wild type *D. melanogaster*. For array experiments *D. melanogaster* (Oregon-R) were fed yeast paste for two days prior to being used for egg lays. Egg lays were prepared for 3 to 5 hours in petri dishes (60 mm diameter) containing fly food (sugar/yeast/cornmeal). Three days later (72-74 hr), sixty early third instar larvae were gently transferred to smaller petri dishes (35 mm) containing a very thin layer of fly food (1 ml). Nine plates with 60 larvae in each were infected for two hours with 6 LH14 females, 9 plates were infected with 6 LB17 females, and 9 were left uninfected (control). All the wasps used were 1 to 2 weeks old and were pre-trained by allowing them to infect for 2 hr. At three different time points after infection (3-5 hr, 10-12 hr, and 20-22 hr), three sets of sixty larvae, infected by each wasp, and three uninfected sets were rinsed in phosphate buffered saline (pH 7.0) and frozen at -70°C. Thus, three identical sets of infected larvae were frozen separately at each time point after infection and similarly three uninfected controls were prepared for each time point.

**RNA extraction and first strand cDNA synthesis** Total RNA was extracted using the Trizol method (DeGregorio *et al.*, 2001). Larvae were homogenized in 1 ml of Trizol reagent (Gibco), left on ice for 5 min and centrifuged for 2 min at 5000 rpm and 4°C. The supernatant (750 µl) was transferred to a fresh microfuge tube containing 200 µl of chloroform and vigorously mixed for 15 sec. The samples were allowed to rest for 3 min and then centrifuged at 12,000 rpm for 15 min at 4°C. The aqueous phase (500 µl) was transferred to a fresh tube, 500 µl of isopropanol were added to each tube and the sample was mixed for 10 min, followed by centrifugation at 12,000 rpm for 10 min and 4°C. The pellet was rinsed in 75% ethanol, and resuspended in Tris-EDTA buffer prepared with diethyl pyrocarbonate-treated water. Each RNA sample was treated with 10 units of RNase-free DNase, and incubated at 37°C for 4 hr. The enzyme was deactivated by heating the sample at 95°C for 5 min. For first strand cDNA synthesis, the samples were first heated at 70°C for 10 min and placed on ice. Then, 4 µl of 5X first strand buffer, 2 µl of 0.1 mM DTT, 10 mM of dNTP mix, and 1 µl of Superscript II Reverse Transcriptase were added to 9 µl of total RNA followed by incubation at 37°C for 1 hr. The tubes were then placed on ice for 5 min to terminate the reaction and stored at -20°C. The cDNA samples were sent to the array facility at Weill Medical College at Cornell University for labeling, hybridization to Affymetrix *Drosophila_2* GeneChips, and scanning. Each replica was hybridized to a separate GeneChip.

**Analysis of array data** Twenty seven "cel" files, one for each array, were uploaded into ArrayAssist version 3.0 (Stratagene). The expression of each gene is assessed by

16-20 bases long probe set with perfect match (PM) corresponding to each gene coding sequence in the *D. melanogaster* genome. Probes with one base change are incorporated into each probe set as mismatch (MM), and used to subtract non-specific binding or background (PM-MM). Because intensity values can vary due to array manufacturing, RNA sample preparation, and scanning, the intensity values detected by each probe set must undergo normalization. A master data table was generated using ArrayAssist Robust Multi-array Algorithm (RMA) to normalize the expression values. The RMA subtracts background noise and normalizes the expression values using expression values from all the arrays (Irizarry *et al.*, 2003). Baseline definition was then performed using all three uninfected controls to define the baseline expression value for each probe set (Log2 = 0). Statistical tests, multiclass *t*-test with variance inflation error stabilization, were done separately for each set of three control arrays (uninfected) versus three experimental (infected animals) for each wasp at each specific time point. The same control samples for were used for statistical tests of each set of arrays done on wasp infected larvae.

Probe sets which represent genes with differential expression two-fold or higher between infected larvae versus uninfected larvae were selected at different probabilities ($p < 0.05$, $< 0.1$, and $< 0.2$), this was done to compare the number of genes selected at different p values. Because the number of genes regulated at $p < 0.1$ and $p < 0.2$ was not greatly different (or in the same range, see Table 1), $p < 0.1$ was considered to be appropriate for the selection of genes differentially regulated in response to wasp infection. Lists of differentially regulated genes (up-regulated or down-regulated, two-fold or more, $p < 0.1$) were first compiled for each time point

and each wasp infection using the query function in ArrayAssist. The lists of genes were exported into Microsoft Excel and compiled into a "non-redundant list" containing all the wasp regulated genes along with the average expression value at each time point. Affymetrix probe sets corresponding to all the genes regulated by wasp infection were "batch queried" for annotations using the program NetAffx available at the Affymetrix website. Using the "GO Biological Function" annotations, each gene was assigned to one of four categories and color coded accordingly: immunity genes (red) (DeGregorio *et al.*, 2001, 2002), genes with other known function (blue), annotated genes with unknown function (green), and genes or probe sets without annotation (black). The genes annotated as immune or defense response genes regulated by either wasp were separated into another table for further analysis. Further analysis was done as follows.

In order to identify the common set of genes regulated by both wasps, genes regulated by LB17 infection were compared to genes regulated by LH14 infection at each time point using the Venn diagram function in ArrayAssist. To obtain a time course of gene expression, genes regulated by each wasp at all three time points were compared to identify those whose expression remained up-regulated or those whose expression remained down-regulated at different time points.

***Drosomycin* expression *in vivo*** In order to examine if the expression profile of *Drosomycin* in response to wasp infection as shown by array experiments correlates to *in vivo* expression, transgenic flies with a *Drosomycin promoter-GFP* reporter gene were infected by wasps and their fat bodies were monitored for GFP fluorescence.

These flies were infected by LB17, LH14, or left uninfected (control) using the same infection protocol used in the array experiments. Each larva was dissected in PBS (pH 7.0) to visually confirm the presence of a wasp egg prior to observation of their fat body cells. Observations of their fat body cells were made at the same time points as those used in the array experiments (3-5 hr, 10-12 hr, and 20-22 hr). A fluorescence microscope (Zeiss Axioscope 40 Plus) fitted with a FITC filter and a digital camera (Zeiss MRc) was used to make observations. All images were taken at the same magnification (40 X) and the same time of exposure (2 sec). Data were pooled from singly-infected hosts.

# RESULTS

## Gland morphology

Both *L. heterotoma* and *L. victoriae* were previously shown to have canal structures lined with F-actin. These structures can be visualized by rhodamine-tagged phalloidin (Chiu *et al.*, submitted). To determine if *L. boulardi-17* (LB17) has similar canals, we stained dissected glands with phalloidin. Similar staining reaction was performed for glands from *L. hetertoma-14* (LH14). Glands from both LH14 and LB17 have F-actin-lined canals oriented towards the lumen of the long gland (Fig. 1 c-f). LB17 glands have fewer, more sparsely distributed canals (Fig. 1f). As reported previously (Morales *et al.*, 2005), equivalent structures are found in *L. victoriae.* One such *L. victoriae* canal is shown at higher resolution, using transmission electron microscopy (TEM) on a section of dissected long gland (Fig. 1g-h). The orientation of the canal observed in the TEM preparation is the same as that of F-actin canals observed in whole glands stained with phalloidin. A comparison of 1c and 1g reveals a "funnel-like" organization of these canals that appear to collect materials produced by "secretory cells". Secretory cells synthesize and secrete precursors of virus-like particles and other unidentified factors present in the wasp gland fluid (Fig. 1 g and h, Morales *et al.*, 2005). Once in the lumen, VLP precursors undergo assembly and maturation.

## Bipolar assay

The formation of bipolar lamellocytes (which indicates their lysis) has been used as a method for comparison of virulence between different wasp species (Chiu *et*

*al.*, 2002; Morales *et al.*, 2005). To test quantitative differences in effects on lamellocyte morphology, we exposed lamellocytes to wasp fluid dissected from LB17 and LH14 and containing the same protein concentration. We found that *L. heterotoma-14* fluid induces the formation of bipolar cells *in vitro*, whereas *L. boulardi-17* does not (Fig. 2). After four hours 31% of the lamellocytes incubated with fluid from LH14 become bipolar (Fig. 2). Virtually no bipolar cells were observed in lamellocytes incubated with LB17 fluid or in the control sample.

**Encapsulation assay**

The virulence of *L. heterotoma* has been previously compared to other wasp parasites in "suppression of encapsulation assays (Rizki *et al.*, 1990; Chiu *et al.*, 2002; Morales *et al.*, 2005). None of the Oregon-R hosts show encapsulation when larvae are infected with either *L. heterotoma-14* or *L. boulardi-17*. To determine if differences in virulence between the two wasp strains can be detected in an egg encapsulation assay, we infected $hop^{Tum\text{-}l}$ (tumor-bearing) larvae with either wasp. Comparison of encapsulation of supernumerary LH14 and LB17 larvae showed a dramatic difference. Whereas all supernumerary LB17 wasp larvae (n = 55) were encapsulated and melanized by host lamellocytes, none of the LH14 supernumerary larvae were encapsulated, or melanized (n = 19, Table 1, and Fig. 3 d-g). Dominant wasp larvae in either singly-infected or superinfected hosts remained free of lamellocytes. A difference in host self encapsulation was also observed: infection by LB17 appears to reduce the number of small melanotic tumors compared to uninfected control larvae, but in response to LH14 infection the number of both large and small

tumors appears to increase (compare panels a, b, and c in Fig. 3). Unexpectedly, almost all LH14 infected animals die within five days after infection.

**Analysis of expression array data**

The Gene Ontology (GO, www.geneontology.org) project dictates the nomenclature used to group genes into functional categories across different organisms. GO assignments are based on the literature using structural and functional similarities, including subcellular localization of the protein. This is a useful paradigm when comparing the function of a large number of genes/proteins, as one can easily identify and select the genes/proteins grouped under the same gene ontology. In our array studies we used NetAffx (http://www.affymetrix.com/analysis/index.affx), an online database at the Affymetrix website, to download annotations for all the Affymetrix probe sets corresponding to genes that were differentially expressed. NetAffx annotations are updated using FlyBase (http://flybase.bio.indiana.edu/) and the literature, and use GO assignments. We group genes into four categories. (i) The "immunity" category includes those annotated as immune or defense response genes. (ii) The "other known function" category includes those genes whose function is known but do not play a known role in host defense. (iii) The "unknown" category includes genes that have a Celera Genomics (CG) designation, but their function is not known. (iv) The "unknown (unannotated)" category includes "genes" that do not have a CG designation, gene ontology entry, or any annotated biological or molecular function, and at this time refer probe set identification only.

**(a) Total number of regulated genes**

Table 2 shows a comparison of the number of genes that are differentially expressed by at least 2-fold when comparing data from infected and uninfected animals at a specific time point. This comparison was done at three different probability values (Table 2). Since the number of genes at $p < 0.1$ is roughly the same as at $p < 0.2$, the genes regulated at $p < 0.1$ were pooled into a "non redundant list". The non redundant list consists of 840 genes that are up- or down-regulated by either or both wasps (not shown). Total numbers of induced genes are 597 for LB17 and 33 for LH14, and repressed genes are 327 for LB17 and 35 for LH14 (Fig. 6).

**(b) Functional groups of regulated genes**

(i) Most genes regulated by wasp infection are in the "unknown" category (61%), followed by genes with other known function (25%, Fig. 4e). (ii) A small proportion of genes belong to the "unannotated unknown" genes category (6%, Fig. 4e). (iii) Significantly, 62 genes (7%) were identified in the "immunity genes category" using the current annotations in NetAffx (Fig. 4e) and will be discussed in more detail below. (iv) Interestingly, 41 proteolysis genes were regulated by LB17 and only two by LH14 infection (data not shown). In LB17, the regulation of proteolysis genes peaks at the midpoint with fewest proteolysis genes regulated at 20-22 hr. (v) Known and immunity genes represent the largest proportions of genes regulated by LH14 (Fig. 4b and d).

**(c) Wasp-specific genes**

The number of genes induced/repressed at any of the three time points studied is higher when LB17 was used for infection, as compared to when LH14 was used for

infection. In all, LB17 changed the expression (up and down-regulation) of 230 genes at 3-5 hr post infection (PI), 588 genes at 10-12 hr, and 263 genes at 20-22 hr PI. LH14 changed the expression of significantly fewer genes: 49 genes at 3-5 hr, 14 genes at 10-12 hr and 16 genes at 20-24 hr (Table 2, $p < 0.1$). As gene expression is not strongly affected after LH14 infection, the common set of regulated genes is not very high (Fig. 5). The strongest overlap is found in the induced category of genes at the earliest time point studied and a majority of these genes belong to the immunity class (see below).

**(d) Time course of gene expression**

Time course comparisons of genes regulated by each wasp are shown in Fig. 6. There are 23 genes out of 597 genes that are induced by LB17 infection at all time points. Among these are stress response molecules (*Turandot A, Turandot C*), one thiolester containing molecule (*Tep I*), and three immune induced molecules (*IM1, IM4,* and *IM10*). The expression of none of these 23 genes is induced by LH14 infection (Table 3a). Of the 327 genes repressed by LB17 infection, only 4 remain repressed at each of the three time points.

LH14 shows a sustained repression of only *Turandot A*. Thus, *Turandot A* is interesting because it is the only gene induced at all time points by LB17, but repressed at all time points by LH14 infection. The expression of none of the 33 LH14-induced genes is sustained throughout the first 24 hours (Fig. 6b).

**(e) Regulation of immunity genes**

To determine if the 62 genes identified in our analysis based on Affymetrix website annotations represents all the genes identified as immunity genes, or if additional

wasp-induced genes might also have immune functions (but may not be annotated as such), we manually compared the non-redundant list of wasp-regulated genes with the list of 95 induced and 26 repressed genes, that were previously determined to be regulated by microbial pathogens, and are also under the control of the Imd or Toll, or both these pathways (see DeGregorio *et al.*, 2002). We reasoned that this exercise might also indicate if the wasp-induced immunity genes fall in one or the other categories (Imd or Toll categories) of gene regulation. (i) We found that there are additional genes in the non-redundant list that are clearly in the immunity category. Table 3a consists of all 81 immunity genes regulated by wasp infection and is organized based on gene functions. Of these genes, 55 are induced, 21 are repressed and 5 are both induced and repressed. (ii) For LB17, 57 genes are induced, 19 are repressed and 3 are induced and repressed at different time points. (iii) For LH14, 11 are induced, 5 are repressed. (iv) There are 11 genes induced by both wasps (*Att A, B, C; Cec C, Dipt B, IM2, Metch, PGRP-SB1, PGRP-SD, prx25401,2*), but only one gene repressed by both wasps (*Lsp1*). (v) Genes induced by LB17, but repressed by LH14 are *TotA* and *Tep1* (also see above); there are no genes that are induced by LH14 and whose expression is not modulated by LB17. However, two genes (*CG6865, Hml*) are uniquely repressed by LH14.

Table 3b shows results of a comparison of the 81 wasp-induced immunity genes with the previously characterized immunity genes (Table 1 of DeGregorio *et al.*, 2002). This comparison revealed the following. (i) Of the 16 genes that are completely Relish dependent in their induction when flies are infected with microbes, only 1 is induced by wasp infection. (ii) Of the 51 completely or partially Spatzle-dependent

genes known to be induced by microbial infection, 13 are induced by the wasp. Eleven of the 28 genes that show complete dependence on Spatzle for induction are up-regulated by wasps. (iii) Of the 3 known Relish-dependent genes repressed by microbial infection, 2 are also repressed by wasp infection. (iv) Out of the 17 genes completely or partially requiring Spatzle for down-regulation upon microbial infections, 2 are also repressed by wasp infection. (v) Finally, of the 6 genes exclusively repressed by Spatzle in bacterial infections, 2 are repressed by wasp infection. These results suggest that the Toll pathway may play a significant role in the activation of the same genes that are also regulated by microbial infection.

### *Drosomycin-GFP* expression

The array analysis identified *Drosomycin* as one of the genes that is differentially regulated by LB17 (Log2 = +2.18) and not LH14 infection (Table 3). To validate these observations *in vivo* and to determine the extent to which the gene is up-regulated, we infected hosts carrying *Drom-GFP* transgene. *Drom-GFP* is normally expressed in the adult or larval fat body after bacterial or fungal infection (Ferrandon *et al.*, 1998). The *Drosophila* fat body is an immune-responsive tissue involved in the production of antimicrobial peptides. At 3-5 hr post infection, more than 70% of the LB17-infected larvae had fat bodies with the highest fluorescence (90-100% GFP+ fat body cells), the remaining 30% of the infected larvae showed moderately high fluorescence (50-90% GFP+ fat body cells, Fig. 7a, Fig. 8 panels 1a-1b). In contrast, less than 20% larvae (n = 32) infected with LH14 showed fluorescence in a few cells of the fat body (Fig. 7a, Fig. 8 1c-1d). Similarly, at 10-12 hr and 20-22 hr post

infection, LB17-infected larvae had a higher number of individuals (n > 20) with more intensely fluorescing fat bodies than LH14-infected animals (Fig 7a, and compare Fig. 8 2a-2b to 2c-2d). *Drosomycin* is not detected in the array experiment at the last (20-22 hr) time point relative to its control (Fig. 7a, Fig. 8 3a-3b, and Table 3a). Except for one larva at 3-5 hr, none of the uninfected larvae showed any fluorescence (Fig. 7a, Fig. 8 1e, 2e, and 3e) and fat bodies of bacterially-challenged animals showed high fluorescence (Fig. 7b).

When *CecA1-GFP* carrying transgenic flies were infected with wasps, we found that infection (by either wasp) did not induce GFP expression (n > 10 for each wasp, and uninfected control). Surprisingly, the transgenic strain did not respond to bacterial infection either. However, 19 out of the 65 larvae carrying the transgene and also the *Toll* gain-of-function allele (*10b*), showed GFP-positive fat bodies (not shown), suggesting that the stock carries a transgene, and that the expression of the transgene is only partially under the control of the Toll pathway.

# DISCUSSION

The goal of this study was to identify a set of immunity and other genes that are modulated upon wasp infection. To this end, we have used two parasitoid wasps of *D. melanogaster* that differ in their immune mechanisms and degree of virulence. Our thrust here was to examine, if a subset of "immunity genes" defined in previous studies using microbial pathogens are also regulated by wasp infections, and if there is a difference in the expression of "wasp-induced immunity genes" induced or repressed by the two wasps. In addition, we examined whether the expression of other genes, whose functions are implicated in host metabolism and development, is also regulated by wasp infection.

## Virulence and immune suppression

*L. boulardi-17* and *L. heterotoma-14* are successful parasites and reproduce in wild type larvae of *D. melanogaster*. Their eggs are almost never encapsulated by these hosts (our unpublished observations). Phylogenetic studies (Schilthuizen *et al.*, 1998) suggest that these two wasp species belong to two of the four distinct "species groups" of the genus *Leptopilina*. Consistent with this notion, we and others have found that VLPs from these species are different from each other in their structure and mode of action. While *L. heterotoma* and *L. victoriae* clearly affect the viability of hematopoietic immune cells of the host, virulent strains of *L. boulardi* (e.g., G431) elicit a weaker response *in vivo* (egg encapsulation assay) and more restricted response on hemocytes in culture, where hemocyte viability is apparently not compromised (Rizki and Rizki, 1994; Dupas *et al.*, 1996; Russo *et al.*, 2001; Labrosse *et al.*, 2003;

Morales *et al.*, 2005; Chiu *et al.*, submitted). Evidence from both in vivo and in vitro experiments demonstrate that these differences in virulence, noted for other *L. heterotoma* and *L. boulardi* strains, also apply to the new strains used in our studies.

Encapsulation assays in this study show that while both LB17 and LH14 can suppress encapsulation of all their dominant eggs in *hopscotch*$^{Tum\text{-}l}$ larvae (Table 1, Fig. 3), only LH14 can protect all of its supernumerary eggs and larvae, whereas LB17 cannot protect *any* of the supernumerary individuals. It is striking that this difference is complete and independent of the number of supernumerary individuals per infected host (Table 1, Fig. 3 d-g arrowhead). These observations suggest that *hop*$^{Tum\text{-}l}$ larvae do not recognize LH14 as foreign, or that LH14 infection efficiently blocks the host's capacity to encapsulate any LH14 larvae, either the dominant or the smaller, supernumerary larvae.

In contrast, LB17, while successful at protecting the dominant egg, is unable to protect the supernumerary eggs/larvae, suggesting that, either the supernumerary eggs are recognized as non-self or that the mechanism of immune suppression is not strong enough to fully counteract host encapsulation. The ability of LH14 fluid (but not that of LB17 fluid) to promote the formation of bipolar lamellocytes is likely to account for its higher degree of virulence.

### *L. boulardi* infection modulates gene expression

In the last few years, gene expression studies using Affymetrix arrays have assessed global changes in adult *D. melanogaster* (De Gregorio *et al.*, 2001; Irving *et al.*, 2001, Boutros *et al.*, 2002, Roxstrom-Lindquist *et al.*, 2004). These studies have

provided an overview of the genes and pathways involved in the immune response to bacterial, fungal, protozoan, and viral infection, and contributed to the identification of many more genes genome-wide, which were previously not known for their functions in host defense. In the first study, adult male flies were immune challenged by septic injury using a tungsten needle dipped in a mixture of *E. coli* and *M. luteus* (De Gregorio *et al.*, 2001). In the same study, flies were also infected externally with the entomopathogenic fungus *Beauvaria bassiana*. Of the 13,197 genes tested (version 1 of *Drosophila* GeneChip Affymetrix Array), 400 genes were selected as *Drosophila* immune-regulated genes (DIRGs) that were up- or down-regulated 2 fold or more upon immune challenge. This selection threshold was used because it included 32 of 33 immunity-responsive genes previously identified. Among the 270 up-regulated genes, De Gregorio et al. found genes that code for PGRPs, GNBPs, serpins, proteases, Toll and Imd pathway proteins, and antimicrobial peptides. The up-regulation of the Toll and Imd pathways seems to account for most immunity genes regulated in response to either bacterial or fungal infection (De Gregorio *et al.*, 2002).

In a similar study, up to 543 genes were found to be up-regulated 2-fold or more after septic injury and fungal infection (Irving *et al.*, 2001). Many unknown genes were also found to be modulated by microbial infection in both studies. Interestingly, the expression of most antimicrobial peptide genes is highest between 9 and 12 hours after bacterial challenge, but *Metchinikowin* and *Drosomycin* were found to be highly up-regulated 72 hrs after fungal infection (Irving *et al.*, 2001).

Results in this study constitute the first set of expression data from parasitic wasp-infected *Drosophila* larvae. One of the most striking findings is that LB17 infection

induces an overall stronger molecular response (597 genes induced, 327 genes repressed) relative to LH14 infection (33 genes induced, 35 genes repressed; Fig. 6). These wasp-induced genes belong to several different functional groups including those with functions in host development and metabolism.

Pair-wise comparisons of induced or repressed genes by each wasp at each time point indicates that there is a mild overlap in the number of genes, including immunity genes, regulated in response to infection by either wasp (Fig. 5): of the 20 induced genes that intersect at 3-5 hr, 9 are immunity genes. Among these are six antimicrobial peptide (AMP) genes (*Attacin A, B, C, Cecropin C, Diptericin B, Metchnikowin*), and two recognition molecules (*PGRP-SB1, and PGRP-SD)*. Of the 5 genes that overlap in the comparison of up-regulated genes at 10-12 hr, 4 are immunity genes. This similar trend in the expression profiles of antimicrobial peptide and other genes possibly points to a common initial response to oviposition (along with VLPs and possible a few microbes) and local wound healing reaction. This interpretation of our data suggests that humoral components may play a minor, albeit significant role during the early phase of infection.

That the response to LB17 is more vigorous and overlaps significantly with genes in the Toll/Imd pathways (Tables 3a and 3b) is somewhat surprising as in a previous study, induction of antimicrobial peptide genes was not observed in a Northern analysis (Nicolas *et al.*, 1996). This discrepancy in observations may have to do with differences in sensitivities of the experimental approaches used. Whether the RNA of the immune-related molecules (see Table 3) are translated and actually participate in host defense against LB17 remains to be demonstrated, although

experiments in the literature support a clear role for many of the immunity genes in defense against microbial pathogens.

**Differences in virulence and gene expression**

The differences in the global gene expression profiles as well as on immunity genes (LB17 can elicit a clear and robust molecular response, whereas LH14 cannot) might suggest that LH14 has a mechanism to suppress the activation of these genes. If this is the case, then a surge of gene expression activity should be observed prior to the 3 hour time point. Instead, LH14 eggs, or presence of VLPs with the wasp eggs, do not provoke gene expression. A third scenario is that the destructive effect of LH14 VLPs on host hemocytes leads to blocking/disruption/attenuation of global gene expression in the larval fat body and other organs. Genetic evidence from the *domino* mutant, lacking hemocytes, supports the idea that hemocytes are necessary for the activation of antimicrobial peptide genes in the larval fat body (Braun *et al.*, 1998).

The observation that LH14 affects the expression of only two genes encoding proteases (in comparison to LB17 infection which regulates 41 proteolysis genes; or in comparison to bacterial or fungal infection which regulates 35 protease and 8 serpin genes, DeGregorio *et al.*, 2001), introduces the possibility that the proteolytic cascade (necessary for example for Toll pathway activation) is not triggered in LH14-infected larvae. These results are consistent with the idea that the major effect of LH14 is on the cellular immune response, and it only has a weak effect on gene expression as such. A weak effect of on gene expression is also observed when *Drosophila* adults are infected by *Drosophila* C virus, where only 11 genes were modulated in response

to the infection (Roxtrom-Lindquist *et al.*, 2004). Given that LH14 also introduces VLPs into its host, it raises the question if antiviral response is limited to hemocytes and because of the small number of hemocytes, gene expression changes are not reflected in RNA samples prepared from the entire body.

**Validation of the *Drosomycin* expression results *in vivo***

*In vivo* expression profiles of *Drosomycin-GFP* in wasp-infected transgenic larvae follow the same general trend of expression observed in the array experiments (2.18 and 1.16-induction level at 3-5 hours and 10-12 hours after infection, respectively; highest GFP levels at 3-4 hr, very high levels at 10-12 hr, and still clearly detectable, 20-22 hours after infection with LB17; Fig. 7a, Fig. 8 panels a-b; Table 3a). GFP fluorescence is continually detected at the last time point, most likely due to perdurance of GFP protein after its RNA levels decline. Consistent with previous findings, there is virtually no expression of *Drom-GFP* in larvae infected with LH14 as compared to uninfected controls at any of the three time points (Fig. 7a, Fig. 8 compare panels c-d with panel e).

*Drosomycin* provided an interesting "test case" for validation of array data as it is differentially regulated by the two wasps. *Drom-GFP* activation by LB17 *in vivo* clearly demonstrates that at least one of the two parasitic wasps tested can activate the expression of antifungal peptide gene in the appropriate immune organ of the larva, the fat body. The lack of *CecA1* activation by wasp infection may not be surprising as the *CecA1* gene does not appear to be activated by wasp infection as observed in the array analysis. Together the *Drom-GFP* and *CecA1-GFP* results suggest that there is

specificity in regulation of antimicrobial peptide genes and even within a small region of DNA where 4 members of the *Cecropin* gene family (99E2) are clustered. While *CecC* is activated by both wasps, *CecB* is uniquely regulated only by LB17 infection. These latter results with *CecB* and *CecC* need to be validated in molecular experiments. The relatively uniform levels of *Drom-GFP* expression in all the cells of the fat body suggests that gene activation in response to introduction of the wasp egg is not local, rather it reflects changes in the activation of the Toll pathway uniformly in the fat body.

**Concluding remarks**

Results of the preliminary study described here suggest that there are significant differences in the molecular outputs of gene expression when larval hosts are infected by wasps differing in their manner and degree of virulence. Our results suggest that infection by LB17 evokes an immune response as measured by changes in gene expression. A set of the genes regulated by LB17 is under the control of the Imd/Toll pathways raising the possibility that these genetic mechanisms participate in determining parasitoid virulence. It is clearly important to determine if other parasitic wasps of *D. melanogaster* that are also highly virulent (e.g., *L. victoriae and Ganaspis xanthopoda*), evoke weak responses similar to LH14 or if they first activate gene expression and then repress it. Conversely, it would be important to determine if avirulent strains of *L. boulardi* promote an even stronger gene expression response and, if so, whether additional genes are regulated or the genes identified in this study are more strongly regulated. Validation of our molecular data in follow-up

experiments is clearly important, as is the establishment of the role of products of immunity genes in host defense. In addition, characterization of development-specific genes identified in this study will be useful in understanding the effect of infection at very early stages of wasp development. Finally, a careful examination of genes that are downregulated will also reveal mechanisms of host-parasite interactions.

## REFERENCES

Asha, H., Nagy, I., Kovacs, G., Stetson, I.A., and Dearolf, C.R., 2003. Analysis of Ras-Induced Overproliferation in *Drosophila* Hemocytes. Genetics 163, 203-215.

Boutros, M., Agaisse, H., Perrimon, N., 2002. Sequential Activation of Signaling Pathways During Innante Immune Response in *Drosophila*. Developmental Cell 3, 711-722.

Bettencourt, R., Asha, H., Dearolf, C., Ip, Y.T., 2004, Journal of Cellular Biochemistry 92, 849-863.

Braun, A., Hoffmann, J.A., and Meister, M., 1998. Analysis of the Drosophila host defense in domino mutant larvae, which are devoid of hemocytes. Proc Natl Acad Sci 95, 14337-14342.

Brennan, C.A., and Anderson, K.V., 2004. *Drosophila*: the genetics of innate immune recognition and response. Annu. Rev. Immunol. 22, 457-483.

Bodian, D.L., Leung, S., Chiu, H., and Govind, S., 2004. Cytokines in *Drosophila* hematopoiesis and cellular immunity. Prog. Mol. Subcell. Biol. 34, 27-46.

Cerritelli, M.E., Cheng, N., Rosenberg, A.H., McPherson, C.E., Booy, F.P., and Steven, A.C., 1997. Encapsidated Conformation of Bacteriphage T7 DNA. Cell 91, 271-280.

Chiu, H., and Govind, S., 2002. Natural infection of D. melanogaster by virulent parasitic wasps induces apoptotic depletion of hematopoietic precursors. Cell Death and Differentiation 9, 1379-1381.

Dupas, S., Frehelin, F.F., and Carton, Y., 1996. Immune suppressive virus-like particles in a *Drosophila* parasitoid: significance of their intraspecific morphological variations.

De Gregorio, E., Spellman, P.T., Rubin, G.M., Lemaitre, B., 2001. Genome-wide analysis of the *Drosophila* immune response by using oligonucleotide microarrays. PNAS 98 (22), 12591-12595.

De Gregorio, E., Spellman, P.T., Tzou, P., Rubin, G.M., and Lemaitre, B., 2002. The Toll and Imd pathways are the major regulators of the immune response in *Drosophila*. The EMBO Journal, 21 (11), 2568-2579.

Eslin, P., Giordanengo, P., Fourdrain, Y., and Prevost, G., 1996. Avoidance of encapsulation in the absence of VLP by a braconid parasitoid of *Drosophila* larvae: and ultrastructural study. Canadian Journal of Zoology 74, 2193-2198.

Ferrandon, D., Jung, A.C., Criqui, M., Lemaitre, B., Uttenweiler-Joseph, S., Michaunt, L., Reichhart, J.M., Hoffmann, J.A., 1998. A drosomycin-GFP reporter transgene reveals a local immune response in *Drosophila* that is not dependent on the Toll pathway. EMBO Journal 17, 1217-1227.

Govind, S., and nehm, R.H. 2004. Innate immunity in fruit flies: a textbook example of genomic recycling. PLoS Biology 2(8), e276.

Hoffmann, B.A., and Meister, J.A. 1998. Analysis of *Drosophila* host defense in domino mutant larvae, which are devoid of hemocytes. Proc. Natl. Acad. Sci. 95(24), 14337-14342.

Hoffmann, J.A., 2003. The immune response of *Drosophila*. Nature 426, 33-38.

Hultmark, D., 2003. *Drosophila* immunity: paths and patterns. Curr. Opin. Immunol. 15, 12-19.

Irizarry, R.A., Hobbs, B., Collin, F., Beazer-Barclay, Y.D., Antonellis, K.J., Scherf, U.,and Speed, T.P., 2003. Exploration, Normalization, and Summaries of High Density Oligonucleotide Array Probe Level Data. Biostatistics. 4(2), 249-264.

Irving, P., Troxler, L., Heuer, T.S., Belvin, M., Kopczynski, C., Reichhart, J., Hoffman, J.A., and Hetru, C., 2001. A genome-wide analysis of immune responses in *Drosophila*. Proceedings to the National Academy of Science 98 (26), 15119-15124.

Khush, R.S., and Lemaitre, B., 2000. Genes that fight infection. Genetics of *Drosophila* Immunity. TIG, 16 (10), 442-449.

Labrosse, C., Carton, Y., Dubuffet, A., Drezen, J.M., Poirie, M., 2003. Active suppression of *D. melanogaster* immune response by long gland products of the parasitic wasp Leptopilina boulardi. Journal of Insect Physiology 49, 513-522.

Lanot, R., Zachary, D., Holder, F., Meister, M. 2001. Post-embryonic hematopoiesis in *Drosophila*. Developmental Biololgy 230, 243-257.

Lemaitre, B., Nicolas, E., Michaut, L., Reichhart, J., and Hoffmann, J.A., 1996. The dorsoventral regulatory gene cassette *spatzle/Toll/cactus* controls the potent antifungal response in *Drosophila* adults. Cell 86, 973-983.

Lemaitre, B., 2004. The road to Toll., Nat. Rev. Immunol. 4, 521-527.

Luo, H., Hanratty, W.P., and Dearolf, C.R., 1995. An Amino acid substitution in the *Drosophila* hopTum-l Jak kinase causes leukemia-like hematopoietic defects. EMBO J. 21, 1412-1420.

Meister, M., and Lagueux, M., 2003. *Drosophila* blood cells. Cellular Microbiology 5 (9), 573-580.

McGraw, L.A., Gibson, G., Clark, A.G., and Wolfner, M.F., 2004. Genes regulated by mating, sperm, or seminal proteins in mated female *Drosophila melanogaster*. Current Biology, 14, 1509-1514.

Morales, J., H. L. Chiu, R. Plaza, T. Oo, S. Hoskins, and S. Govind., 2005. Biogenesis, structure, and immune suppressive effects of virus-ike particles of a *Drosophila* parasitoid, Leptopilina victoriae. J. Insect Physiology, Special Issue "Physiological and biochemical relationships among non-poly-DNA viruses, parasitic wasps, and Their hosts". In press.

Nappi, A.J., Vass, E., Malagoli, D., and Carton, Y., 2004. The effects of parasite-derived immune-suppressive factors on the cellular innate immune and autoimmune responses of *Drosophila* melanogaster. J. Parasitol., 90, 1139-1149.

Nicolas, E., Nappi, A.J., Lemaitre, B., 1996. Expression of antimicrobial peptide genes after infection by parasitoid wasps in *Drosophila*. Developmental and Comparative Immunology 20(3), 175-181.

Qiu, P., Pan, P.C., and Govind, S., 1998. A role for the *Drosophila* Toll/cactus pathway in larval hematopoiesis. Development 125, 1909-1520.

Rizki, R.M., and Rizki, R.M., 1984a. The cellular defense system of Drosophila melanogaster. In Insect Ultrastructure, Vol. 2. Ed. by King, RC, and Akai, H. Plenum Publishing Corp. pp. 579-604.

Rizki, R.M., and Rizki, R.M., 1984b. Selective Destruction of a host blood cell type by parasitoid wasp. Proceedings to the National Academy of Science 81, 6154-6158.

Rizki, R.M, and Rizki, T.M., 1990. Parasitoid virus-like particles destroy *Drosophila* cellular immunity. Proceedings to the National Academy of Science 87, 8388-8392.

Rizki, T.M., Rizki, R.M., and Carton, Y., 1990. *Leptopilina heterotoma* and *L. boulardi*: Strategies to avoid Cellular Defense Responses of *Drosophila melanogaster*. Experimental Parasitology 70, 466-475.

Rizki, T.M., Rizki, R.M. 1991. Effects of lamellolysin from a parasitoid wasp on *Drosophila* blood cells in vitro. J. of Experimental Zoology 257, 236-244.

Rizki, T. M., and R. M. Rizki. 1992. Lamellocyte differentiation in *Drosophila* larvae parasitized by *Leptopilina*. Developmental and Comparative Immunology 16,103-110.

Rizki, T. M., and R. M. Rizki. 1994. Parasitoid-induced cellular immune deficiency in *Drosophila*. Primordial Immunity: Foundations for the Vertebrate Immune system. Annals of the New York Academy of Sciences 712, 178-194.

Roxstrom-Lindquist, K., Terenius, O., and Faye, I., 2004. Parasite-specific immue response in adult *Drosophila* melanogaster: a genomic study. EMBO reports 5 (2), 207-212.

Russo, J., Dupas, S., Frey, F., Carton, Y., and Brehelin, M., 1996. Insect immunity: early events in the encapsulation process of parasitoid (*Leptopilina boulardi*) eggs in resistant and susceptible strains of *Drosophila*. Parasitology 112, 135-142.

Russo, J., Brehelin, M., and Carton, Y., 2001. Haemocyte changes in resistant and susceptible strains of *D. melanogaster* caused by virulent and avirulent strains of the parasitic wasp Leptopilina boulardi. Journal of Insect Physiology, 47, 167-172.

Schilthuizen, M., Nordlander, G., Stouthamer, R., and Van Alphen, J.M. 1998. Morphological and molecular phylogenetics in the genus Leptopilina (Hymenoptera: Cynipoidea: Eucoilidae). Systematic Entomology 23, 253-264.

Sorrentino, R.P., Carton, Y., and Govind, S., 2002. Cellular Immune Response to Parasite Infection in the *Drosophila* Lymph Gland Is Developmentally Regulated. Developmental Biology 243, 65-80.

Sorrentino, R.P., Melk, J.P., and Govind, S.G., 2004. Genetic Analysis of Contributions of Dorsal Group and JAK-Stat92E Pathway Genes to Larval Hemocyte Concentration and the Egg Encapsulation Response in *Drosophila*. Genetics Society of America 166, 1343-1356.

Smith, P.K., Drohn, R.I., Hermanson, G.T., Mallia, A.K., Gartner, F.H., Provenzano, M.D., Fujimoto, E.K., Goeke, N.M., Olson, B.J., and Kenk, D.C. 1985. Measurement of protein using bichinoic acid. Anal. Biochem. 150, 76-85.

Takehana, A., Yano, T., Mita, S., Kotani, A., Oshima, Y., and Kurata, S., 2004. Peptidoglycan recognition protein PGRP-LE and PGRP-LC act synergistically in *Drosophila* immunity. EMBO 23, 4690-4700.

Tzou, P., Ohresser, D.F., Capovilla, J.R., Lemaitre, B., Hoffmann, J.A., and Imler, J., 2000. Tissue-specific inducible expression of antimicrobial peptide genes in *Drosophila* surface epithelia. Immunity 13, 737-748.

Tzou, P., De Gregorio, E., Lemaitre, B., 2002. How *Drosophila* combats microbial infection: a model to study innate immunity and host-pathogen interactions. Current Opinion in Microbiology, 5, 102-110.

Wang, J., Kean, L., Yang, J., Allan, A.K., Davies, S.A., Herzyk, P., and Dow, J.A., Function-informed transcriptome analysis of *Drosophila* renal tubule. Genome Biology 5, R69

Zettervall, C., Anderl, I., Williams, M.J., Palmer, R., Durucz, E., Ando, I., and Hultmark, D., 2004. A directed screen for genes involved in *Drosophila* blood cell activation. PNAS 101 (39), 14192-14197.

**Table 1.** *L. boulardi-17* wasp supernumerary larvae are encapsulated by *hopscotch*$^{Tum\text{-}l}$ larvae. Host *Drosophila* larvae (*hopscotch*$^{Tum\text{-}l}$) were infected with *L. hetertoma-14* (LH14) or *L. boulardi-17* (LB17). Five days after infection, host larvae were observed for the presence of melanotic tumors, and dissected to observe encapsulation of wasp egg or wasp larva. In the first row, **n** refers to the number of host larvae scored. In all other rows, **n** refers to the number of wasp eggs or larvae dissected from 101 LB17-infected hosts, or 47 LH14-infected hosts. N/A = not applicable.

| | **Control Uninfected** | **LB17 Infected** | **LH14 Infected** |
|---|---|---|---|
| **Host larvae with tumors** | 100% (n=122) | 100% (n = 101) | 100% (n = 47) |
| **Encapsulation of of dominant larvae** | N/A | 0% (n = 101) | 0% (n = 47) |
| **Encapsulation of supernumerary larva** | N/A | 100% (n = 55) | 0% (n = 19) |
| **Encapsulation of supernumerary eggs** | N/A | 100% (n = 4) | 0% (n = 2) |

**Table 2.** Comparison of differentially expressed genes at three different probability values. Statistical t-tests were performed to compare the expression level of genes from three arrays done on *D. melanogaster* infected with wasp versus the expression level of genes from three arrays done on uninfected hosts at each time point. The wasps used to infect were *L. boulardi-17* (LB17) and *L. heterotoma-14* (LH14). Genes (probe sets) differentially expressed 2-fold or more ($\log2 \geq +1$, or $\log2 \leq -1$) were identified at $p < 0.2$, $< 0.1$, and $< 0.05$. The statistical analyses were done in ArrayAssist. Note that the number of genes regulated at $p < 0.2$ is not much higher than that at $p < 0.1$.

**1a**

| Genes up-regulated at 3-5 hr | | |
|---|---|---|
| **P** | **LB17 Inf.** | **LH14 Inf.** |
| <0.05 | 110 | 28 |
| <0.10 | 113 | 29 |
| <0.20 | 114 | 29 |

**1b**

| Genes down-regulated at 3-5 hr | | |
|---|---|---|
| **P** | **LB17 Inf.** | **LH14 Inf.** |
| <0.05 | 111 | 19 |
| <0.10 | 117 | 20 |
| <0.20 | 118 | 20 |

**1c**

| Genes up-regulated at 10-12 hr | | |
|---|---|---|
| **P** | **LB17 Inf.** | **LH14 Inf.** |
| <0.05 | 454 | 5 |
| <0.10 | 457 | 8 |
| <0.20 | 459 | 9 |

**1d**

| Genes down-regulated at 10-12 hr | | |
|---|---|---|
| **P** | **LB17 Inf.** | **LH14 Inf.** |
| <0.05 | 126 | 5 |
| <0.10 | 131 | 6 |
| <0.20 | 133 | 10 |

**1e**

| Genes up-regulated at 20-22 hr | | |
|---|---|---|
| **P** | **LB17 Inf.** | **LH14 Inf.** |
| <0.05 | 127 | 3 |
| <0.10 | 128 | 3 |
| <0.20 | 128 | 3 |

**1f**

| Genes down-regulated at 20-22 hr | | |
|---|---|---|
| **P** | **LB17 Inf.** | **LH14 Inf.** |
| <0.05 | 134 | 13 |
| <0.10 | 135 | 13 |
| <0.20 | 139 | 16 |

**Table 3a.** Immunity genes regulated by wasp infection in *Drosophila melanogaster.*

## PGRPs

| Affy Probe | Gene Title | Gene Symbol | 3-5_Bou | 10-12_Bou | 20-22_Bou | 3-5_Het | 10-12_Het | 20-22_Het | GO Biological Process Description |
|---|---|---|---|---|---|---|---|---|---|
| 1625486_a_at | Peptidoglycan recognition protein LA | PGRP-LA | * | 1.15 | * | * | * | * | immune response /// defense response /// detection of bacteria |
| 1628884_at | Peptidoglycan recognition protein SA | PGRP-SA | 1.29 | * | * | * | * | * | response to pest, pathogen or parasite /// anti-Gram-positive bacterial polypeptide induction /// immune response /// defense response /// detection of bacteria /// immune response /// regulation of Toll signaling pathway /// defense response to Gram-positive bacteria |
| 1636490_at | --- | PGRP-SB1 | 3.09 | * | * | 3.80 | * | * | immune response /// defense response |
| 1633545_at | --- | PGRP-SD | 1.42 | * | * | 1.67 | * | * | immune response /// defense response |

## Immune Induced Molecules

| Affy Probe | Gene Title | Gene Symbol | 3-5_Bou | 10-12_Bou | 20-22_Bou | 3-5_Het | 10-12_Het | 20-22_Het | GO Biological Process Description |
|---|---|---|---|---|---|---|---|---|---|
| 1633053_at | Immune induced molecule 1 | IM1 | 4.46 | 3.51 | 1.00 | * | * | * | defense response |
| 1640360_at | Immune induced molecule 2 | IM2 | 3.36 | 3.61 | * | * | 1.25 | * | defense response |
| 1622893_at | Immune induced molecule 3 | IM3 | 3.27 | 3.41 | * | * | * | * | defense response /// antibacterial humoral response /// Toll signaling pathway |
| 1626345_at | Immune induced molecule 4 | IM4 | 3.12 | 2.72 | 1.24 | * | * | * | defense response /// immune response |
| 1626319_a_at | Immune induced molecule 10 /// | IM10 /// CG33470 | 3.01 | 1.54 | 1.02 | * | * | * | defense response /// antibacterial humoral response /// Toll signaling pathway |
| 1639019_s_at | Immune induced molecule 10 /// | IM10 /// CG33470 | 3.88 | 3.32 | 2.41 | * | * | * | defense response /// antibacterial humoral response /// Toll signaling pathway |

Table 3a. (cont.)

| | | | | | | | | | |
|---|---|---|---|---|---|---|---|---|---|
| 1629530_at | Immune induced molecule 23 | IM23 | 4.04 | 3.54 | * | * | * | * | defense response /// antibacterial humoral response /// Toll signaling pathway |

## Antimicrobial Peptides

| Affy Probe | Gene Title | Gene Symbol | 3-5_Bou | 10-12_Bou | 20-22_Bou | 3-5_Het | 10-12_Het | 20-22_Het | GO Biological Process Description |
|---|---|---|---|---|---|---|---|---|---|
| 1625124_at | Attacin-A | AttA | 3.99 | * | * | 3.25 | * | * | Defense response to Gram-negative bacteria |
| 1627551_s_at | Attacin-A /// Attacin-B | AttA /// AttB | 3.62 | * | * | 2.95 | * | * | Defense response to Gram-negative bacteria |
| 1641419_at | Attacin-C | AttC | 3.02 | 2.99 | * | 2.49 | 2.53 | * | Defense response to bacteria |
| 1626530_at | Cecropin B | CecB | 1.18 | * | * | * | * | * | Defense response to Gram-negative and Gram-positive bacteria and fungi/salivary gland cell death |
| 1632719_at | Cecropin C | CecC | 2.91 | * | * | 2.25 | * | * | Defense response to Gram-negative, Gram-positive bacteria and fungi |
| 1638235_at | Diptericin B | DptB | 1.99 | 2.30 | * | 2.55 | 2.58 | * | antibacterial humoral response |
| 1635189_at | Drosomycin | Drs | 2.18 | 1.16 | * | * | * | * | Defense response to fungi |
| 1627613_at | Metchnikowin | Mtk | 2.50 | 1.67 | * | 2.58 | 1.64 | * | Defense response to Gram-positive bacteria and fungi |

## Tots and Heat Shock Proteins

| Affy Probe | Gene Title | Gene Symbol | 3-5_Bou | 10-12_Bou | 20-22_Bou | 3-5_Het | 10-12_Het | 20-22_Het | GO Biological Process Description |
|---|---|---|---|---|---|---|---|---|---|
| 1638872_at | Heat shock protein 68 | Hsp68 | * | * | -1.23 | * | * | * | protein folding /// protein complex assembly /// defense response /// response to heat |
| 1632841_x_at | Heat-shock-protein-70Bc /// Heat-shock-protein-70Aa /// Heat-shock-protein-70Ab /// Heat-shock-protein-70Ba /// /// Heat-shock-protein-70Bb | Hsp70Bc /// Hsp70Aa /// Hsp70Ab /// Hsp70Ba /// Hsp70Bbb /// Hsp70Bb | -1.94 | * | * | * | * | * | protein folding /// protein complex assembly /// defense response /// response to heat /// response to heat |

**Table 3a.** (cont.)

| | | | | | | | | | |
|---|---|---|---|---|---|---|---|---|---|
| 1639571_s_at | Heat-shock-proteins-70Ab, -70Aa, -70Bc, -70Ba, -70Bb | Hsp70Ab /// Hsp70Aa /// Hsp70Bc /// Hsp70Ba /// Hsp70Bbb /// Hsp70Bb | -1.76 | -1.48 | * | * | * | * | protein folding /// protein complex assembly /// defense response /// response to heat /// response to heat |
| 1626821_s_at | Heat-shock-proteins-70Bb, 70Bc, -70Ba, -70Aa, -70Ab | Hsp70Bb /// Hsp70Bc /// Hsp70Ba /// Hsp70Bbb /// Hsp70Aa /// Hsp70Ab | -1.83 | * | * | * | * | * | protein folding /// protein complex assembly /// defense response /// response to heat /// response to heat |
| 1635549_at | Turandot A | TotA | 5.23 | 3.97 | 1.54 | -1.88 | -2.18 | -1.85 | response to stress///humoral defense mechanism/// response to heat |
| 1627975_at | Turandot B | TotB | 1.64 | 1.39 | * | * | * | * | humoral defense mechanism |
| 1639323_at | Turandot C | TotC | 6.27 | 6.53 | 5.20 | * | * | * | humoral defense mechanism |

## Teps

| Affy Probe | Gene Title | Gene Symbol | 3-5_Bou | 10-12_Bou | 20-22_Bou | 3-5_Het | 10-12_Het | 20-22_Het | GO Biological Process Description |
|---|---|---|---|---|---|---|---|---|---|
| 1637734_at | Thiolester containing protein I | TepI | 3.60 | 4.25 | 1.81 | * | * | -1.00 | antibacterial humoral response |
| 1630067_a_at | Thiolester containing protein II | TepII | 2.29 | 1.74 | * | * | * | * | antibacterial humoral response |

## Melanization Related and Clotting

| Affy Probe | Gene Title | Gene Symbol | 3-5_Bou | 10-12_Bou | 20-22_Bou | 3-5_Het | 10-12_Het | 20-22_Het | GO Biological Process Description |
|---|---|---|---|---|---|---|---|---|---|
| 1628298_at | Diphenol oxidase A3 | Dox-A3 | * | * | 1.31 | * | * | * | defense response |
| 1639320_a_at | Dopa decarboxylase | Ddc | * | 1.24 | * | * | * | * | dopamine biosynthesis from tyrosine /// serotonin biosynthesis from tryptophan /// melanin biosynthesis /// pigmentation |

Table 3a. (cont.)

| | | | | | | | | | |
|---|---|---|---|---|---|---|---|---|---|
| 1639321_s_at | Toll | Tl | 1.34 | * | * | * | * | * | defense response to bacteria and fungi /// dorsal/ventral axis specification /// hemopoiesis /// melanization defense response /// hemocyte proliferation |
| 1628018_at | Hemolectin | Hml | * | * | * | -1.00 | * | * | cell adhesion /// hemostasis /// hemostasis /// defense response |

## Peroxidase, Peroxiredoxin, Response to Toxin, and Reactive Oxygen Species

| Affy Probe | Gene Title | Gene Symbol | 3-5_Bou | 10-12_Bou | 20-22_Bou | 3-5_Het | 10-12_Het | 20-22_Het | GO Biological Process Description |
|---|---|---|---|---|---|---|---|---|---|
| 1623410_at | Peroxidase | Pxd | -1.26 | * | * | * | * | * | insect chorion formation |
| 1630927_x_at | Peroxidase | Pxd | -1.08 | * | * | * | * | * | insect chorion formation |
| 1631628_s_at | Peroxiredoxin 2540 /// /// Peroxiredoxin 2540 | Prx2540-1 /// CG12896 /// Prx2540-2 | 3.18 | 1.43 | * | 2.52 | * | * | oxygen and reactive oxygen species metabolism /// defense response /// mesoderm development |
| 1633471_at | Peroxiredoxin 2540 /// Peroxiredoxin 2540 /// | Prx2540-2 /// Prx2540-1 /// CG12896 | 2.37 | * | * | 2.05 | * | * | oxygen and reactive oxygen species metabolism /// defense response /// mesoderm development |
| 1638182_at | --- | CG5999 | * | -1.56 | -1.26 | * | * | * | polysaccharide metabolism /// defense response /// steroid metabolism /// response to toxin |
| 1623752_at | --- | CG5959 | * | 2.02 | * | * | * | * | defense response /// response to toxin |
| 1638006_at | --- | CG10211 | * | 1.30 | * | * | * | * | oxygen and reactive oxygen species metabolism /// defense response |
| 1623372_at | --- | CG5873 | * | 3.19 | * | * | * | * | oxygen and reactive oxygen species metabolism /// defense response |
| 1631111_at | --- | CG6879 | * | 1.24 | * | * | * | * | oxygen and reactive oxygen species metabolism /// defense response |

## Serine Proteases and Serpins

| Affy Probe | Gene Title | Gene Symbol | 3-5_Bou | 10-12_Bou | 20-22_Bou | 3-5_Het | 10-12_Het | 20-22_Het | GO Biological Process Description |
|---|---|---|---|---|---|---|---|---|---|
| 1623312_s_at | --- | CG11836 | * | 1.15 | * | * | * | * | defense response /// proteolysis |
| 1626903_at | --- | CG3355 | * | 4.39 | * | * | * | * | Defense response /// proteolysis |

**Table 3a.** (cont.)

| | | | | | | | | | |
|---|---|---|---|---|---|---|---|---|---|
| 1632933_at | --- | CG6865 | * | * | * | * | -1.54 | * | defense response /// proteolysis and peptidolysis |
| 1625130_at | --- | CG8170 | * | 3.14 | * | * | * | * | defense response /// proteolysis and peptidolysis |
| 1626272_s_at | --- | CG3066 | 1.53 | * | * | * | * | * | proteolysis /// defense response |
| 1630598_at | --- | CG18179 | * | -1.57 | -1.94 | * | * | * | proteolysis and peptidolysis |
| 1638413_at | --- | CG18180 | * | -1.03 | * | * | * | * | proteolysis and peptidolysis |
| 1638413_at | --- | CG18180 | * | -1.03 | * | * | * | * | proteolysis and peptidolysis |
| 1636946_at | --- | CG6687 | 1.57 | 1.27 | * | * | * | * | proteolysis and peptidolysis |
| 1636653_at | necrotic | nec | 1.44 | * | * | * | * | * | proteolysis and peptidolysis /// antifungal humoral response, /// defense response /// Toll signaling pathway /// |
| 1634848_at | /// | CG16705 /// CG18754 | 2.54 | 1.55 | * | * | * | * | regulation of amino acid biosynthesis /// proteolysis and peptidolysis |

## Cytochrome P450s

| Affy Probe | Gene Title | Gene Symbol | 3-5_Bou | 10-12_Bou | 20-22_Bou | 3-5_Het | 10-12_Het | 20-22_Het | GO Biological Process Description |
|---|---|---|---|---|---|---|---|---|---|
| 1631300_at | Cytochrome P450-18a1 | Cyp18a1 | -1.37 | 1.52 | * | * | * | * | steroid biosynthesis |
| 1641022_a_at | Cytochrome P450-18a1 | Cyp18a1 | -1.37 | 1.67 | * | * | * | * | steroid biosynthesis |

## Others

| Affy Probe | Gene Title | Gene Symbol | 3-5_Bou | 10-12_Bou | 20-22_Bou | 3-5_Het | 10-12_Het | 20-22_Het | GO Biological Process Description |
|---|---|---|---|---|---|---|---|---|---|
| 1639724_at | --- | CG14250 | * | 3.27 | * | * | * | * | --- |
| 1631660_at | --- | CG15065 | 4.13 | 4.04 | 3.14 | * | * | * | --- |
| 1624057_at | --- | CG16713 | 1.05 | * | * | * | * | * | --- |
| 1623871_at | --- | CG18563 | 3.44 | 2.60 | * | * | * | * | --- |
| 1635968_at | --- | CG3604 | * | * | 1.93 | * | * | * | --- |
| 1640399_at | --- | CG3775 | -1.01 | -1.19 | * | * | * | * | --- |
| 1625698_at | --- | CG6639 | 4.88 | 4.00 | 2.91 | * | * | * | --- |
| 1633812_at | --- | CG9080 | * | * | -1.12 | * | * | * | --- |
| 1640037_at | --- | CG7798 | * | -1.86 | * | * | * | * | antimicrobial humoral response (sensu Protostomia) |
| 1637198_at | --- | CG10345 | * | 1.01 | * | * | * | * | apoptosis /// defense response |

**Table 3a.** (cont.)

| | | | | | | | | | |
|---|---|---|---|---|---|---|---|---|---|
| 1640616_at | --- | CG17974 | * | -1.63 | * | * | * | * | defense response |
| 1637851_at | --- | CG7422 | -1.47 | 2.15 | * | * | * | * | defense response |
| 1623710_at | --- | CG5847 | -1.16 | 2.09 | -1.08 | * | * | * | defense response /// cell adhesion |
| 1631280_at | --- | CG9095 | * | 2.53 | * | * | * | * | defense response /// cell adhesion |
| 1630260_at | --- | CG31832 | * | 1.60 | 1.35 | * | * | * | Defense response to bacteria |
| 1633251_at | --- | CG15829 | * | -1.43 | * | * | * | * | lipid transport /// cell acyl-CoA homeostasis |
| 1627271_at | --- | CG13422 | 2.44 | 2.31 | * | * | * | * | polysaccharide metabolism /// defense response to Gram-negative bacteria |
| 1633167_s_at | /// | CG32496 /// CG6788 | * | 1.21 | 1.06 | * | * | * | Defense response to bacteria /// cell adhesion |
| 1625276_a_at | Ecdysone-induced protein 28/29kD | Eip71CD | * | 1.10 | * | * | * | * | protein modification /// response to stress /// defense response /// salivary gland cell death /// autophagic cell death /// sulfur amino acid metabolism |
| 1640565_at | Ejaculatory bulb protein III | PebIII | * | 0.99 | * | * | * | * | sensory perception /// response to virus /// metamorphosis (sensu Insecta) |
| 1626429_at | Larval serum protein 1 | Lsp1 | -1.51 | * | * | -1.35 | * | * | --- |
| 1628699_at | Larval serum protein 1 | Lsp1 | -1.54 | -1.02 | * | -1.54 | * | * | --- |
| 1631803_at | Larval serum protein 1 | Lsp1 | -4.48 | -4.51 | -1.44 | -4.12 | * | * | --- |
| 1641634_at | Larval serum protein 2 | Lsp2 | * | -5.67 | -1.64 | * | * | * | --- |
| 1632591_at | Pherokine 3 | Phk-3 | * | 1.24 | * | * | * | * | sensory perception /// response to bacteria /// metamorphosis/// signal transduction /// embryogenesis/// spermatogenesis /// oogenesis development (sensu Insecta) |
| 1638512_at | Stubble | Sb | * | 1.35 | * | * | * | * | defense response /// cytoskeleton organization and biogenesis /// proteolysis and peptidolysis /// morphogenesis of larval imaginal disc epithelium |
| 1635267_s_at | Tetraspanin 66E | Tsp66E | * | 1.66 | * | * | * | * | defense response /// signal transduction /// cell-cell adhesion |

**Table 3a.** (cont.)

| | | | | | | | | | |
|---|---|---|---|---|---|---|---|---|---|
| 1626546_s_at | Tetraspanin 74F | Tsp74F | * | 1.09 | * | * | * | * | cell motility /// defense response /// cytoskeleton organization and biogenesis /// signal transduction /// cell-cell adhesion |
| 1639299_at | UDP-glycosyltransferase 37c1 | Ugt37c1 | * | * | 1.25 | * | * | * | polysaccharide metabolism /// defense response /// steroid metabolism /// response to toxin |

**Table 3b.** Wasp-regulated *Drosophila* immunity genes mediated by Relish and/or Spatzle.

**Induced DIRGs**

Genes regulated by Relish

| Affy Probe | Gene Title | Gene Symbol | 3-5_Bou | 10-12_Bou | 20-22_Bou | 3-5_Het | 10-12_Het | 20-22_Het | GO Biological Process Description |
|---|---|---|---|---|---|---|---|---|---|
| 1633545_at | --- | PGRP-SD | 1.42 | * | * | 1.67 | * | * | *immune response /// defense response* |
| 1633251_at | --- | CG15829 | * | -1.43 | * | * | * | * | lipid transport /// cell acyl-CoA homeostasis |

Genes regulated by Relish and Spatzle

Group A

| Affy Probe | Gene Title | Gene Symbol | 3-5_Bou | 10-12_Bou | 20-22_Bou | 3-5_Het | 10-12_Het | 20-22_Het | GO Biological Process Description |
|---|---|---|---|---|---|---|---|---|---|
| 1625698_at | --- | CG6639 | 4.88 | 4.00 | 2.91 | * | * | * | --- |
| 1636946_at | --- | CG6687 | 1.57 | 1.27 | * | * | * | * | proteolysis and peptidolysis |
| 1625124_at | Attacin-A | AttA | 3.99 | * | * | 3.25 | * | * | Defense response to Gram-negative bacteria |
| 1627551_s_at | Attacin-A /// Attacin-B | AttA /// AttB | 3.62 | * | * | 2.95 | * | * | Defense response to Gram-negative bacteria |
| 1635189_at | Drosomycin | Drs | 2.18 | 1.16 | * | * | * | * | Defense response to fungi |
| 1627613_at | Metchnikowin | Mtk | 2.50 | 1.67 | * | 2.58 | 1.64 | * | Defense response to Gram-positive bacteria and fungi |

Group B

| Affy Probe | Gene Title | Gene Symbol | 3-5_Bou | 10-12_Bou | 20-22_Bou | 3-5_Het | 10-12_Het | 20-22_Het | GO Biological Process Description |
|---|---|---|---|---|---|---|---|---|---|
| 1628884_at | Peptidoglycan recognition protein SA | PGRP-SA | 1.29 | * | * | * | * | * | response to pest, pathogen or parasite /// anti-Gram-positive bacterial polypeptide induction /// immune response /// defense response /// detection of bacteria /// immune response /// regulation of Toll signaling pathway /// defense response to Gram-positive bacteria |
| 1630067_a_at | Thiolester containing protein II | TepII | 2.29 | 1.74 | * | * | * | * | antibacterial humoral response |
| 1635968_at | --- | CG3604 | * | * | 1.93 | * | * | * | --- |

**Table 3b.** (cont.)

| | | | | | | | | | |
|---|---|---|---|---|---|---|---|---|---|
| 1639320_a_at | Dopa decarboxylase | Ddc | * | 1.24 | * | * | * | * | dopamine biosynthesis from tyrosine /// serotonin biosynthesis from tryptophan /// melanin biosynthesis /// pigmentation |
| 1633812_at | --- | CG9080 | * | * | -1.12 | * | * | * | --- |
| 1626530_at | Cecropin B | CecB | 1.18 | * | * | * | * | * | Defense response to Gram-negative and Gram-positive bacteria and fungi/salivary gland cell death |
| 1632719_at | Cecropin C | CecC | 2.91 | * | * | 2.25 | * | * | Defense response to Gram-negative, Gram-positive bacteria and fungi |

Group C

| Affy Probe | Gene Title | Gene Symbol | 3-5_Bou | 10-12_Bou | 20-22_Bou | 3-5_Het | 10-12_Het | 20-22_Het | GO Biological Process Description |
|---|---|---|---|---|---|---|---|---|---|
| 1638235_at | Diptericin B | DptB | 1.99 | 2.30 | * | 2.55 | 2.58 | * | antibacterial humoral response |

Genes regulated by Spatzle

| Affy Probe | Gene Title | Gene Symbol | 3-5_Bou | 10-12_Bou | 20-22_Bou | 3-5_Het | 10-12_Het | 20-22_Het | GO Biological Process Description |
|---|---|---|---|---|---|---|---|---|---|
| 1627271_at | --- | CG13422 | 2.44 | 2.31 | * | * | * | * | polysaccharide metabolism /// defense response to Gram-negative bacteria |
| 1623871_at | --- | CG18563 | 3.44 | 2.60 | * | * | * | * | --- |
| 1626272_s_at | --- | CG3066 | 1.53 | * | * | * | * | * | proteolysis /// defense response |
| 1634848_at | /// | CG16705 /// CG18754 | 2.54 | 1.55 | * | * | * | * | regulation of amino acid biosynthesis /// proteolysis and peptidolysis |
| 1624057_at | --- | CG16713 | 1.05 | * | * | * | * | * | --- |
| 1640360_at | Immune induced molecule 2 | IM2 | 3.36 | 3.61 | * | * | 1.25 | * | defense response |
| 1631660_at | --- | CG15065 | 4.13 | 4.04 | 3.14 | * | * | * | --- |
| 1639724_at | --- | CG14250 | * | 3.27 | * | * | * | * | --- |
| 1636653_at | necrotic | nec | 1.44 | * | * | * | * | * | proteolysis and peptidolysis /// antifungal humoral response, /// defense response /// Toll signaling pathway /// |

**Table 3b.** (cont.)

| | | | | | | | | | |
|---|---|---|---|---|---|---|---|---|---|
| 1639321_s_at | Toll | Tl | 1.34 | * | * | * | * | * | defense response to bacteria and fungi /// dorsal/ventral axis specification /// hemopoiesis /// melanization defense response /// hemocyte proliferation |
| 1623410_at | Peroxidase | Pxd | -1.26 | * | * | * | * | * | insect chorion formation |
| 1630927_x_at | Peroxidase | Pxd | -1.08 | * | * | * | * | * | insect chorion formation |

**Repressed DIRGs**

Genes regulated by Relish

| Affy Probe | Gene Title | Gene Symbol | 3-5_Bou | 10-12_Bou | 20-22_Bou | 3-5_Het | 10-12_Het | 20-22_Het | GO Biological Process Description |
|---|---|---|---|---|---|---|---|---|---|
| 1638413_at | --- | CG18180 | * | -1.03 | * | * | * | * | proteolysis and peptidolysis |
| 1630598_at | --- | CG18179 | * | -1.57 | -1.94 | * | * | * | proteolysis and peptidolysis |

Genes regulated by Spatzle

| Affy Probe | Gene Title | Gene Symbol | 3-5_Bou | 10-12_Bou | 20-22_Bou | 3-5_Het | 10-12_Het | 20-22_Het | GO Biological Process Description |
|---|---|---|---|---|---|---|---|---|---|
| 1640399_at | --- | CG3775 | -1.01 | -1.19 | * | * | * | * | --- |
| 1631300_at | Cytochrome P450-18a1 | Cyp18a1 | -1.37 | 1.52 | * | * | * | * | steroid biosynthesis |
| 1641022_a_at | Cytochrome P450-18a1 | Cyp18a1 | -1.37 | 1.67 | * | * | * | * | steroid biosynthesis |

Genes regulated by Relish and Spatzle

| Affy Probe | Gene Title | Gene Symbol | 3-5_Bou | 10-12_Bou | 20-22_Bou | 3-5_Het | 10-12_Het | 20-22_Het | GO Biological Process Description |
|---|---|---|---|---|---|---|---|---|---|
| 1626429_at | Larval serum protein 1 | Lsp1 | -1.51 | * | * | -1.35 | * | * | --- |
| 1628699_at | Larval serum protein 1 | Lsp1 | -1.54 | -1.02 | * | -1.54 | * | * | --- |
| 1631803_at | Larval serum protein 1 | Lsp1 | -4.48 | -4.51 | -1.44 | -4.12 | * | * | --- |
| 1641634_at | Larval serum protein 2 | Lsp2 | * | -5.67 | -1.64 | * | * | * | --- |

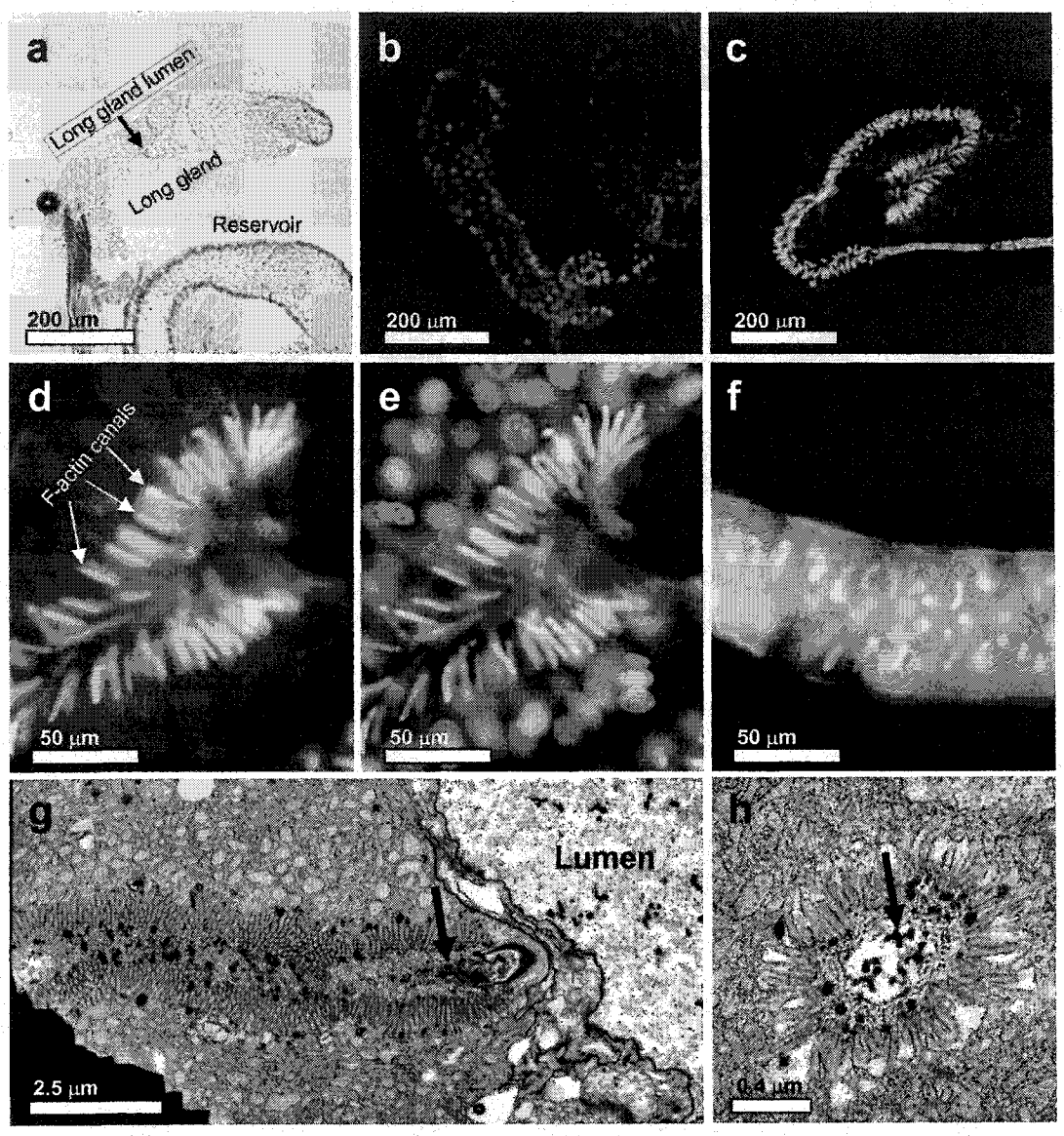


**Figure 1.** Intracellular canals in the long glands of *L. heterotoma-14*, *L. boulardi-17*, and *L. victoriae* connect secretory cells and the long gland lumen. Bright field microscopy reveals the overall morphology of the long gland from *L. heterotoma-14* (**a**). Ultra-violet fluorescence microscopy allows visualization of Hoechst-stained nuclei in the long gland of *L. heterotoma-14*, which surround the long gland lumen (**b** and **e**). Rhodamine-labeled phalloidin stains F-actin within canals found in the long glands of *L. heterotoma-14* (**c, d, e**), and *L. boulardi-17* (**f**), and *L. victoriae*. Large nuclei are located peripherally, whereas the canals are oriented towards the lumen (e). Panels **g** and **h** are transmission electron micrographs showing canals from *L. victoriae* in longitudinal (**g**) and transverse (**h**) views. Note that canals are surrounded by microvilli-like structures, which appear to contain filamentous actin, arrows in panels **g** and **h** point to VLP precursors found within canals.

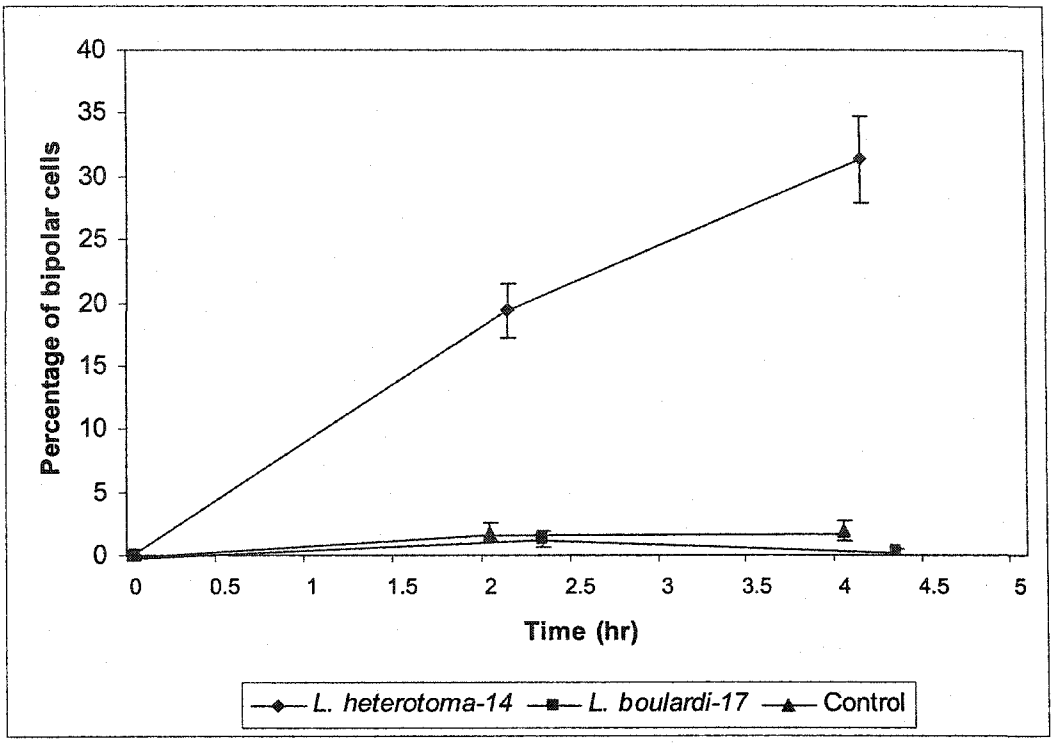


**Figure 2**. *Drosophila* lamellocytes are susceptible to lysis by the long gland reservoir fluid from *L. heterotoma-14* females, but not from *L. boulardi-17* females. Hemocytes obtained from *hopscotch*$^{Tum\text{-}l}$ mutant larvae were incubated *in vitro* with 2.1 μg of wasp fluid protein, or with PBS (control). The same amount of protein (2.1 μg) was used in each experiment.

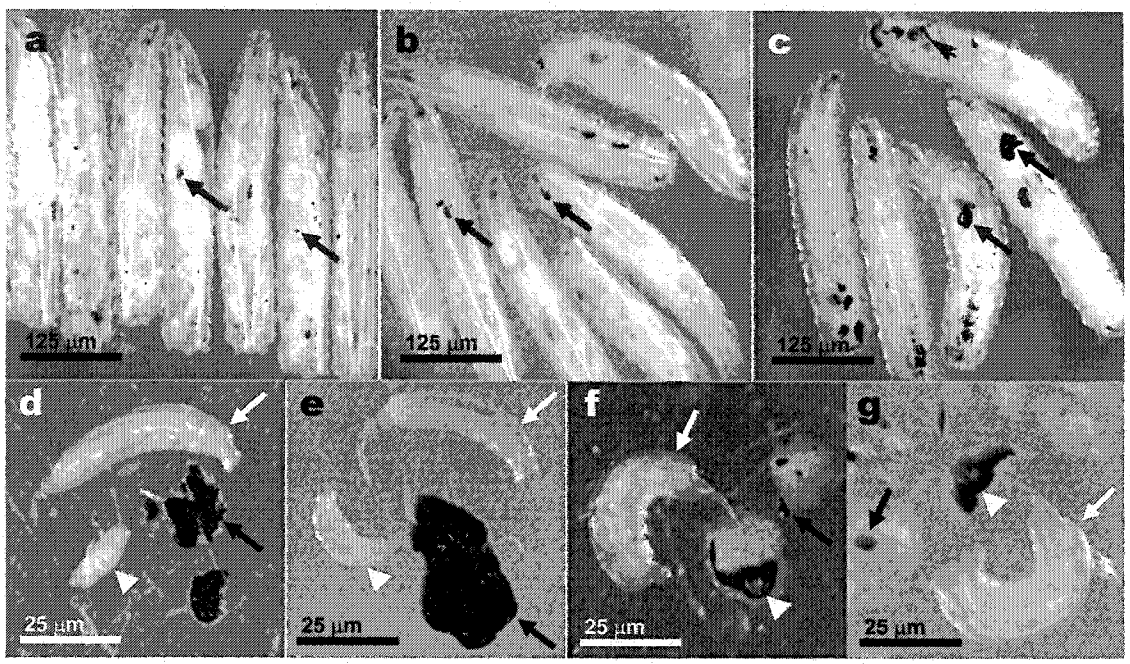


**Figure 3.** Encapsulation of supernumerary *L. boulardi-17* larval parasites in tumorous *Drosophila* mutant host larvae (*hopscotch*$^{Tum\text{-}l}$). (**a**) All control larvae show the formation of multiple melanotic tumors (black arrows in **a**), as do hosts infected with either *L. boulardi-17* (**b, f, g**) or *L. heterotoma-14* (**c-e**). Dominant larvae of (either wasp species) are not encapsulated (white arrows in **d, e, f,** and **g**). In *L. heterotoma-14,* supernumerary eggs or larvae are not encapsulated (arrowhead in **d** and **e** respectively). *L. boulardi-17* supernumerary larvae are encapsulated and melanized (white arrowhead in **f** and **g**).

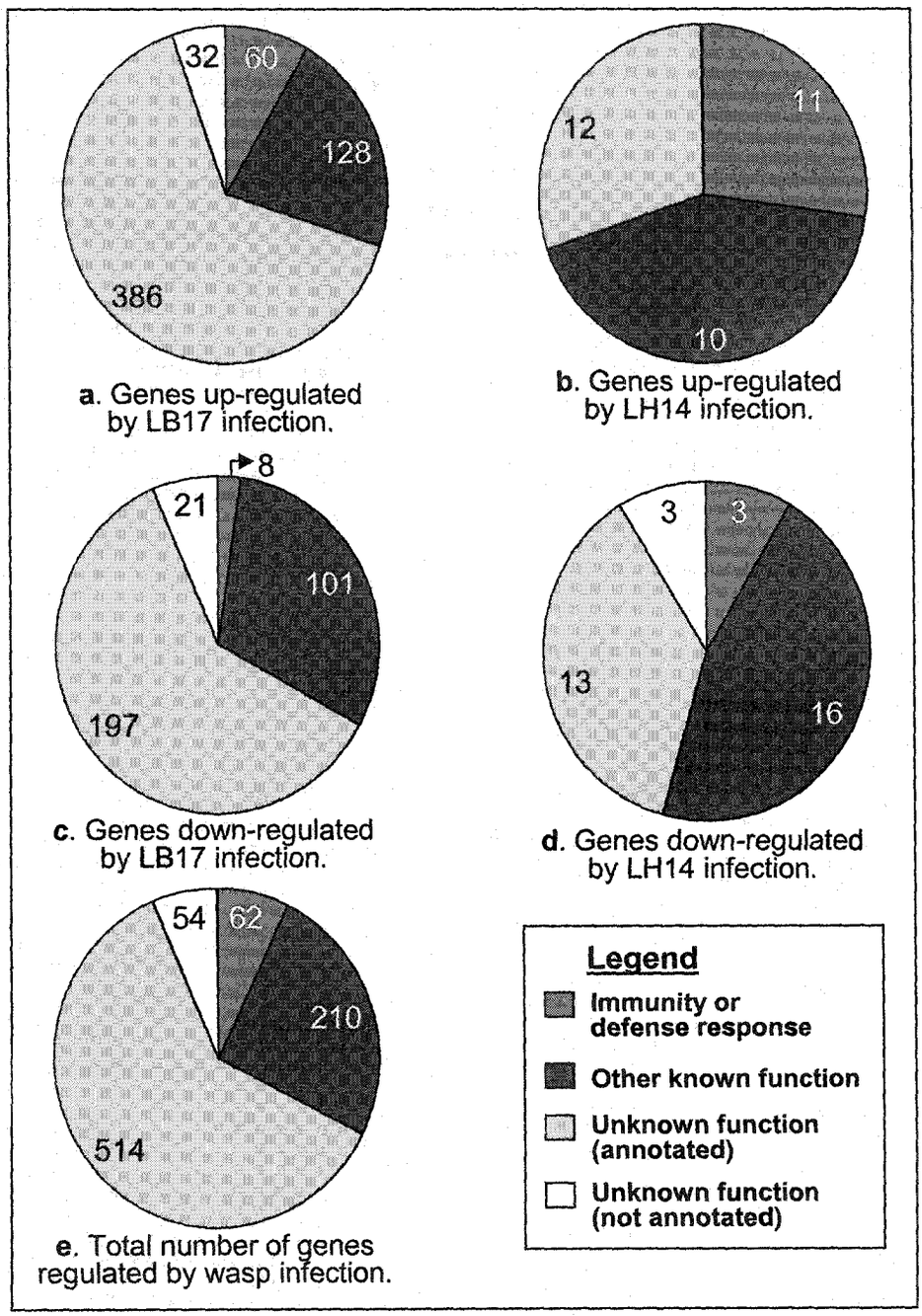


**Figure 4.** Percentage of immunity or defense response genes compared to the other gene categories regulated by *L. boulardi-17* (LB17) or *L. heterotoma-14* (LH14) infection of *D. melanogaster*. Each pie chart was generated from a list of genes showing differential regulation (two-fold or more; $p < 0.1$), relative to their corresponding uninfected controls. The proportions of different classes of genes are based on annotations from NetAffx. Nineteen additional genes were found to be regulated by infection (from the known and unknown categories) and have been added to Tables 3a and 3b. These nineteen genes were not annotated as "immunity genes" by NetAffx, but were previously identified to be in the immunity category (DeGregorio et al., 2002).

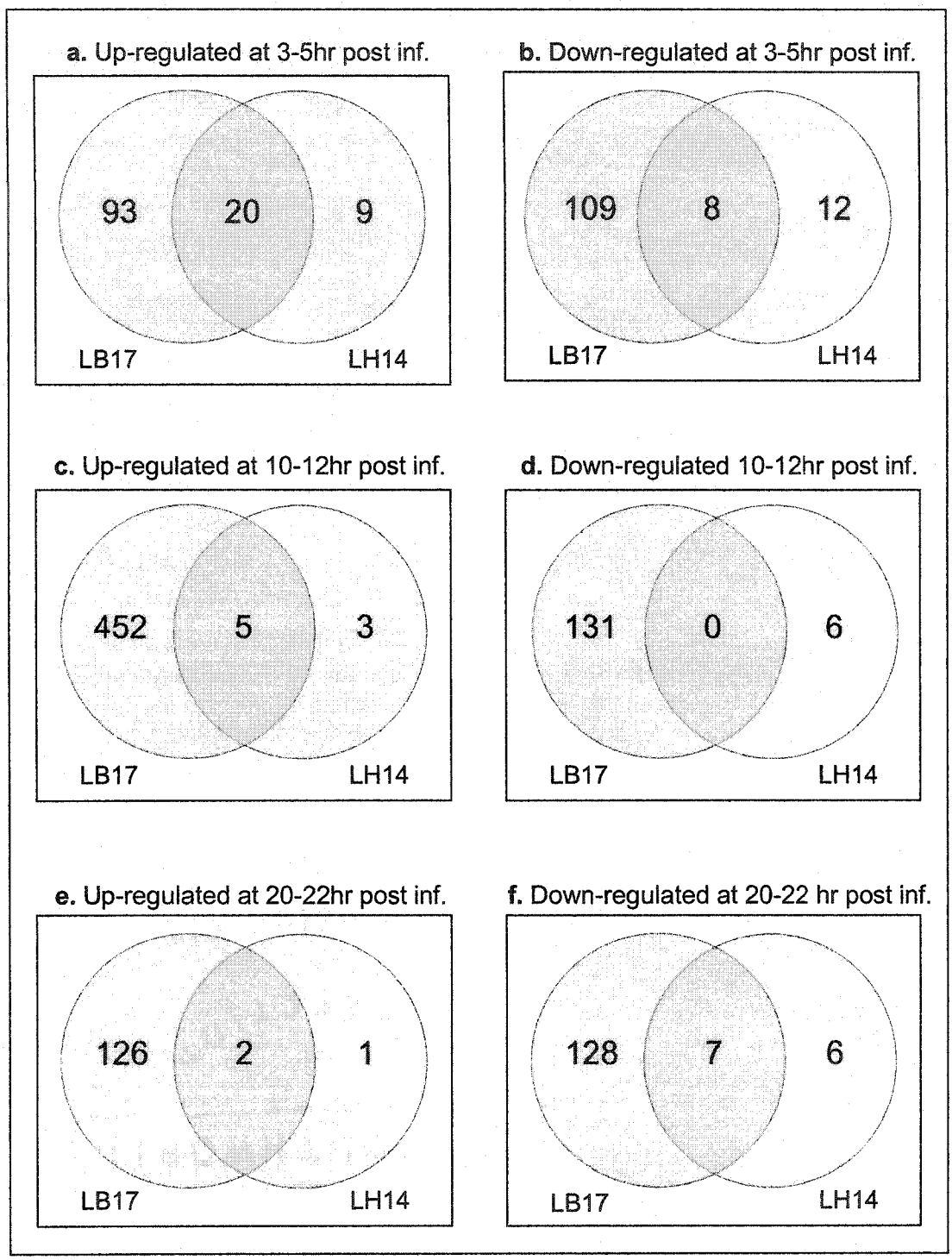


**Figure 5**. Venn diagrams showing the number of genes regulated by *L. boulardi-17* (LB17) infection compared to genes regulated by *L. heterotoma-14* (LH14) infection of *D. melanogaster* at three different time points: 3-5 hr, 10-12 hr, and 20-22 hr post-infection. Intersection sets show the number of genes regulated by both wasps. Analyses were done in ArrayAssist (Stratagene) from lists of probe sets generated by multiclass *t*-tests with a probability value < 0.10 and a 2-fold or more differential expression.

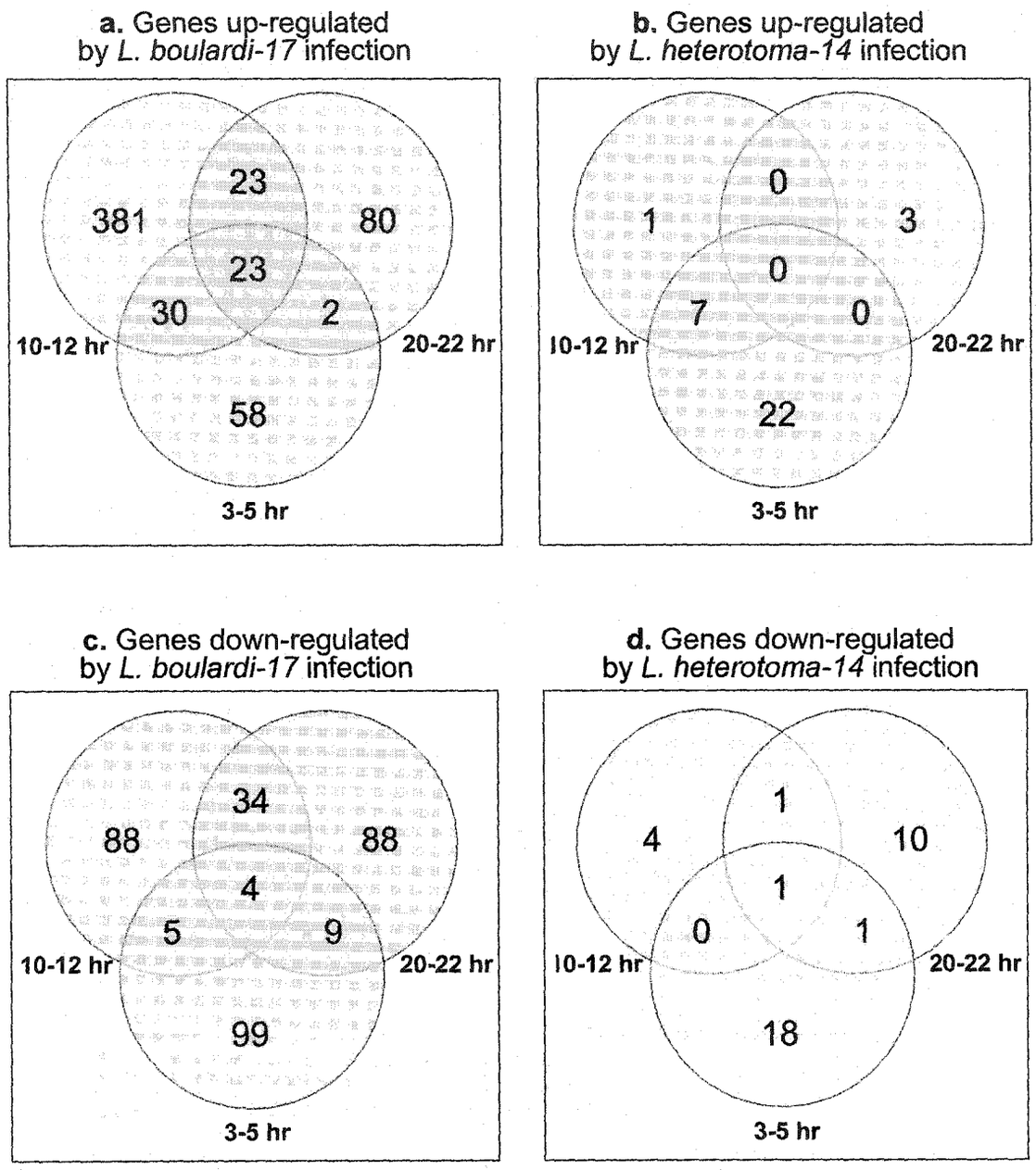


**Figure 6.** Time course comparisons of *D. melanogaster* genes regulated by wasp infection. (**a**) The number of genes significantly up-regulated ($p < 0.1$) in *Drosophila* larvae with two-fold or higher differential expression at 3-5 hr after infection by *L. boulardi-17* are compared with the genes up-regulated by the same wasp at 10-12 hr and 20-22 hr post infection. For example, 23 genes are induced at all three time points in response to *L. boulardi-17* infection (intersection in **a**). Genes induced by *L. heterotoma-14* are compared in a similar manner (**b**) as well as genes down-regulated by either wasp (**c** and **d**).

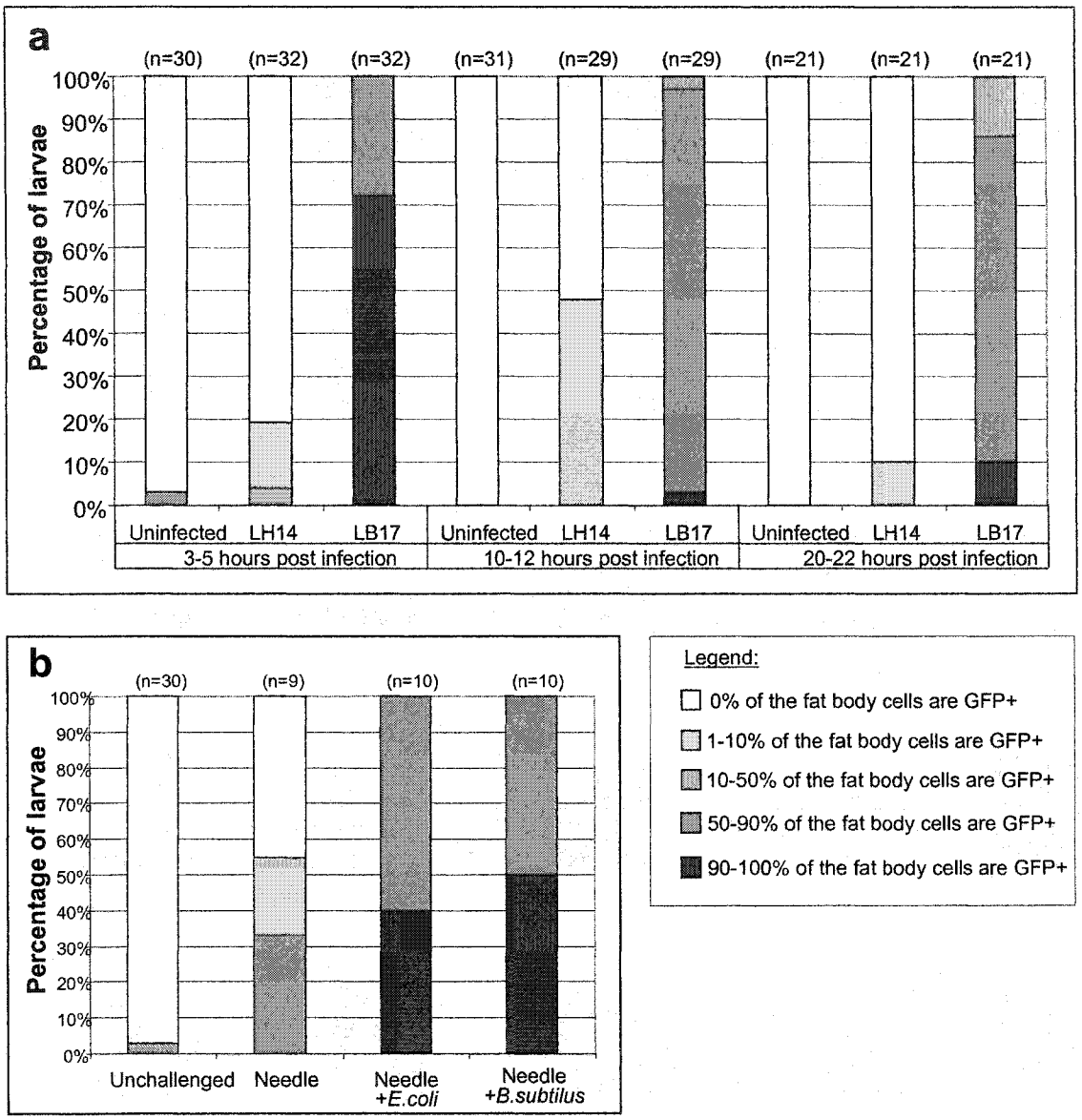


**Figure 7. (a)** Expression of *Drosomycin-GFP* reporter as detected by observations of green fluorescent protein (GFP) levels in the fat bodies of transgenic flies after wasp infection. All the larvae were dissected under a stereomicroscope to visually confirm infection prior to observations under a UV microscope using the FITC channel. **(b)** Expression of *Drosomycin-GFP* in transgenic L3 larvae after being challenged with a clean tungsten needle, or a needle dipped in either *E. coli* or *B. subtilis*. Observations were made 4 hr after immune challenge. Percentage of cells fluorescing was determined visually by observing entire dissected larvae at low magnification (100 X).

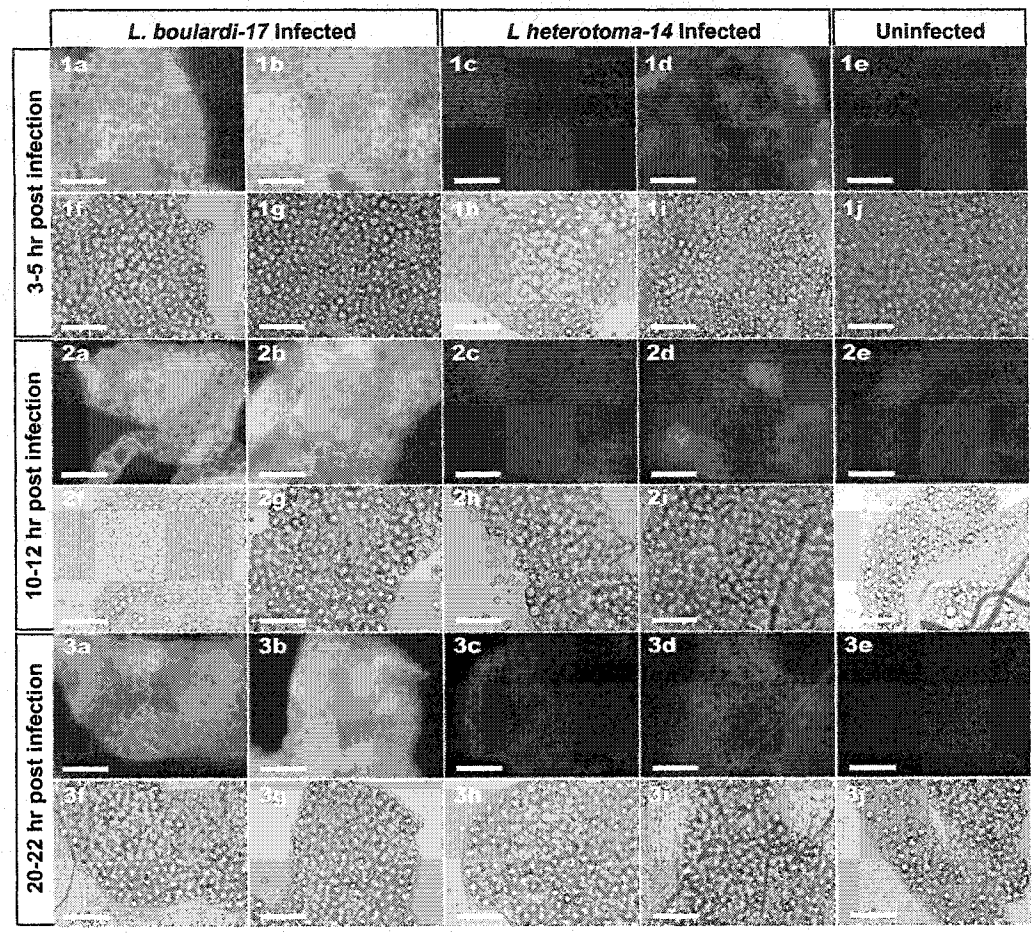


**Figure 8.** Expression of *Drosomycin (promoter)-GFP* in response to wasp infection. Transgenic larvae were infected with *L. boulardi-17*, *L. heterotoma-14*, or left uninfected (control) and their fat bodies were dissected and observed at the indicated times under the fluorescence microscope using the FITC filter. Two representative images are shown from a portion of the fat body. Phase images (**f-j**) corresponding to images photographed with fluorescence optics (**a-e**) are also included.